Local and Global Sensitivity Analysis of Thin Ply Laminated Carbon Composites

Thomas A. Neigh

Thesis submitted to the Faculty of the
Virginia Polytechnic Institute and State University
in partial fulfillment of the requirements for the degree of

Master of Science
in
Engineering Mechanics

Rakesh K. Kapania, Chair
Scott W. Case
Thomas D. McQuigg

April 25 2024
Blacksburg, Virginia

Keywords: Sensitivity Analysis, Laminated Composites

Local and Global Sensitivity Analysis of Thin Ply Laminated Carbon Composites

Thomas A. Neigh

(ABSTRACT)

Recent work in the area of composite laminates has focused on the characterization of the strength of laminates constructed from very thin plies. Interlaminar shear and normal stress components have been shown to be concentrated on the edges, the so-called edge effect, of unidirectional laminates at the interface between plies of different fiber orientation. Research has shown that decreasing ply thickness can reduce these interlaminar stress edge effects, and delay delamination in quasi-isotropic laminate specimen for laminates of equal total thickness. First ply failure stress has also been shown to increase with decreasing ply thickness. For these reasons, there has been a great deal of interest in laminated composites constructed from very thin plies. This work studies the impact of manufacturing tolerances on ply orientation on the mechanical properties of the constructed laminate. Direct Monte-Carlo simulation is used to model the variance introduced in the manufacturing process. First-order variance-based sensitivity analysis using a local analysis of variance technique is used to study the contribution of each individual ply to the variation in as built mechanical properties. Variation in mechanical properties of thick-ply and thin-ply laminate designs are compared to study if thin-ply laminate designs show more or less variation than their thick-ply counterparts. This work has found potential impacts of ply angle variation on variance of as-built stiffness in laminates of different ply thicknesses. These differences are attributable to the total ply count in a laminate. For a fixed height laminate, the ply count is inversely proportional to thickness, yielding the apparent benefit of thin plies. Using thinner plies

in a sub-laminar stacking arrangement, repeating a sublaminate instead of repeating plies, reduces sensitivity to manufacturing errors and would suppress tranverse failure modes.

Local and Global Sensitivity Analysis of Thin Ply Laminated Carbon Composites

Thomas A. Neigh

(GENERAL AUDIENCE ABSTRACT)

Carbon fiber reinforced polymer composites, a material consisting of carbon fiber filaments bound within a polymer matrix, are commonly used in aerospace applications for their excellent strength to weight ratio. This class of materials is highly tailorable, with strength and stiffness controlled by the number of fiber layers, their thickness, and each layer's respective orientation. Variability in these characteristics arising from manufacturing processes can result in changes in the laminate's engineering properties. This work shows that characterizing the impacts to the engineering properties through Monte-Carlo simulation of variability in the orientation is possible. A Monte-Carlo simulation is a type of statistical simulation where a sample population is generated using an assumed mean and standard deviation. Engineering and statistical analyses can then be performed on this sample population to determine the variability in the engineering properties of the population. In addition, the variability in the population can be studied as a function of each individual fiber layer to understand individual impacts based on orientation and position within the larger composite. Using these analysis techniques presented in this work allows for the study of laminate variability prior to manufacturing, allowing engineers to better understand the material during the design of complex aerospace structures.

Dedication

Dedicated to my friends and family, without whom this journey would never have been possible.

Acknowledgments

I would like to thank my committee members for their generosity with their wisdom and time. A special thank you to Dr. Kapania, my committee chair, for his guidance and patience throughout my journey.

Contents

List of Figures

List of Tables

List of Abbreviations

CFRP Carbon Fiber Reinforced Polymer

CLT Classical Lamination Theory

mil $\frac{1}{1000}$ inch

NASA National Aeronautics and Space Administration

Chapter 1

Introduction

Thin ply composites are gaining an increasing interest due to their apparent ability to delay first ply failure of CFRP composites. Analytical evidence of such behavior was first shown in [11]. Modern manufacturing techniques have allowed for the construction of composites from thin plies without damaging fibers [16]. Minimizing imperfections in the fiber, cured ply, and layup are critical to ensuring that laminated composites perform as designed. Statistical analyses can be completed based on expected errors to determine bounding cases for the expected performance. These bounds establish an expectation for both stiffness and strength, which is critical to design of aerospace hardware to meet strength and stiffness requirements This work is built upon the intersection of these fields of study, composite analysis, statistical analysis, and thin ply composites. A brief introduction to each of these fields is given in this chapter, followed by literature review in subsequent chapters.

1.1 Composite Analysis

Laminated CFRP composites are popular due to their high specific strength and specific stiffness. Engineering properties of these materials, called laminated composites through the remainder of the paper, are highly tailorable for desirable characteristics [6]. Material selection for fiber and matrix, processing of raw material during manufacturing, environmental conditions during layup, layup techniques, and stacking sequence all contribute to

the engineering properties of the final layup.

Variation in any step of the manufacturing process can affect the engineering properties of the final laminate. Fluctuation in temperature during fiber curing, excessive moisture during cure, and deviations from nominal ply orientation during stacking are all examples of variation/errors that can contribute to differences between as-designed and as-manufactured engineering properties. This work focuses on ply angle error that arises in hand layup techniques. Variation of the ply angle orientation impacts the final laminated composite engineering properties.

1.2 Statistical Analysis

The impact of variation in manufacturing processes on the laminate's stiffness and strength can be simulated with statistical models. For a given model of the errors introduced in manufacturing, the Monte-Carlo method may be used to generate a simulated sample of as-built composites containing manufacturing defects. Variation in the model output is studied using a combination of uncertainty and sensitivity analysis. Uncertainty analysis studies variation in the output, while sensitivity analysis studies how the variation in model output may be attributed to variation in the model input [15]. In the case of laminated composites, these processes are applied to studying the resulting stiffness matrices of as built composites. Sensitivity analysis is used to study how variation in stiffness may be attributed to variation in the manufacturing process. In this work, the variation of ply angle that arises from errors during hand layup is focused on as a source of variation. Additional sources of variations, such as void content, ply thickness, and other defects, could be included in the mathematical models but are not studied in this work.

1.3 Thin Ply Composites

Thin-ply composite laminates are defined by NASA as those that are constructed from plies that measure 2.5mil or thinner [19]. Such laminates are gaining increasing interest in the aerospace industry due their ability to suppress through thickness failure modes of a laminate. This delay in delamination is thought to be due to suppression of interlaminar stresses on the ply boundaries at the free edge of a laminate. In exchange for damage suppression, composite laminates constructed from thin plies fail in a more brittle manner [11, 16]. This research studies how variation from the nominally designed configuration introduced in the manufacturing process affects the mechanical properties of the laminate.

Chapter 2

Literature Review

2.1 Thin Ply Composites

Ply thickness has been shown analytically to be connected to interlaminar stresses, which are concentrated at laminate edges in specimen subjected to axial extension [11]. These stresses contribute to transverse micro-cracking and delamination failures. Experimental studies have shown that decreasing ply thickness in quasi-isotropic laminates suppresses these failure modes, increasing laminate strength up to the ultimate fiber strength [11, 16, 20]. This increase in strength and simplification of failure mode make thin ply composites attractive to aerospace designers.

2.1.1 Experimental Studies

The size effect of ply thickness has been studied extensively by [16, 2, 21]. Four sources of potential size effect: probability of flaws, crack propagation, laminate scaling, and manufacturing were proposed in [2]. Total laminate volume was conserved in all experimental studies to eliminate this size effect, though the effect of volume of an individual ply on probability of a defect persists. Crack propagation is thought to be blunted at the boundary of plies with different orientation angle, due to the discontinuity in ply angle. In-situ strength models have been proposed by [4, 21] showed that repetition of a sub-laminate $[45, 90, -45, 0]_n$,

as opposed to ply block scaling $[45_n, 90_n, -45_n, 0_n]$, was critical to laminate performance. Sub-laminate scaling showed an increase in unnotched tensile strength and increase in onset of damage stress for open hole tension. In exchange for the increase in onset of damage, laminates failed in a more brittle manner at a lower ultimate strength than the ply block scaling. Studies performed by [2, 21] demonstrated that thick ply laminates behave similarly to ply block scaled thin ply laminates. Thin ply laminates were shown to provide significant improvements in strength compared to thick ply counterparts. Unnotched tensile specimen demonstrated an ultimate strength comparable to the ultimate strength of the constituent fibers [2, 16]. Onset of damage in open hole tension was demonstrated to be at a higher load than for their thick ply counterparts [2, 16]. In open hole fatigue testing, thin ply composites were demonstrated to have a quasi-infinite life for sufficiently low loading, which was not observed for any level of loading for thick ply laminates [2]. Thin ply laminates were also shown to have improved hot/wet performance and resistance to onset of damage from impact testing [2].

2.1.2 Manufacturing Techniques

Ply thickness of carbon fiber composites is controlled by the thickness of the tow of carbon fiber used to manufacture the ply. Thinner plies are achieved through spreading of fiber tows. Modern tow spreading techniques reduce tension in the filaments during spreading using air flow to prevent fiber damage [16, 12]. Air is pulled downwards using a vacuum, which results in a tension free state in the fibers. A vibrating spreader is then used to decrease tow thickness uniformly. This technique is referred to as pneumatic tow spreading or the pneumatic method [12]. Unidirectional laminates studied in [16] of both thin and thick ply laminates created from prepreg sheets from the same original tow using this tow spreading technique showed comparable moduli and strength, demonstrating that thin ply

laminates can be constructed without introducing any fiber damage. Standard deviations of the tested samples were also comparable, suggesting that any manufacturing errors are independent of the ply thickness.

2.1.3 Modeling Techniques

Analytical prediction of experimentally observed laminate failure strengths generated by [2] using a variety of techniques. Techniques employed included CLT without damage, CLT with damage considerations, in-situ strength techniques, and shell modeling in Abaqus/CAE [5]. Damage was introduced into the CLT model though progressive load steps where the stiffness of any ply is penalized by 99% when the Tsai-Hill failure criterion of that ply reached a value of one. Ultimate failure was defined as failure of the 0° ply. Their calculations showed that strength predictions with CLT reasonably predicted failure strengths of laminates with predicted first ply failure corresponding with the onset of damage observed in thick ply laminates. Ultimate strength predictions with damage matched well with observed failure strength of intermediate ply laminates and ultimate strength predictions without damage. The in-situ strength model, which was first proposed in [4], postulates that apparent transverse strength of a ply is increased by its neighbors constraining crack propagation. This model for strength prediction is based on linear elastic fracture mechanics. This method did not agree well with experimental results in [2], whose results follow a linear relationship as opposed to an asymptotic relationship proportional to the inverse of the square root of ply thickness. Other limiting mechanisms such as free edge delamination and matrix damage are suspected of contributing to these differences [2]. Shell modeling was found to be a poor predictor of first ply failure in thick ply laminates, with improved accuracy for thin and intermediate ply laminates. These results have shown that simple model techniques such as shell modeling and CLT are reliable for predicting strength of laminates with thin plies due

to the suppression of delamination and other transverse failure modes [2].

2.2 Composite Analysis

Composite analysis performed in this work is completed using CLT. The two key assumptions that accompany this theory are plane stress and the Kirchhoff hypothesis, which states that a line normal to the mid-plane does not deform, but instead only translates and rotates [6]. This hypothesis assumes no out of plane shear deforms the normal to the mid-plane, which is typically applicable for a structure whose thickness is small compared to in-plane dimensions. Through thickness normal and shear stresses are not considered in CLT. Methods such as first-order shear deformation theory, or higher-order shear deformation theory include the effects of through the thickness shear effects, but are not considered in this work.

2.2.1 Laminate Stiffness Matrix

To perform analysis with laminated composites, laminate level properties are developed from the properties of the individual plies. Using the plane stress assumption, the orthotropic stiffness properties can be reduced to a 3x3 matrix for in-plane extensional stiffness and shear stiffness, the so called reduced stiffness matrix. This matrix and subcomponents are defined in Eqs. 2.1 through 2.5 [6]:

$$Q_{ij} = \begin{bmatrix} Q_{11} & Q_{12} & 0 \\ Q_{12} & Q_{22} & 0 \\ 0 & 0 & Q_{66} \end{bmatrix} \tag{2.1}$$

$$Q_{11} = \frac{E_1}{1 - \nu_{12}\nu_{21}} \tag{2.2}$$

$$Q_{12} = \frac{\nu_{12}E_2}{1 - \nu_{12}\nu_{21}} \tag{2.3}$$

$$Q_{22} = \frac{E_2}{1 - \nu_{12}\nu_{21}} \tag{2.4}$$

$$Q_{66} = G_{12} \tag{2.5}$$

The stress strain relations for a single ply are given by 2.6:

$$\begin{Bmatrix} \sigma_1 \\ \sigma_2 \\ \tau_{12} \end{Bmatrix} = \begin{bmatrix} Q_{11} & Q_{12} & 0 \\ Q_{12} & Q_{22} & 0 \\ 0 & 0 & Q_{66} \end{bmatrix} \begin{Bmatrix} \epsilon_1 \\ \epsilon_2 \\ \gamma_{12} \end{Bmatrix} \tag{2.6}$$

Ply orientation is then used to transform the lamina level stiffness into the laminate coordinate system for the transformed reduced stiffness $\overline{Q}_{ij}$, i=1,2,6. The transformation matrix T and transformation equation are defined in Eqs. 2.7 and 2.8, respectively. The shorthand notation $m = \cos(\theta)$ and $n = \sin(\theta)$, where θ is the ply orientation angle relative to the laminate X-direction is used for cleanliness [6]. Errors in ply orientation at any individual ply impact the larger laminate stiffness matrix by changing the transformed reduced stiffnesses. The stiffness of each individual ply is then assembled into the laminate stiffness matrix.

$$T = \begin{bmatrix} m^2 & n^2 & 2mn \\ n^2 & m^2 & -2mn \\ -mn & mn & m^2 - n^2 \end{bmatrix} \tag{2.7}$$

$$\overline{Q} = [T]^{-1}[Q][T] \tag{2.8}$$

The laminate stiffness matrix can then be constructed by relating the mid-plane strains and curvatures to the laminate force and moment resultants, respectively. The matrix shown in Eq. 2.9, commonly referred to as the **ABD** Matrix, is comprised of the extensional matrix **A**, the extensional bending coupling **B**, and the bending matrix **D**. Each of the 3 submatrices are computed from the transformed reduced stiffnesses of each lamina using the following, i=1, 2, and 6:

$$ABD = \begin{bmatrix} A & B \\ B & D \end{bmatrix} \tag{2.9}$$

$$A_{ij} = \sum_{k=1}^{N} \overline{Q}_{ij_k}(z_k - z_{k-1}) \tag{2.10}$$

$$B_{ij} = \frac{1}{2}\sum_{k=1}^{N} \overline{Q}_{ij_k}({z_k}^2 - z_{k-1}^2) \tag{2.11}$$

$$D_{ij} = \frac{1}{3}\sum_{k=1}^{N} \overline{Q}_{ij_k}({z_k}^3 - z_{k-1}^3) \tag{2.12}$$

Force and moment resultants **N** and **M**, respectively, are related to mid-plane strains and

curvatures, ε and κ, using:

$$\begin{Bmatrix} N \\ M \end{Bmatrix} = \begin{bmatrix} A & B \\ B & D \end{bmatrix} \begin{Bmatrix} \varepsilon \\ \kappa \end{Bmatrix} \tag{2.13}$$

Certain classifications of laminates, based on their stacking sequences, result in select terms of the ABD matrix reducing to 0. Symmetric, balances, and cross-ply laminates each result in select 0 terms. Definitions of these classifications are given in the following [6]:

- Symmetric: For every ply on one side of the laminate mid-plane with specified thickness, material properties, and ply orientation angle there exists another ply the same distance from the mid-plane with identical thickness, properties, and orientation angle. For these laminates all components of the B matrix reduce to 0, resulting in the decoupling of the A and D matrices.
- Balanced: For every ply with a specified thickness, material properties, and ply orientation angle there exists another ply somewhere in the laminate with identical thickness and properties, but opposite orientation angle. For these laminates, A_{16} and A_{26} are zero.
- Cross-ply: Every ply has its fibers oriented at either 0° or 90°. For these laminates 16 and 26 components of all 3 submatrices are zero. The combination of a symmetric and balanced laminate is frequently used in engineering applications due to the decoupling of the extensional-bending behavior, and the decoupling of in-plane shear from in-plane extensional behavior. Classical techniques exist for writing effective laminate level engineering properties for these laminates, which are discussed in the next section. Variation in ply orientation can result in a final laminate that does not satisfy the symmetric balanced condition. Errors in ply thickness and properties (voids) can also violate these assumptions but are not investigated in this work.

2.2.2 Effective Engineering Properties

Effective engineering properties of a laminate are often used to describe how a laminate will respond to laminate level loading. As the laminate matrix discussed thus far is based on CLT, the discussion will be limited to in-plane loading. These effective engineering moduli are defined to relate the average stress in a laminate to the mid-plane strains [6]. Average stresses can thus be defined as the force resultants divided by laminate thickness H:

$$\overline{\sigma}_x = \frac{N_x}{H}; N_x \equiv \int_{-H/2}^{H/2} \sigma_{xx} dz \tag{2.14}$$

$$\overline{\sigma}_y = \frac{N_y}{H}; N_x \equiv \int_{-H/2}^{H/2} \sigma_{yy} dz \tag{2.15}$$

$$\overline{\tau}_{xy} = \frac{N_{xy}}{H}; N_{xy} \equiv \int_{-H/2}^{H/2} \tau_{xy} dz \tag{2.16}$$

Assuming a symmetric balanced laminate, inverting the ABD matrix, and applying 2-D Hooke's law, the effective engineering properties for a laminate can be written as follows [6]:

$$[abd] = \begin{bmatrix} a & b \\ b^T & d \end{bmatrix} = [ABD]^{-1} \tag{2.17}$$

$$\overline{E}_x = \frac{1}{a_{11} H} \tag{2.18}$$

$$\overline{E}_y = \frac{1}{a_{22} H} \tag{2.19}$$

$$\overline{G}_{xy} = \frac{1}{a_{66}H} \tag{2.20}$$

$$\overline{\nu}_{xy} = -\frac{a_{12}}{a_{11}} \tag{2.21}$$

A modification of the classical approach for development of effective engineering properties where no restrictions are imposed on stacking sequence is outlined in [18]. In this approach curvature of the laminate is suppressed while force and moment resultants are applied. A new matrix, P, is then derived to relate the mid-plane strains to the force resultants. Effective moduli and poisson's ratio are then derived by individually applying N_x, N_y, or N_{xy}.

$$\begin{Bmatrix} \varepsilon \\ 0 \end{Bmatrix} = \begin{bmatrix} a & b \\ b^T & d \end{bmatrix} \begin{Bmatrix} N \\ M \end{Bmatrix} \tag{2.22}$$

$$P = [a] - [b][d]^{-1}[b^T] \tag{2.23}$$

$$\begin{Bmatrix} \epsilon_x \\ \epsilon_y \\ \gamma_{xy} \end{Bmatrix} = \begin{bmatrix} P_{11} & P_{12} & P_{16} \\ P_{12} & P_{22} & P_{26} \\ P_{16} & P_{26} & P_{66} \end{bmatrix} \begin{Bmatrix} N_x \\ N_y \\ N_{xy} \end{Bmatrix} \tag{2.24}$$

The resulting equations for effective engineering properties are shown in the following. For brevity, the variable Δ is introduced to reduce the size of the equations. For a symmetric balanced laminate the classical equations are recovered as P_{16} and P_{26} will reduce to zero [18].

$$\Delta = P_{11}P_{22} - P_{12}^2 \tag{2.25}$$

$$\overline{E}_x = \frac{1}{(P_{11} - \frac{P_{16}^2}{P_{66}})H} \tag{2.26}$$

$$\overline{E}_y = \frac{1}{(P_{22} - \frac{P_{26}^2}{P_{66}})H} \tag{2.27}$$

$$\overline{G}_{xy} = \frac{1}{\left(P_{66} - \frac{P_{16}(P_{22}P_{16} - P_{12}P_{26})}{\Delta} - \frac{P_{26}(P_{11}P_{26} - P_{12}P_{26})}{\Delta}\right)H} \tag{2.28}$$

$$\overline{\nu}_{xy} = -\frac{P_{12} - \frac{P_{16}P_{26}}{P_{66}}}{P_{11} - \frac{P_{16}^2}{P_{66}}} \tag{2.29}$$

Recovery of the classical equations was verified numerically for an example symmetric balanced laminate $[\pm\theta, 0, 90]_S$ using material properties from [6]. The agreement between classical and modified methods for this laminate is demonstrated for E_x in Fig 2.1:

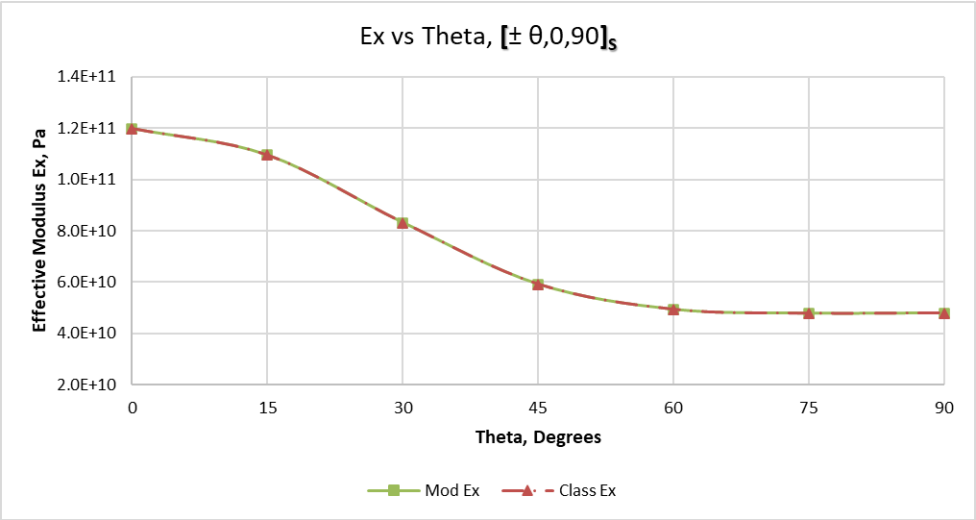

Figure 2.1: Longitudinal Modulus for $[\pm\theta, 0, 90]_S$

For laminates that do not satisfy these classifications, such as the unsymmetric and unbalanced laminate $[\theta_2, 0, 90]_{2T}$ using material properties from [6]. Results of the two methods differ as shown in Fig 2.2 and Fig 2.3 for E_x and E_y, respectively:

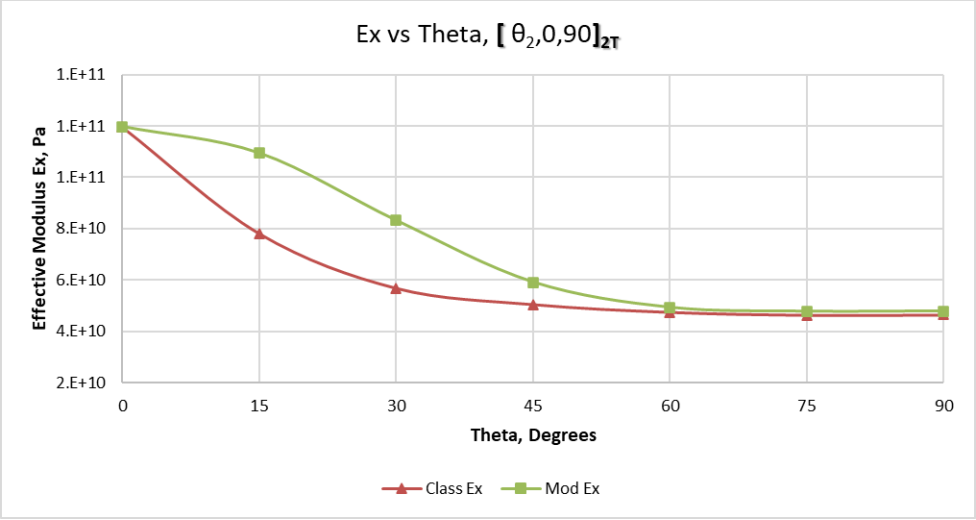

Figure 2.2: Longitudinal Modulus for $[\theta_2, 0, 90]_{2T}$

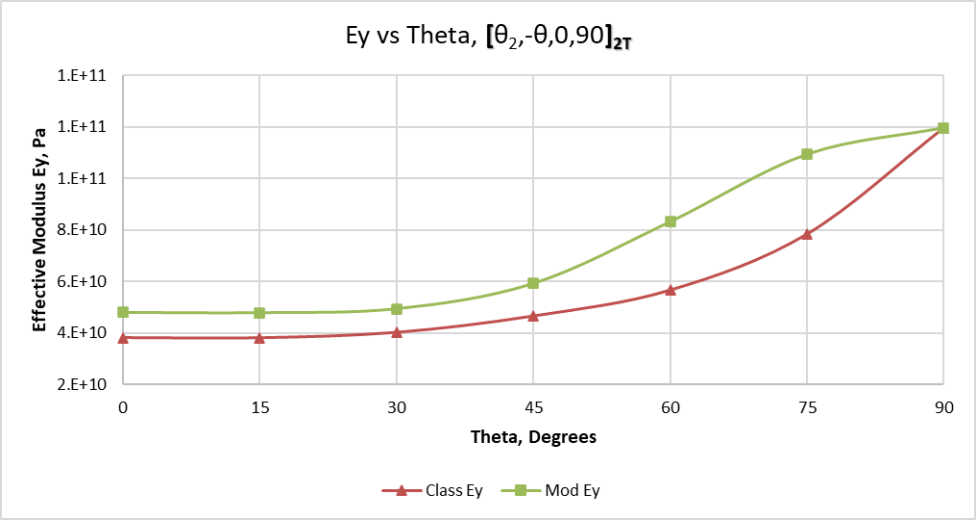

Figure 2.3: Transverse Modulus for $[\theta_2, 0, 90]_{2T}$

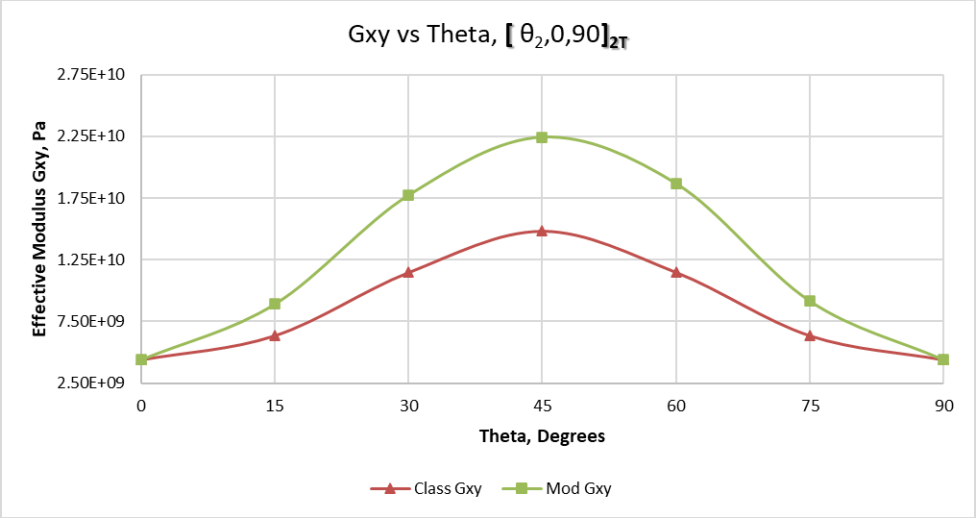

Figure 2.4: Shear Modulus for $[\theta_2, 0, 90]_{2T}$

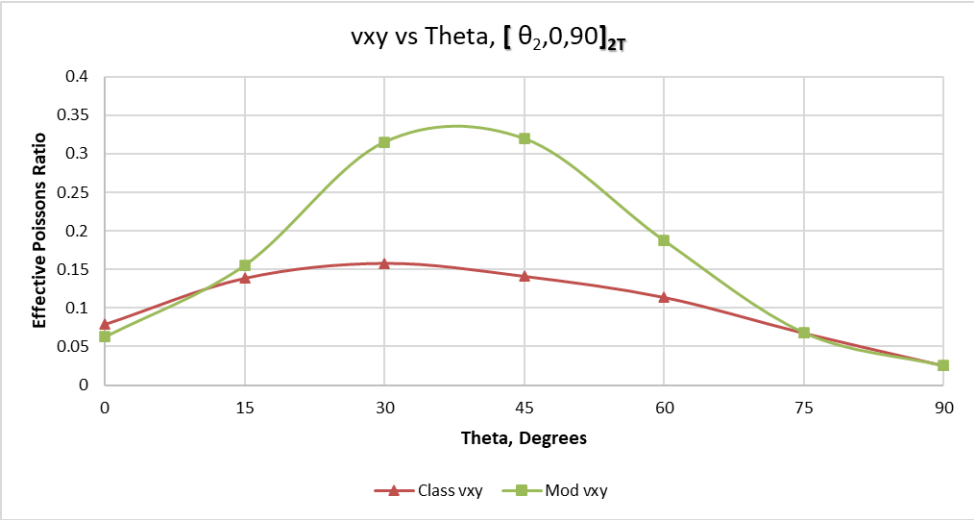

Figure 2.5: Poisson's Ratio for $[\theta_2, 0, 90]_{2T}$

While this modified method provides greater flexibility than the classical method, the laminates studied in this work are nominally symmetric and balanced. Small deviations from the nominal are assumed acceptable. In addition, while the modified method reduces to the classical method analytically in the case of a symmetric and balanced laminate, this reduction is difficult to achieve numerically. The ABD matrix of simulated laminates is not well conditioned for numerical inversion, yielding erroneous results. As a result of the need for numerical implementation the classical method for obtaining the effective engineering properties of a laminated composite is employed in this work.

2.3 Statistical Analysis

Two classes of statistical analysis techniques are employed in this work to study the uncertainty in the model of the manufactured laminated composite layup, uncertainty analysis and sensitivity analysis. Uncertainty analysis is used to quantify variation in the model output, while sensitivity analysis is used to study how the variation in the model output can be attributed to sources of variation in the model input [15]. In this work, the model refers to the composite analysis simulation, the output to the resulting stiffness values, and the input to the properties of each of the plies with variation being limited to the fiber orientation angle. Sensitivity indices can aid in identifying critical plies for a layup's properties. For both analysis methods, the Monte-Carlo method is employed as a common engineering technique for simulating an input population. Common metrics of uncertainty analysis include mean, standard deviation, and confidence intervals of output distributions [15]. These metrics are quantitative and understood by most engineers.

In engineering, sensitivity analysis techniques are typically applied to equations (deterministic models) based on a set of experimental data or randomly generated input variables.

Output of a sensitivity analysis depends on the technique chosen. Derivative, regression, and variance techniques exist for the computation of sensitivity indices. Derivative metrics are quantitative, but difficult to compute for complex problems and are local to the point of computation. Regression techniques, such as least-squares-regression, are a global technique that yield qualitative metrics, but make some assumptions about the model's linearity. Variance based techniques are a set of statistical techniques that do not make any assumptions about the model that can be performed both on a local or global scale [15, 8]. These techniques use both conditional variance, the variance when a variable or set of variables is fixed, and unconditional variance, the variance when all variables are free. These techniques are best suited for problems where the input parameters can be best described by a statistical distribution, such as manufacturing error in composite layup. Variance based techniques will be employed in this work due to their applicability to manufacturing problems.

2.3.1 Analysis of Variance

Variance based sensitivity analysis techniques can be broken down into local and global techniques and are based on statistics analysis of variance techniques. The analysis of variance is a statistical analysis technique for studying the relationship between dependent and independent variables in a model [14]. Within the scope of this work, it is a set of techniques that can be used to study the relationship between the input angle variation and variation in laminate stiffness. Local sensitivity analysis focuses on sensitivities near a fixed value of input variables, x_i. Sensitivity indices are computed by comparing the variance of the output with a fixed input parameter, called conditional variance, to the variance without any fixed input parameters, called the unconditional variance [15]. These methods offer lower computational time than global analysis techniques, at the expense of dependency on the selected x_i [15, 9].

Another downside of local sensitivity analysis techniques is that it is possible, depending on selection of x_i, to obtain a conditional variance greater than the unconditional variance. In this case, the sensitivity index returned by the technique is negative which indicates that fixing the variable leads to greater variation. Global variance based sensitivity analysis techniques do not impose the restrictions of local sensitivity analysis methods. These methods can compute both first-order sensitivity measures, as well as measures of the effects of interaction between input variables. Both local and global sensitivity analysis techniques are used in this work, and the specific techniques are described further below.

Local Analysis of Variance

Local analysis of variance computes a first-order sensitivity index by fixing select input parameters at a selected value while allowing others to vary. One common sensitivity analysis approach is to fix input parameters at the mean value [9]. It is a first-order method where n simulations of the i^{th} random variable are generated while keeping all other variables at their mean value. The standard deviation of the results for each of the i^{th} variables must be computed, as well as the standard deviation of all variables are allowed to vary. This first-order method offers low computation expense but does not account for any interaction between variables. An improvement is proposed in [10] accounts for interaction between variables by reversing the "fixity" of the input variables. Instead of allowing the i^{th} variable to vary, the i^{th} variable is fixed at its mean value and other variables are allowed to vary. Sensitivity index for the i^{th} variable is then computed from the following [10]:

$$O_i = 1 - \frac{\sigma_i}{\sigma_{orig}} \tag{2.30}$$

Where

- O_i is the sensitivity index
- σ_i is the standard deviation of the output when the i^{th} input parameter is fixed at its mean value
- σ_{orig} is the standard deviation of the output when all input parameters are allowed to vary

Larger values of O_i indicate that the i^{th} input parameter has a more significant impact on the variance of the output. Values of O_i are relative and may not sum to 1 across the domain of all input parameters. It should be noted that it is theoretically possible to obtain negative values of O_i using this technique. Negative values happen in the case that $\sigma_i > \sigma_{orig}$, which would indicate that the variance increased when the i^{th} variable was fixed. This is more common in the case of correlated input variables and is a weakness of local sensitivity analysis techniques [10].

Sobol's Method for Analysis of Variance

Sobol's technique for global sensitivity analysis relies on function decomposition [17]. Variance is decomposed into its sub-components and these sub-components are used to compute sensitivity indices. A total sensitivity index is then defined as the sum of the effects of an individual variable across all first-order effects and the effects of interaction across every order of the parameter [17]. An example decomposition of such a total sensitivity index TS across individual indices S for a model with input parameters z_i through z_k:

$$TS(z_1) = S(z_1) + S(z_1, z_2) + \ldots + S(z_1, z_k) + \ldots + S(z_1, ..., z_k) \tag{2.31}$$

Sensitivity indices computed using this method are commonly referred to as Sobol indices,

and will be referred to as such in the remainder of this work. The foundation of Sobol's method is function decomposition. A function $f(x)$ is decomposed into summands of function of increasing dimensionality, as in Eq. 2.32. Sensitivity to the output Y of the function is determined by defining input factor space per [17]. Sobol's method for obtaining sensitivity indices form these equations is summarized below per the process defined in [17] and summarized in [3].

$$f(x_1, ..., x_k) = f_0 + \sum_{i=1}^{k} f_i(x_i) + \sum_{1 \le i \le j \le k} f_{ij}(x_i, x_j) + \ldots + f_{1,2,...,k}(x_1, ..., x_k) \tag{2.32}$$

Where f_0 is the "zeroth" order, and $f_i, f_{i,j,...k}$ are decompositions of increasing order.

The derivation of the method was completed assuming an n-dimensional unit cube domain Ω_k such that:

$$\Omega_k = (x | 0 \le x_i \le 1, i = 1, ..., k) \tag{2.33}$$

However, this method may be applied to problems whose variables exist in non-unit domains.

In order for 2.32 to hold true over domain Ω_k, f_0 must be a constant and the integrals of the components of the decomposition over any of its own variables must be zero [17]:

$$\int_0^1 f_{i1,...,is}(x_{i1}, ..., x_{is})\, dx_{ik} = 0, \text{ if } 1 \le k \le s \tag{2.34}$$

Where $f_{i1,...,is}$ are decompositions of increasing order with interaction between other orders.

From 2.32 and 2.34, it can be seen that the individual summands of the function decomposition must be orthogonal [17]. This orthogonality can be expressed in equation form

as:

$$\int_{\Omega_k} f_{i1,...,is} * f_{j1,...,jl} dx = 0, \text{ if } (i_1, ..., i_s) \neq (j_1, ..., j_l); (i, j, s, l = 1, ..., k) \tag{2.35}$$

Similarly here, $f_{j1,...,jl}$ are decompositions of increasing order with interaction between other orders, indexed independently of $f_{i1,...,is}$.

Since at least one index will not be repeated in 2.35, the equation vanishes due to 2.34. Resulting from both equations is the constant f_0:

$$f_0 = \int_{\Omega_k} f(x) dx \tag{2.36}$$

The decomposition has been shown to be unique and components of the expansion in 2.32 can be expressed in multidimensional integrals [17]. These integrals for first-order and higher order components are shown below. In these integrals, dx/dx_i is used to indicate differentiation across all variables except x_i.

$$f_i(x_i) = -f_0 + \int_0^1 ... \int_0^1 f(x) dx/dx_i \tag{2.37}$$

$$f_{ij}(x_i, x_j) = -f_0 - f_i(x_i) - f_j(x_j) \int_0^1 ... \int_0^1 f(x) dx/dx_i dx_j \tag{2.38}$$

Using the equations for components 2.36 thru 2.38, the total variance D and partial variances $D_{i1}, ..., is$ of function $f(x)$ are defined below for indices $1 \leq i_1 \leq ... \leq i_s \leq k$ and $i, s = 1, ..., k$

$$D = \int_{\Omega_k} f^2(x) dx - f_0^2 \tag{2.39}$$

$$D_{i1,\dots,is} = \int_0^1 \dots \int_0^1 f_{i1,\dots,is}(x_{i1}, \dots, x_{is}) dx_{i1}, \dots, dx_{is} \tag{2.40}$$

The relationship between total and partial variance can be obtained by squaring 2.32 and integrating over k the following can be written after accounting for orthogonality [17]

$$D = \sum_{i=1}^{k} D_i + \sum_{1 \le i < j \le k} D_{ij} + \dots + D_{1,2,\dots,k} \tag{2.41}$$

Using the relationship between the variances, the sensitivity indices of arbitrary order $S(i_1, \dots, i_s)$ can be defined as [17].

$$S_{i_1,\dots,i_s} = \frac{D_{i_1,\dots,i_s}}{D} \text{ for } 1 \le i_1 < \dots < i_s \le k \tag{2.42}$$

The first-order sensitivity index is defined as S_i, the sensitivity index for input parameter x_i. Second order indices $S_{ij}, i \neq j$, for input parameters x_i and x_j, as well as higher order indices are similarly defined in this fashion. The total sensitivity index for a single input parameter can thus be defined as the sum of the first-order index with indices of increasing order for interaction with all other input parameters as shown in 2.31. It therefore follows from 2.41 and 2.42 that the sum across all sensitivity indices for all input parameters must be 1, i.e.,

$$\sum_{i=1}^{k} S_i + \sum_{1 \le i < j \le k} S_{ij} + \dots + S_{1,2,\dots,k} = 1 \tag{2.43}$$

While a powerful tool for computing sensitivity indices of a function $f(x)$, the above formulations of variance and sensitivity index are difficult to apply directly to a set of output data of a statistical population for a set of input parameters. A discrete form of these equations for use in statistical analysis can be obtained using Monte-Carlo integration as shown in

Eqs. 2.44, 2.45, and 2.46 [3, 22]. These equations can be implemented easily into computer algorithms for sensitivity analysis with input parameter simulations generated using the Monte-Carlo method.

$$f_0 = \frac{1}{N}\sum_{k=1}^{N} f(x_k) \tag{2.44}$$

$$D = \frac{1}{N}\sum_{k=1}^{N} [f(x_k)^2 - f_0^2] \tag{2.45}$$

$$D_i = D - \frac{1}{2N}\sum_{k=1}^{N} [f(x_k) - f(x_{ik} - x'_{-ik})]^2 \tag{2.46}$$

$$D_i^{tot} = \frac{1}{2N}\sum_{k=1}^{N} [f(x_k) - f(x'_{ik}, x_{-ik})]^2 \tag{2.47}$$

Where

- D is the total variance
- D_i is the first-order effect variance
- D_i^{tot} is the total effect variance
- N is the sample size
- $x_{-i} = (x_1, \ldots, x_{i-1}, x_{i+1}, x_m)$ is a parameter space complementary to x_i.

Chapter 3

Initial Studies and Methods

3.1 Analysis Method

Statistical analysis in this work is completed using the Monte-Carlo method. Sample populations are generated using MATLAB's random number generator for probability distribution functions. The type of distribution is specified by the user and does not have to be a normal distribution. MATLAB's random number generator is a pseudorandom number generator, meaning that while it captures the statistical properties of a random sequence while the sequence is generated by a deterministic algorithm [13]. These numbers are then fed into the desired function for generating output values. Uncertainty analysis is completed to identify mean and standard deviation. Sensitivity analysis is then completed on the simulation output to assess impact of the input variation. This process is then repeated for a specified number of iterations to generate an average set of sensitivity indices. This generic process is shown in Fig. 3.1. This technique is applied for both the simple reference problems and laminate analysis.

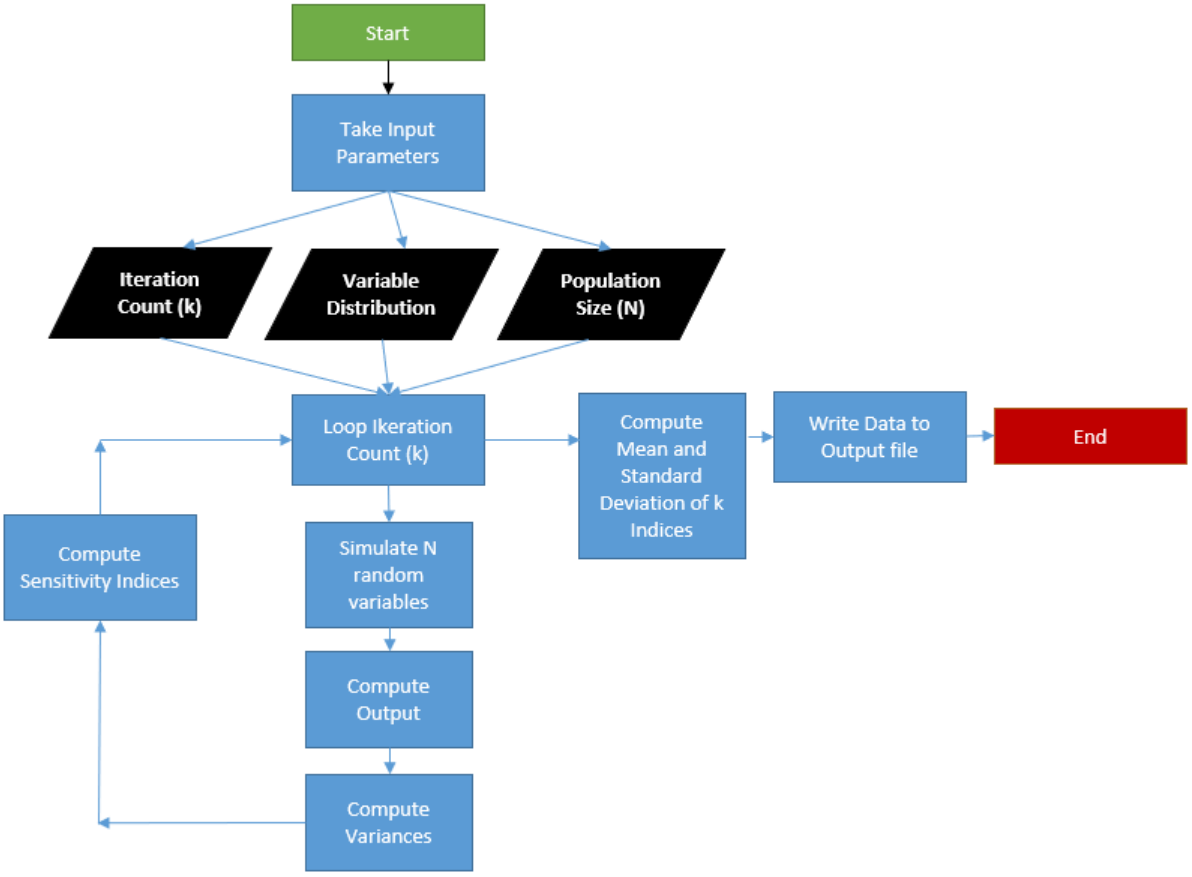

Figure 3.1: Code Structure Flowchart

3.2 Method Verification

To verify the accuracy of the analysis method chosen for this work, sensitivity indices computed using this code were compared to [10] for select problems. Model and probability distributions were used from the reference source. Analysis was completed to determine the mean value and variance of the sensitivity indices for each variable to compare to the reported values in the source text. To ensure convergence of the results, input variable population size was chosen to be 10,000 and 1000 iterations of Monte-Carlo analysis were performed to generate 1000 sets of sensitivity indices for each model. Sensitivity index values obtained

match well with values from the literature. Results for each study are summarized in their respective subsections.

3.2.1 Bivariate Polynomial

The first and simplest example used to test the code was a bivariate polynomial as defined below. Both variables are assumed to have a standard Gaussian distribution per [10].

$$y = x_1 + x_2 + x_2^2 + x_1 * x_2 + 3 \tag{3.1}$$

Sensitivity indices were computed for both input variables using both the local analysis of variance (LANOVA) and Sobol index methods. Monte-Carlo simulation was used to generate a simulated population of input parameters. A histogram of the output distribution for the chosen input probability density functions is shown in Fig. 3.2. The distribution is skewed right, which is expected as the polynomial is quadratic in x_2, with both variables normally distributed over the domain $0 \leq x_i \leq 1, i = 1, 2$.

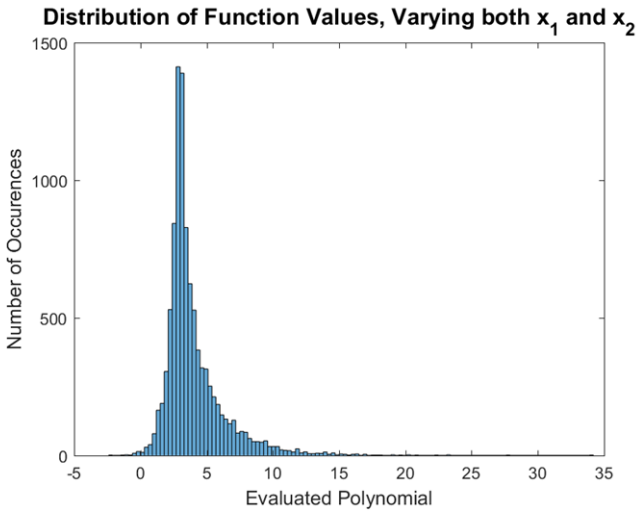

Figure 3.2: Bivariate Polynomial Output Distribution Varying both x_1 and x_2

Local Analysis of Variance: Bivariate Polynomial

LANOVA sensitivity indices are computed for the polynomial by fixing the opposite variable at its mean value. For a Gaussian distribution the mean value is zero. In effect, this means that the sensitivity index with respect to x_2 is computed by removing x_1 terms and vice versa. The sensitivity index for x_2 is greater than x_1, indicating a larger first-order impact on the output distribution. This larger impact is expected due to the variable x_2 possessing a higher maximum exponent than x_1. In addition, the two indices do not sum to one, indicating that the total variation in output cannot solely be explained by first-order effects, due to the interaction between x_1 and x_2. Indices are compared to reference values in Table 3.1. Computed indices compare well with reference values, within one tenth of the standard deviation of the computed sensitivity indices.

Table 3.1: Literature Polynomial LANOVA Sensitivity Index Comparison

Input Variable	Mean LANOVA Index	Std. Dev.	Reference Index [10]	Error in Std. Dev.
x_1	0.2255	0.0095	0.2250	0.05
x_2	0.5527	0.0077	0.5520	0.09

The distribution of the computed indices across the 1000 Monte-Carlo simulation iterations, each with a population size of 10000, are shown in Fig. 3.3 and Fig. 3.4. The distribution of computed indices resembles a normal distribution. A χ^2 goodness of fit test was completed in MATLAB and did not reject the null hypothesis at the 5% significance level that the output distribution matched a normal distribution.

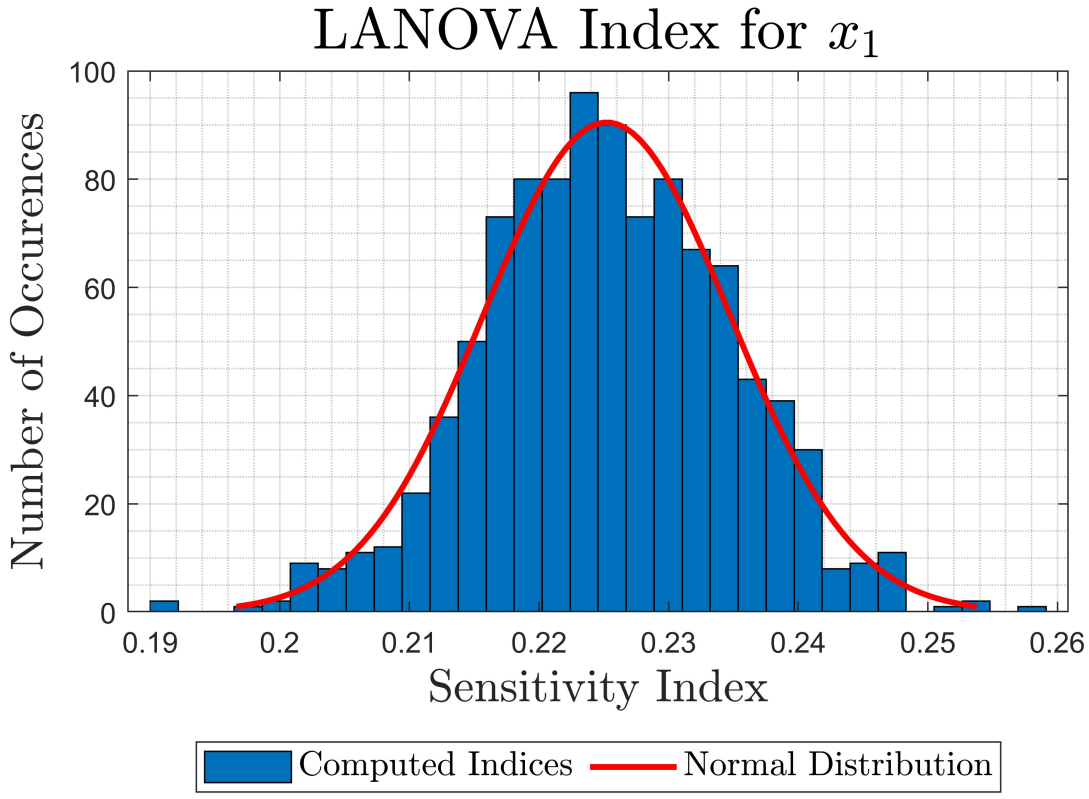

Figure 3.3: Distribution of computed LANOVA indices for x_1

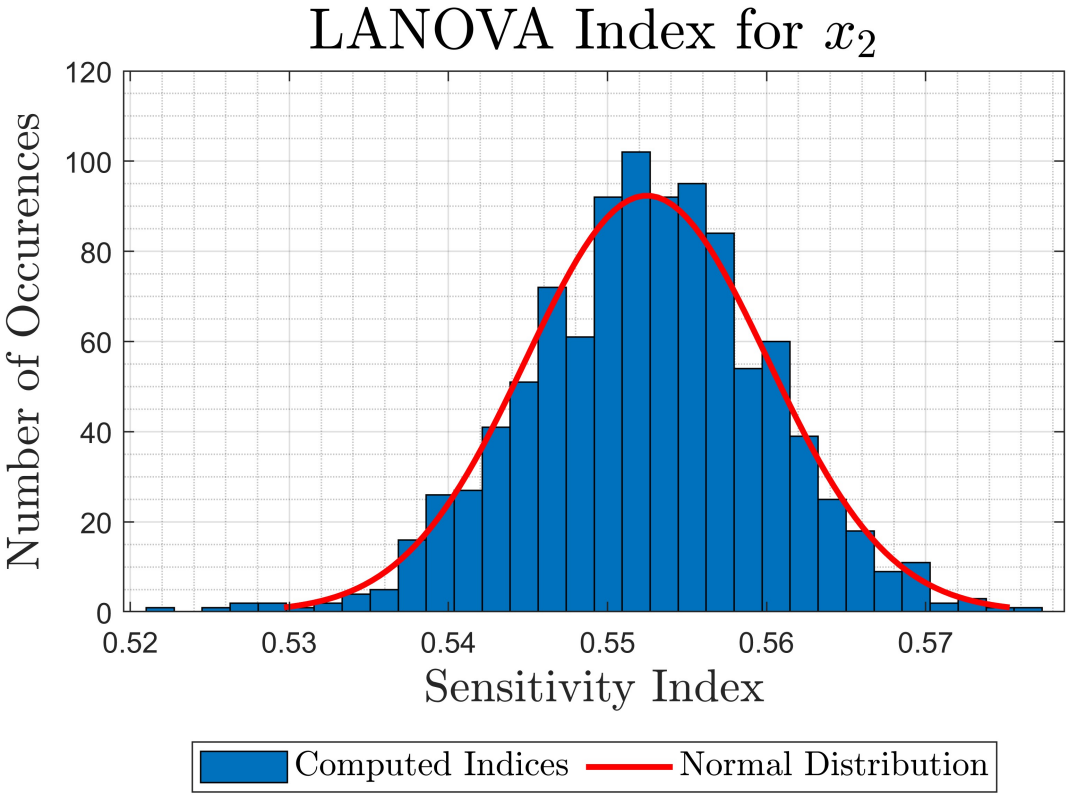

Figure 3.4: Distribution of computed LANOVA indices for x_2

Sobol's Method: Bivariate Polynomial

In addition to LANOVA, Sobol's method was applied to obtain sensitivity indices for the bivariate polynomial problem. Average indices computed from the 1000 Monte-Carlo iterations are shown compared to reference values in Table 3.2. Computed indices compare well with reference values, within one tenth of the standard deviation of the computed sensitivity indices. In addition, the two indices do not sum to one, indicating that the total variation in output cannot solely be explained by first-order effects, due to the interaction between x_1 and x_2.

Table 3.2: Literature Polynomial LANOVA Sensitivity Index Comparison

Input Variable	Mean FOSI	Std. Dev.	Reference Index [10]	Error (Std. Dev.)
x_1	0.1998	0.022	0.2000	-0.01
x_2	0.6001	0.013	0.6000	0.01

The distribution of the computed indices across the 1000 Monte-Carlo simulation iterations, each with a population size of 10000, are shown in Fig. 3.5 and Fig. 3.6. The distribution of computed indices resembles a normal distribution. A χ^2 goodness of fit test was completed in MATLAB and did not reject the null hypothesis at the 5% significance level that the output distribution matched a normal distribution.

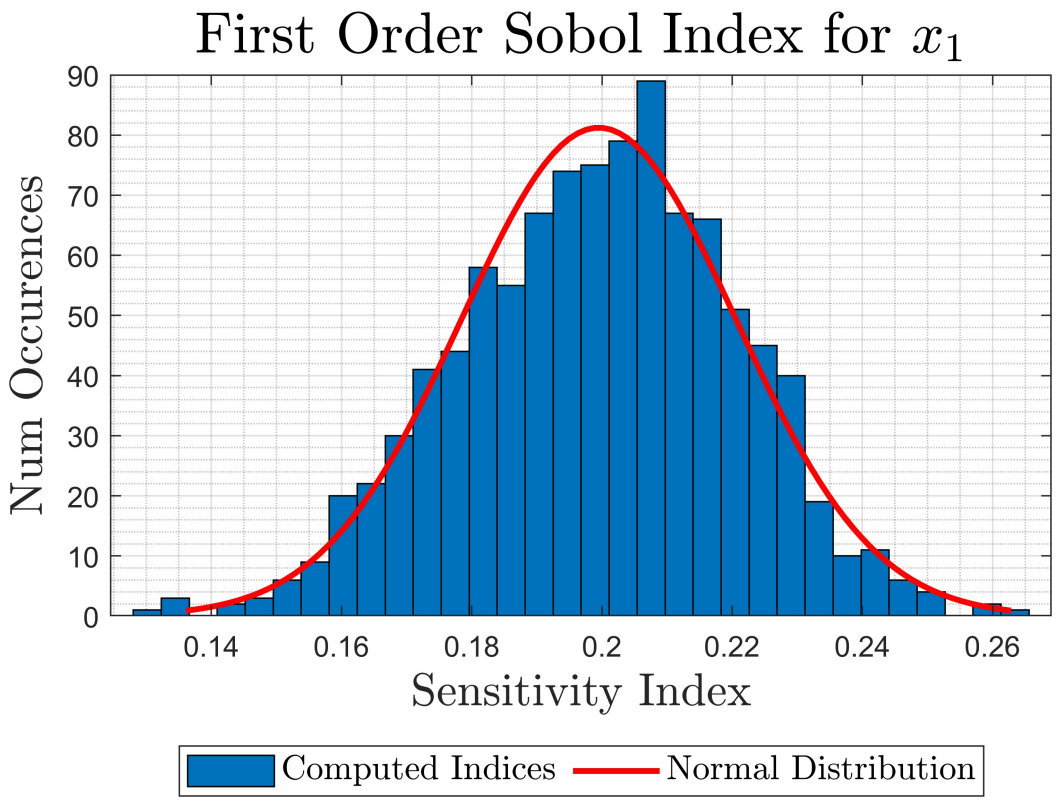

Figure 3.5: Distribution of computed Sobol indices for x_1

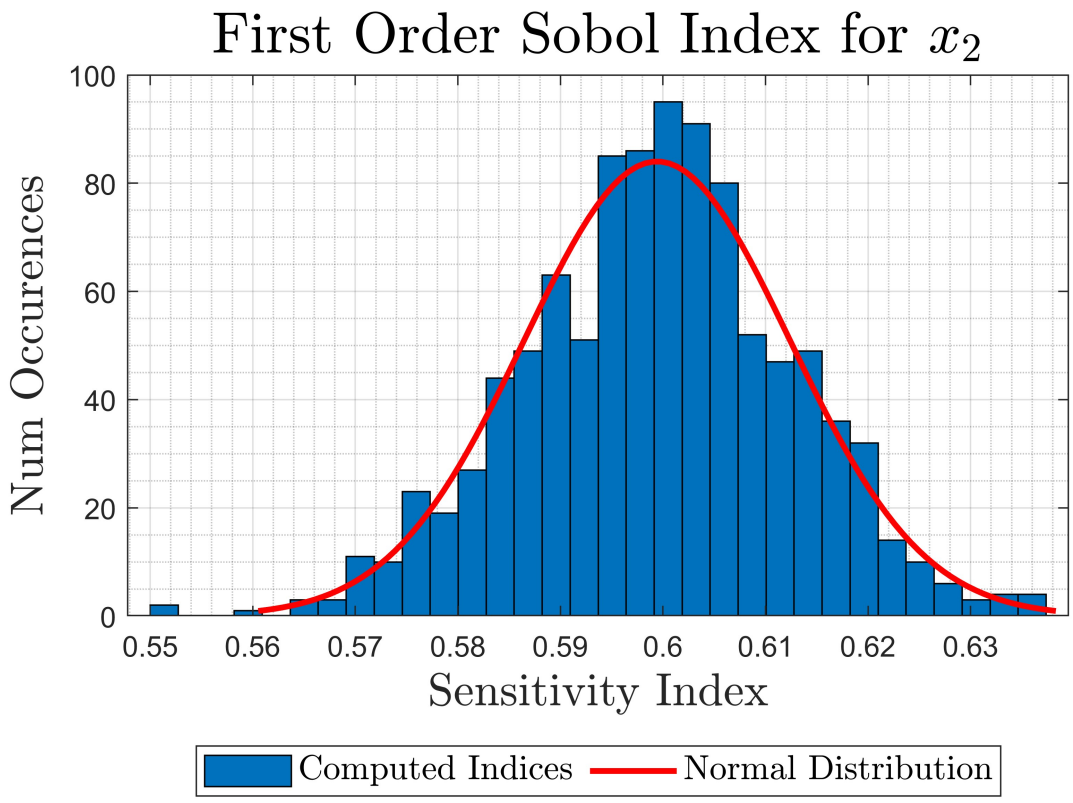

Figure 3.6: Distribution of computed Sobol indices for x_2

3.2.2 Beam Deflection

A simply supported beam uniform rectangular beam with uniform loading, as shown in Fig. 3.7, was also studied to introduce additional input variables and more complex probability functions. The function for midspan displacement is shown in 3.2. Output was chosen to be the midspan deflection of the beam, as described below. Input variables of beam length, height, thickness, Young's modulus, and distributed load intensity were all chosen to have a log-normal probability distribution. Mean and standard deviation of the input variables is shown in Table 3.3.

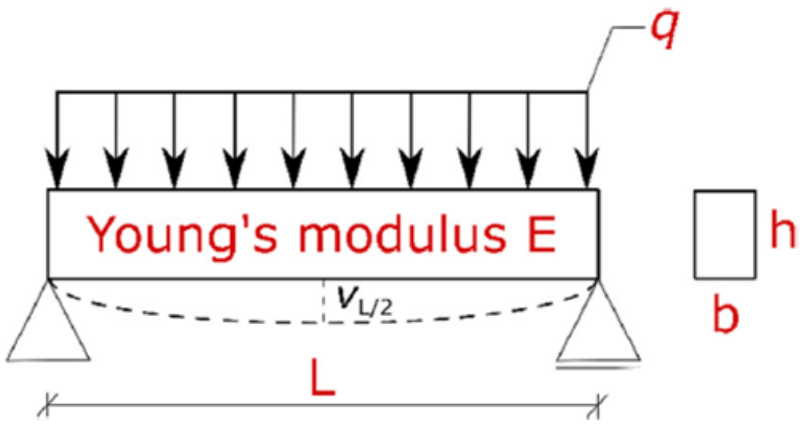

Figure 3.7: Simply Supported Rectangular Beam with Uniform Load [10]

$$v_{L/2} = \frac{5}{32}\frac{qL^4}{EbH^3} \tag{3.2}$$

Table 3.3: Beam Problem Input Variable Statistical Properties [10]

Input Variable	μ	σ	Units
b	0.15	0.0075	m
H	0.30	0.015	m
E	20	4.5	GPa
q	10	2	kN/m
L	5	0.05	m

For a lognormal distribution the expected value $E(X)$ is defined by Eq. 3.3.

$$E(X) = e^{\mu + \frac{\sigma^2}{2}} \tag{3.3}$$

Sensitivity indices were computed for both input variables using both LANOVA and Sobol's method. Monte-Carlo simulation was used to generate a simulated population of input parameters. A histogram of the output distribution of for the chosen input probability density functions is shown in Fig. 3.8.

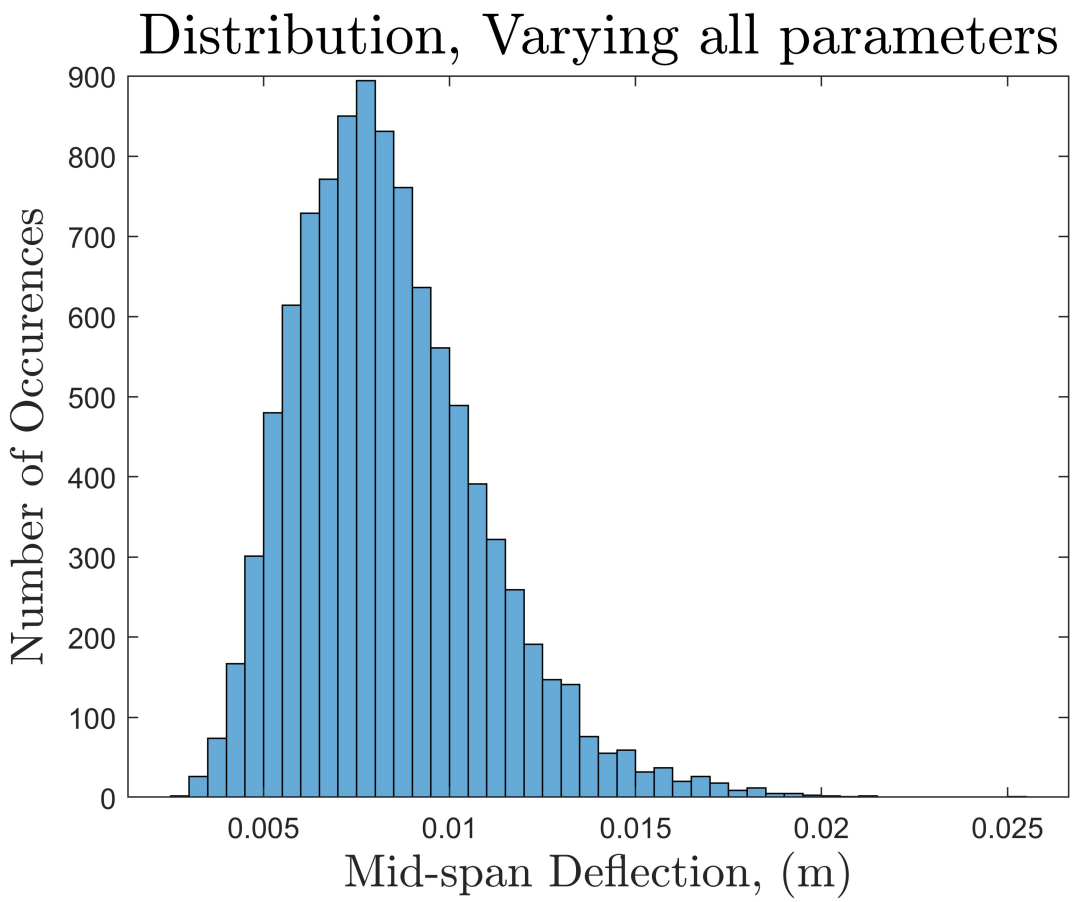

Figure 3.8: Beam Deflection Output Distribution

Local Analysis of Variance: Beam Deflection

LANOVA sensitivity indices are computed for any given input variable for the beam problem by fixing the remaining variables at its mean value.

Sensitivity indices are compared with reference values given in [10] in Table 3.4. Computed indices compare well with reference values, though not within one standard deviation. Reference values were computed using a neural network ensemble, while values presented in this working were computed using direct Monte-Carlo simulation. Ranking of indices compares well with reference values. Both models are in agreement on relative importance of each input variable.

Table 3.4: Literature Beam LANOVA Sensitivity Index Comparison

Input Variable	Mean LANOVA Index	Std. Dev.	Reference Index [10]	Error (Std. Dev.)
b	0.0175	0.0023	0.019	-0.65
H	0.1547	0.0057	0.163	-1.46
E	0.1594	0.0058	0.177	-3.03
q	0.268	0.0061	0.259	1.48
L	0.0101	0.0018	0.002	4.50

The distribution of the computed indices across the 1000 Monte-Carlo simulation iterations, each with a population size of 10000, are shown in Fig. 3.9 through Fig. 3.13. The distribution of computed indices resembles a normal distribution. A χ^2 goodness of fit test was completed in MATLAB and did not reject the null hypothesis at the 5% significance level that the output distribution matched a normal distribution.

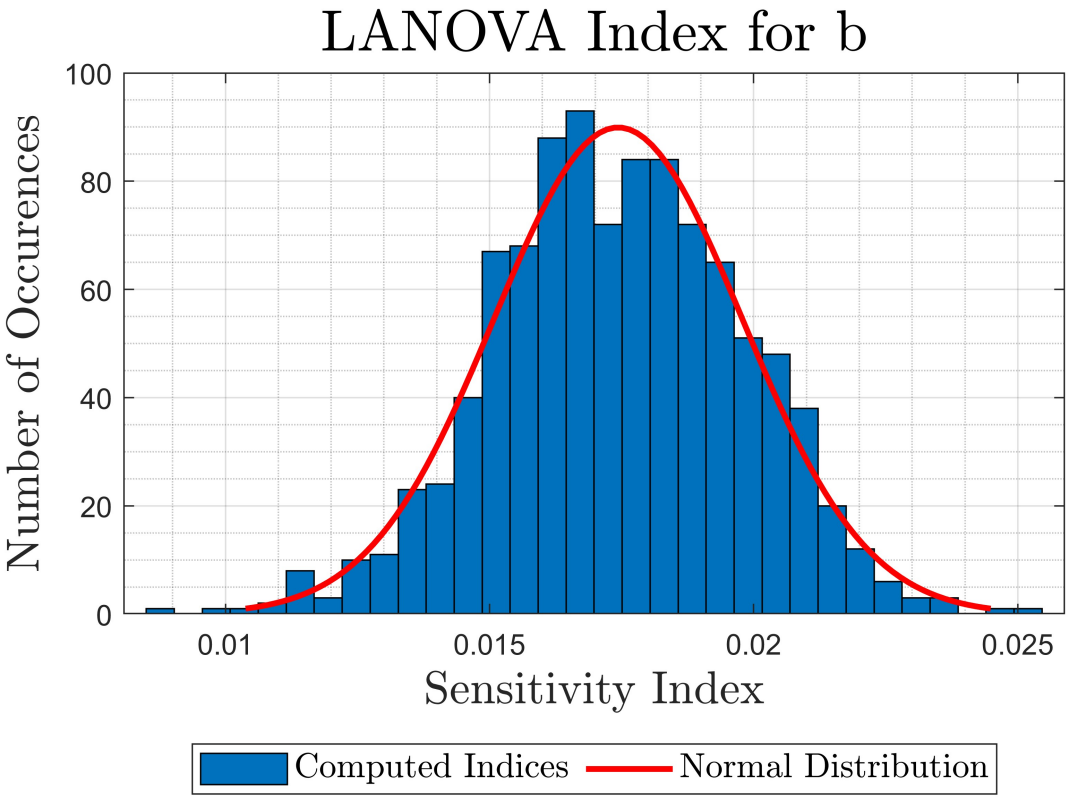

Figure 3.9: Distribution of computed sensitivity indices for b

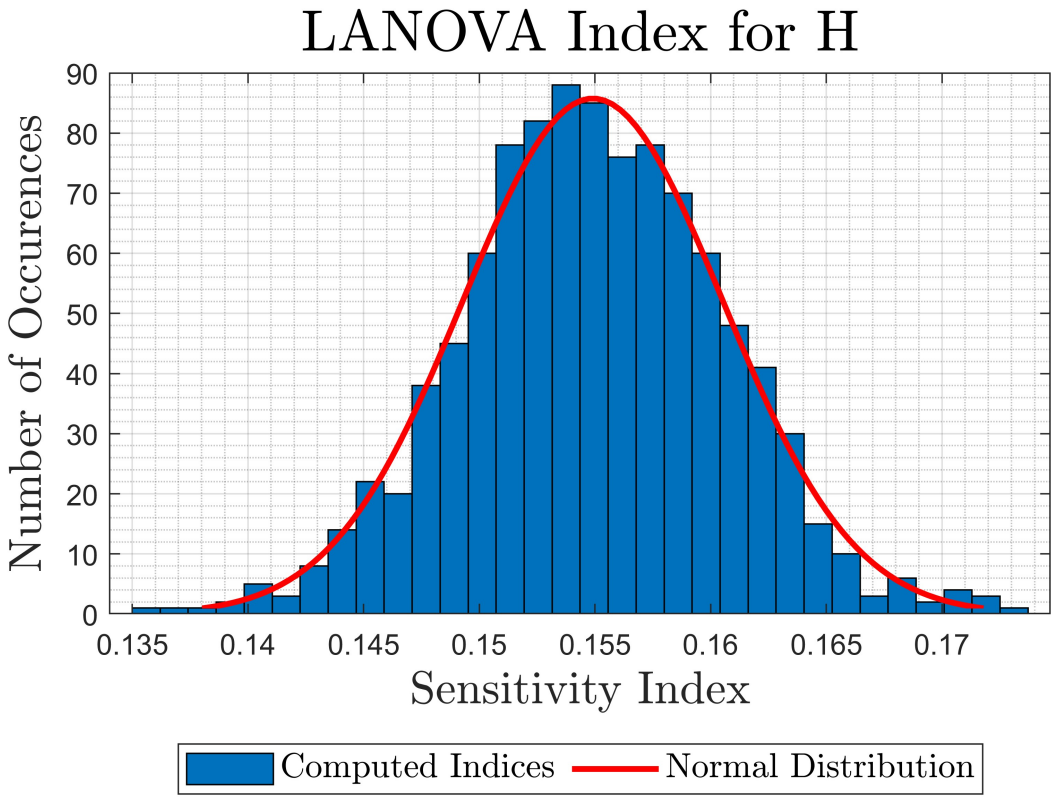

Figure 3.10: Distribution of computed sensitivity indices for H

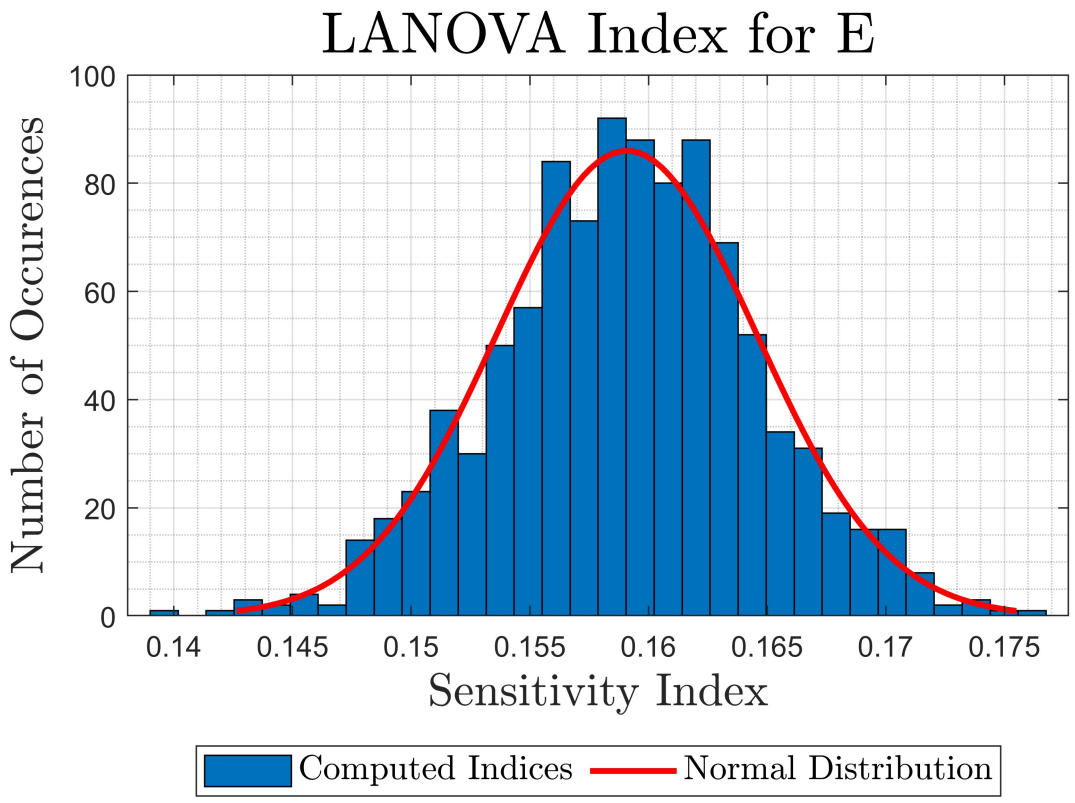

Figure 3.11: Distribution of computed sensitivity indices for E

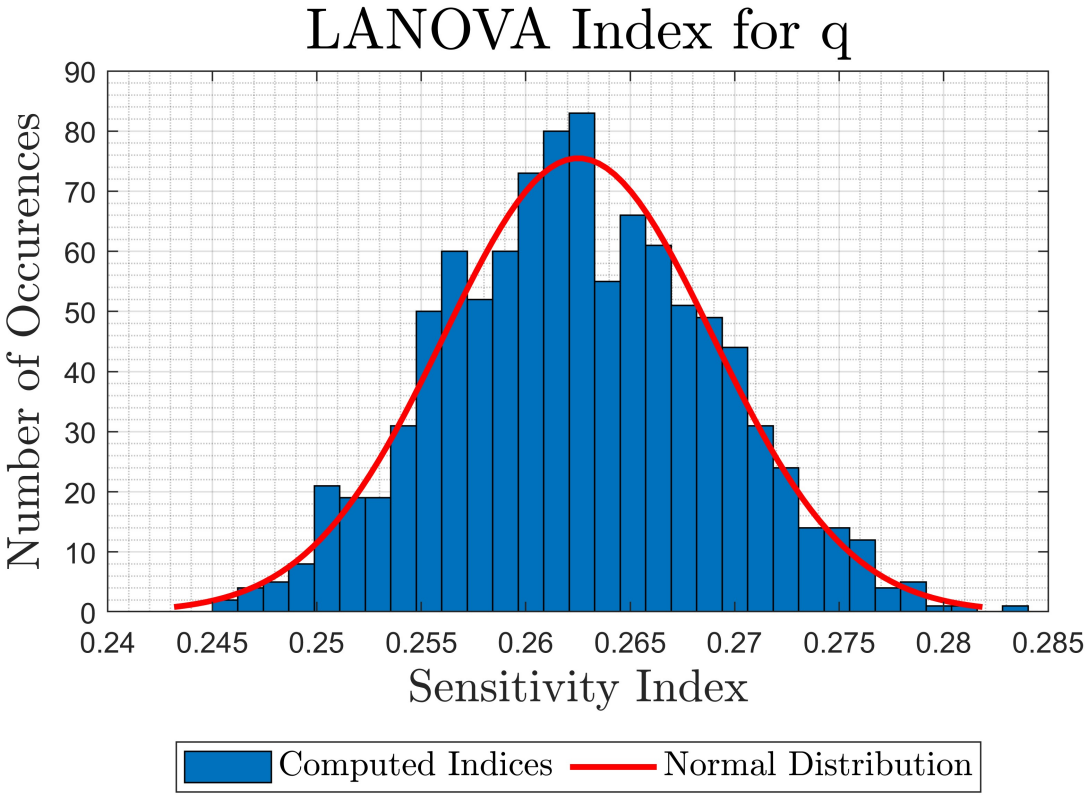

Figure 3.12: Distribution of computed LANOVA indices for q

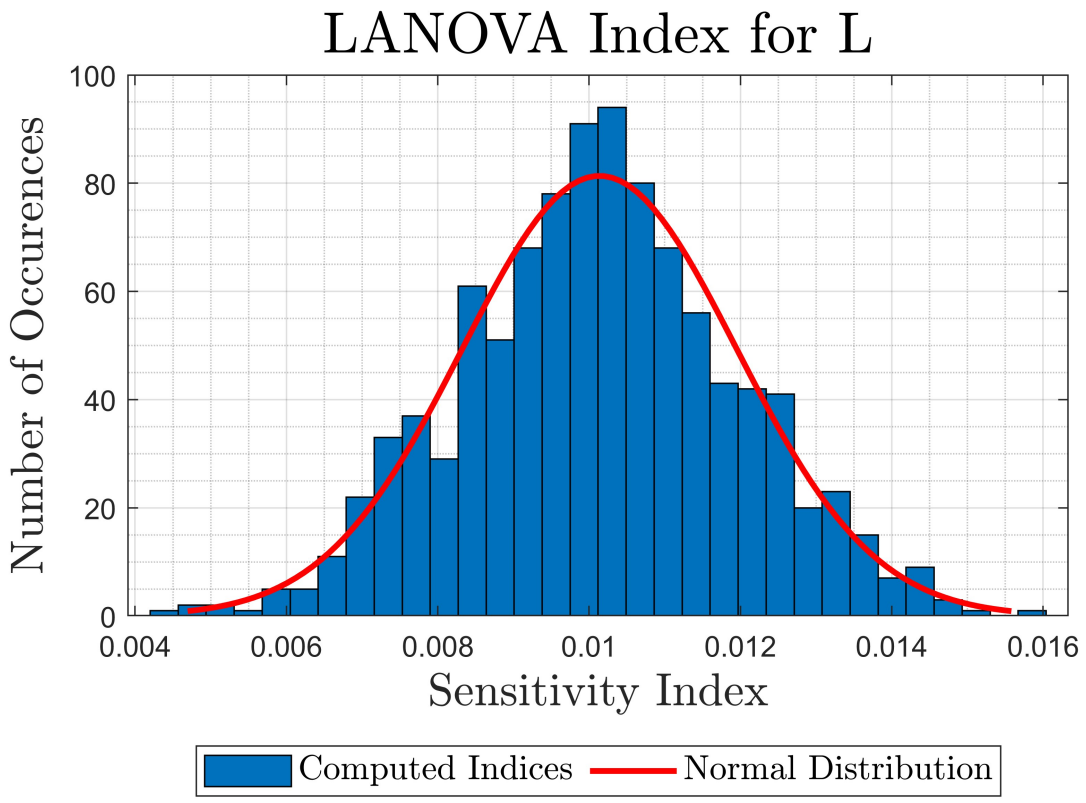

Figure 3.13: Distribution of computed LANOVA indices for L

Sobol's Method: Bivariate Polynomial

In addition to LANOVA, Sobol's method was applied to obtain sensitivity indices for the beam problem. Average indices computed from the 1000 Monte-Carlo iterations are shown compared to reference values in Table 3.5. Similar to as stated in the prior section, the agreement in ranking of input variables is more important than the numerical similarity of the computed sensitivity indices. In addition, the sum of all indices is approximately 0.97, indicating the majority of variation in this model can be explained by first-order effects.

Table 3.5: Literature Beam Sobol's Sensitivity Index Comparison

Input Variable	Mean FOSI	Std. Dev.	Reference Index [10]	Error in Std. Dev.
b	0.0273	0.0165	0.030	-0.16
H	0.2466	0.0136	0.240	0.49
E	0.2440	0.0144	0.250	-0.42
q	0.4344	0.0108	0.420	1.33
L	0.0172	0.0165	0.02	-0.17

The distribution of the computed indices across the 1000 Monte-Carlo simulation iterations, each with a population size of 10000, are shown in Fig. 3.14 and Fig. 3.18. The distribution of computed indices resembles a normal distribution. A χ^2 goodness of fit test was completed in MATLAB and did not reject the null hypothesis at the 5% significance level that the output distribution matched a normal distribution.

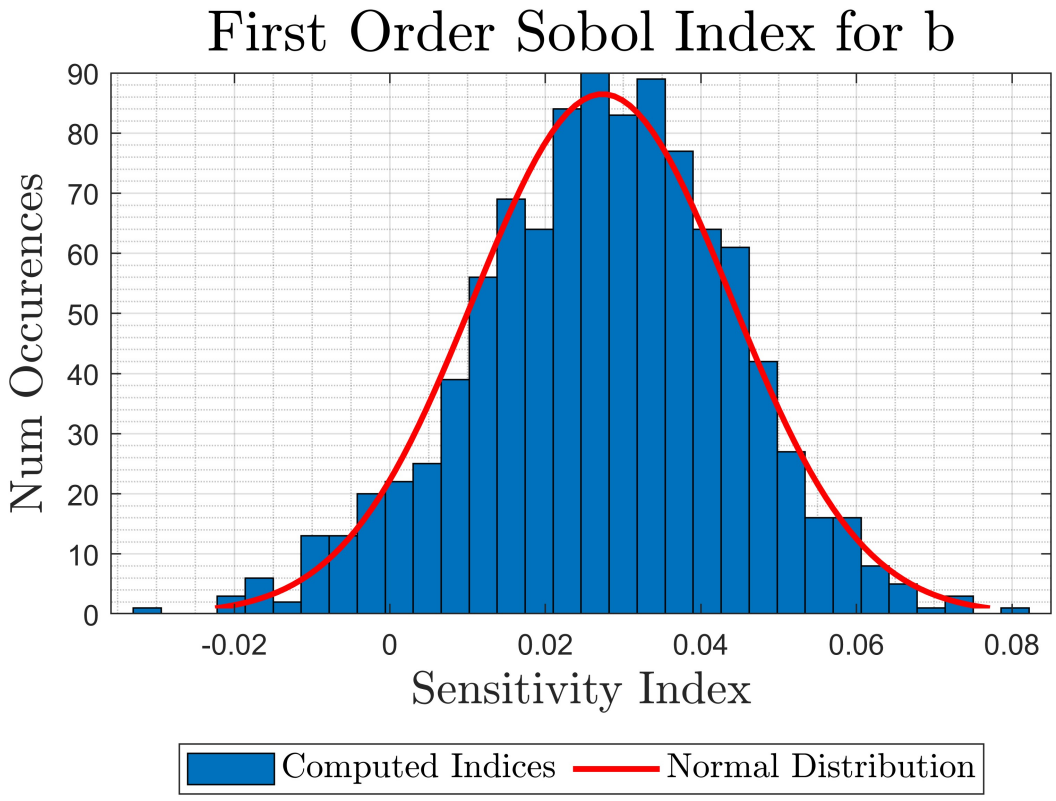

Figure 3.14: Distribution of computed Sobol indices for b

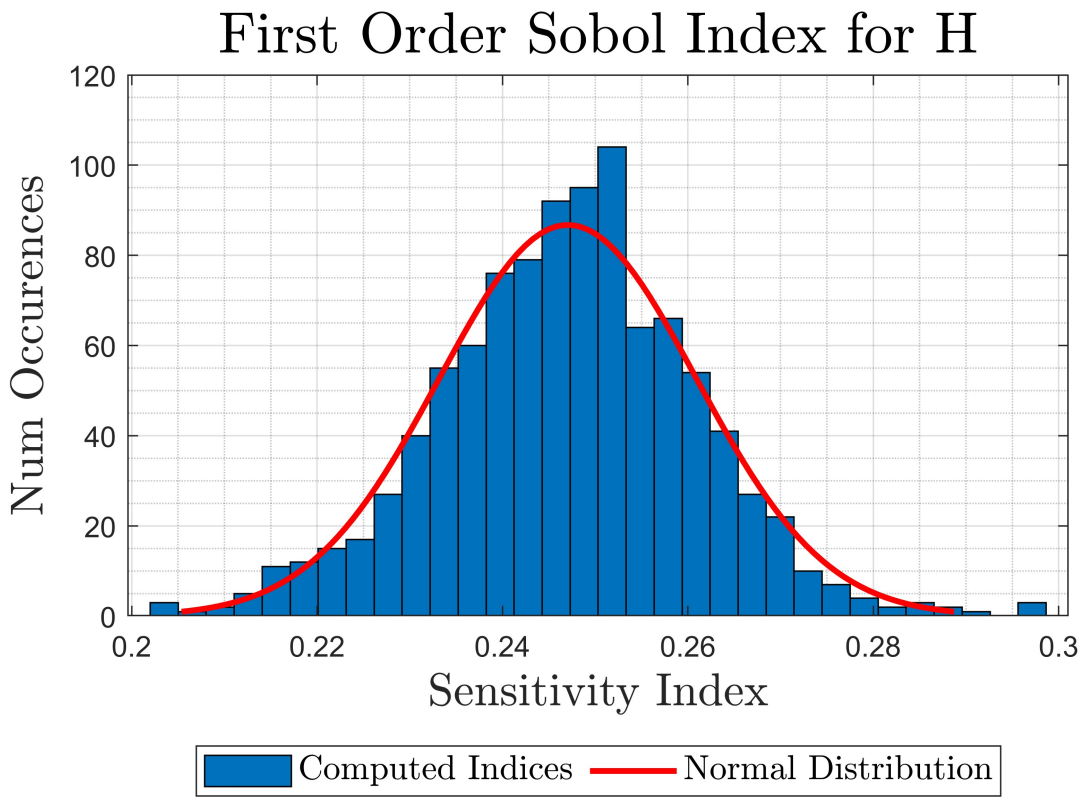

Figure 3.15: Distribution of computed Sobol for H

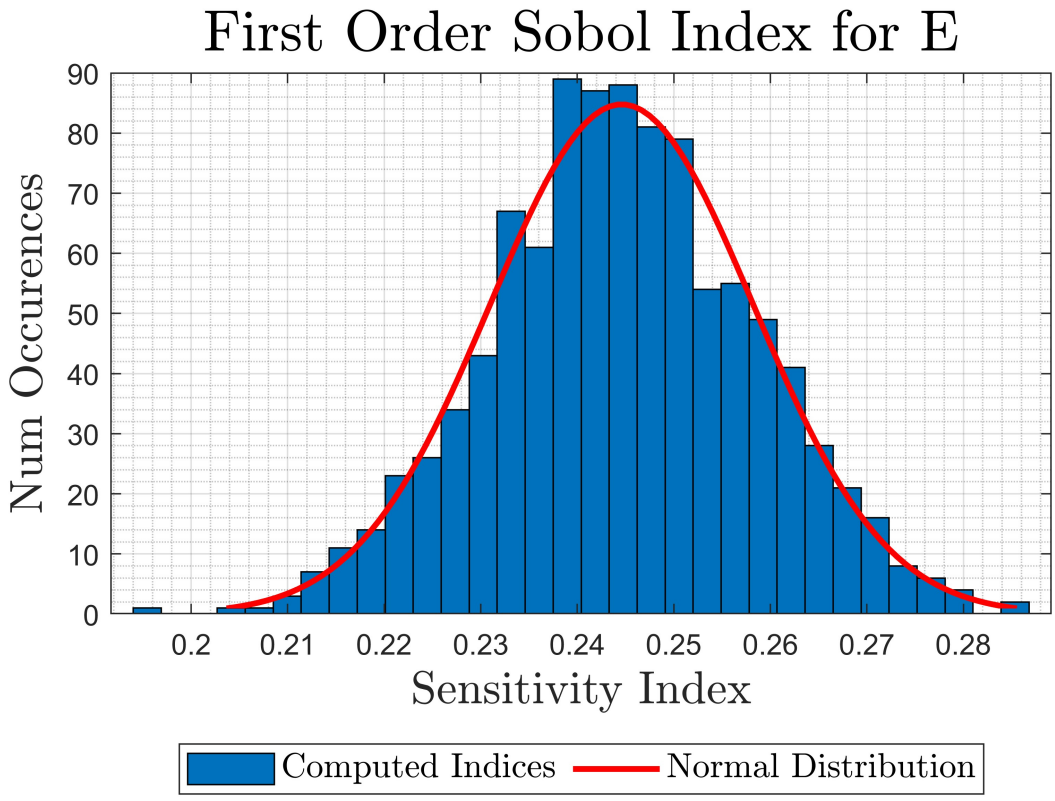

Figure 3.16: Distribution of computed Sobol indices for E

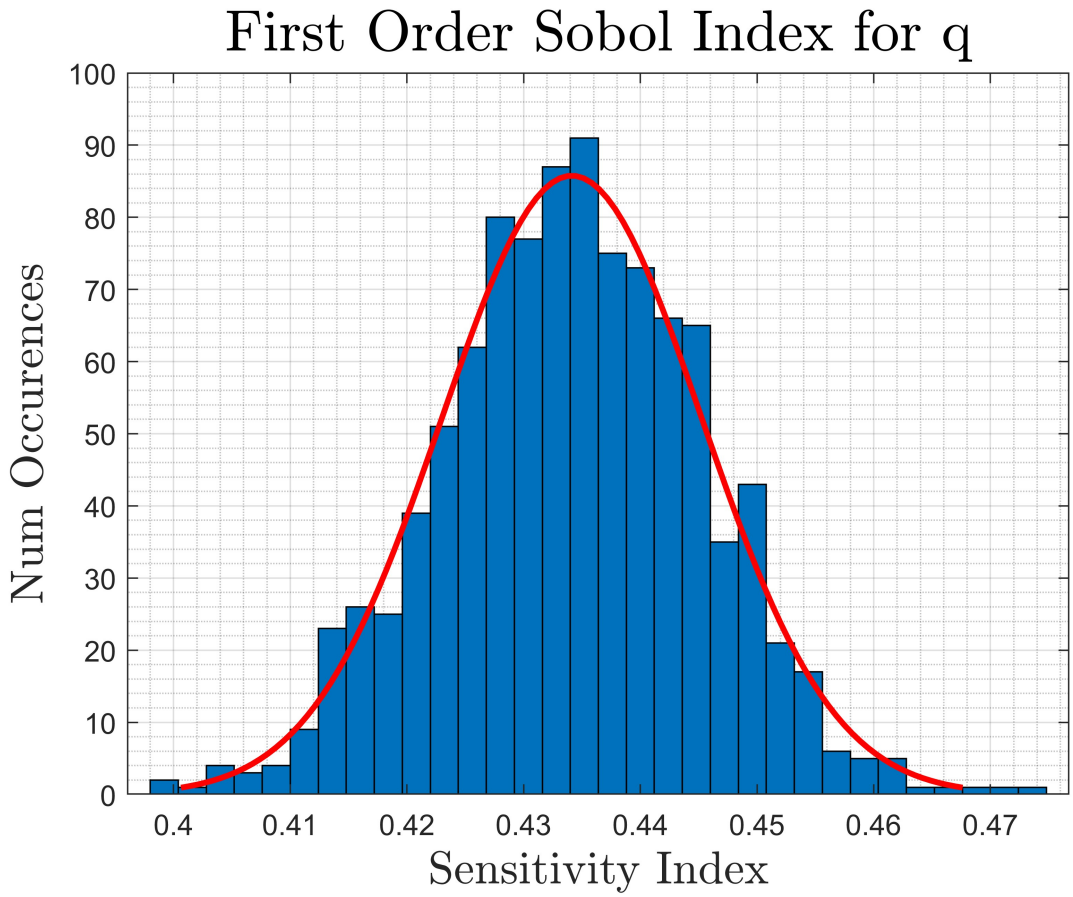

Figure 3.17: Distribution of computed Sobol indices for q

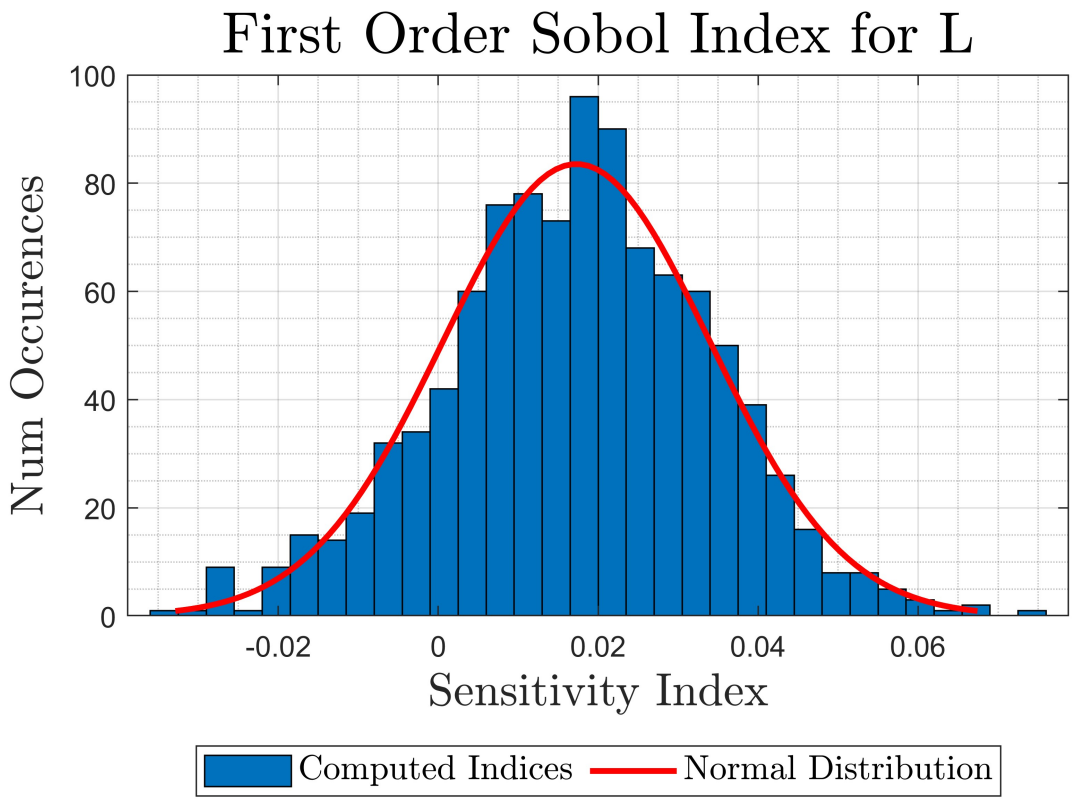

Figure 3.18: Distribution of computed Sobol indices for L

3.2.3 Conclusions

The method presented in this work adequately matches the conclusions obtained from the sensitivity analysis of the reference problems presented in literature. The method presented in this work is therefore considered verified.

3.3 Convergence Studies

Monte-Carlo simulations and sensitivity index computations rely on the ability of the simulation to accurately represent the distributions of the input variables. For method verification, the input variable population size value of 10,000 and iteration count of 1000 ensured accurate prediction of sensitivity index values To identify the minimum size of population and number of iterations allowable in the simulation a convergence study was performed. The following were considered for inputs for the simulation: iterations ranging from 1 to 1,000, and sample numbers ranging from 10 to 10,000. A heatmap of these inputs can be seen in a tabular form in Table 3.6, where red represents a lower total number of simulations and green indicates a higher total number of simulations. The left most column shows the population size per simulation and the upper most row shows the number of simulations performed. The remainder of the table is the product of these headers, indicating the total simulated count. Sensitivity indexes obtained were analyzed with the target of $< 2\%$ change from their neighboring indices. Values highlighted green in Table 3.7 through Table 3.20 indicates this target was achieved. For the polynomial problem, this target was typically achieved within a Monte-Carlo population size of 1,000 and Monte-Carlo iteration count of 1000. On occasion, islands of combinations that do not meet this target are observed within the range of satisfying parameters, which are ignored. For select input parameters in the beam problem, specifically b and L however, these targets are not achieved. The sensitivity

indices for these parameters are an order of magnitude smaller than those for E, q, and H. Therefore it is unsurprising that a 2% change target was not as easily achieved. The successful achievement of this target for the 3 parameters E, q, and H is taken to represent a successful achievement of the <2% change target for the beam problem. Based on this study, a simulation count of 1,000 and population size of 1,000 laminates were selected for laminate sensitivity analysis. This selection balances the convergence objective with computing limitations for large laminates.

Table 3.6: Convergence Study Input Parameters

Simulation Population Size \ Number of Monte Carlo Simulations	1	2	3	4	5	10	20	30	40	50	100	200	300	400	500	1000
10	1.E+01	2.E+01	3.E+01	4.E+01	5.E+01	1.E+02	2.E+02	3.E+02	4.E+02	5.E+02	1.E+03	2.E+03	3.E+03	4.E+03	5.E+03	1.E+04
20	2.E+01	4.E+01	6.E+01	8.E+01	1.E+02	2.E+02	4.E+02	6.E+02	8.E+02	1.E+03	2.E+03	4.E+03	6.E+03	8.E+03	1.E+04	2.E+04
30	3.E+01	6.E+01	9.E+01	1.E+02	2.E+02	3.E+02	6.E+02	9.E+02	1.E+03	2.E+03	3.E+03	6.E+03	9.E+03	1.E+04	2.E+04	3.E+04
40	4.E+01	8.E+01	1.E+02	2.E+02	2.E+02	4.E+02	8.E+02	1.E+03	2.E+03	2.E+03	4.E+03	8.E+03	1.E+04	2.E+04	2.E+04	4.E+04
50	5.E+01	1.E+02	2.E+02	2.E+02	3.E+02	5.E+02	1.E+03	2.E+03	2.E+03	3.E+03	5.E+03	1.E+04	2.E+04	2.E+04	3.E+04	5.E+04
100	1.E+02	2.E+02	3.E+02	4.E+02	5.E+02	1.E+03	2.E+03	3.E+03	4.E+03	5.E+03	1.E+04	2.E+04	3.E+04	4.E+04	5.E+04	1.E+05
200	2.E+02	4.E+02	6.E+02	8.E+02	1.E+03	2.E+03	4.E+03	6.E+03	8.E+03	1.E+04	2.E+04	4.E+04	6.E+04	8.E+04	1.E+05	2.E+05
300	3.E+02	6.E+02	9.E+02	1.E+03	2.E+03	3.E+03	6.E+03	9.E+03	1.E+04	2.E+04	3.E+04	6.E+04	9.E+04	1.E+05	2.E+05	3.E+05
400	4.E+02	8.E+02	1.E+03	2.E+03	2.E+03	4.E+03	8.E+03	1.E+04	2.E+04	2.E+04	4.E+04	8.E+04	1.E+05	2.E+05	2.E+05	4.E+05
500	5.E+02	1.E+03	2.E+03	2.E+03	3.E+03	5.E+03	1.E+04	2.E+04	2.E+04	3.E+04	5.E+04	1.E+05	2.E+05	2.E+05	3.E+05	5.E+05
1000	1.E+03	2.E+03	3.E+03	4.E+03	5.E+03	1.E+04	2.E+04	3.E+04	4.E+04	5.E+04	1.E+05	2.E+05	3.E+05	4.E+05	5.E+05	1.E+06
2000	2.E+03	4.E+03	6.E+03	8.E+03	1.E+04	2.E+04	4.E+04	6.E+04	8.E+04	1.E+05	2.E+05	4.E+05	6.E+05	8.E+05	1.E+06	2.E+06
3000	3.E+03	6.E+03	9.E+03	1.E+04	2.E+04	3.E+04	6.E+04	9.E+04	1.E+05	2.E+05	3.E+05	6.E+05	9.E+05	1.E+06	2.E+06	3.E+06
4000	4.E+03	8.E+03	1.E+04	2.E+04	2.E+04	4.E+04	8.E+04	1.E+05	2.E+05	2.E+05	4.E+05	8.E+05	1.E+06	2.E+06	2.E+06	4.E+06
5000	5.E+03	1.E+04	2.E+04	2.E+04	3.E+04	5.E+04	1.E+05	2.E+05	2.E+05	3.E+05	5.E+05	1.E+06	2.E+06	2.E+06	3.E+06	5.E+06
10000	1.E+04	2.E+04	3.E+04	4.E+04	5.E+04	1.E+05	2.E+05	3.E+05	4.E+05	5.E+05	1.E+06	2.E+06	3.E+06	4.E+06	5.E+06	1.E+07

Table 3.7: Polynomial Problem Parameter x_1 LANOVA Index Convergence

Simulation Population Size \ Number of Monte Carlo Simulations	1	2	3	4	5	10	20	30	40	50	100	200	300	400	500	1000
10	-0.537	0.311	0.643	0.190	0.316	0.329	0.282	0.090	0.246	0.217	0.216	0.211	0.199	0.220	0.206	0.222
20	0.075	0.478	0.183	0.246	0.138	0.229	0.268	0.279	0.225	0.243	0.229	0.224	0.202	0.229	0.216	0.226
30	-0.034	0.369	0.125	-0.012	0.248	0.228	0.256	0.216	0.263	0.200	0.212	0.242	0.217	0.222	0.225	0.216
40	0.399	0.307	0.379	0.158	0.221	0.187	0.283	0.221	0.209	0.212	0.226	0.240	0.233	0.228	0.225	0.220
50	0.296	0.213	0.309	0.310	0.272	0.265	0.252	0.215	0.197	0.216	0.214	0.239	0.244	0.232	0.216	0.229
100	0.116	0.171	0.247	0.179	0.220	0.183	0.203	0.228	0.215	0.232	0.232	0.215	0.230	0.226	0.223	0.228
200	0.123	0.201	0.172	0.228	0.255	0.219	0.243	0.216	0.228	0.233	0.240	0.219	0.221	0.221	0.222	0.222
300	0.204	0.211	0.190	0.179	0.216	0.178	0.216	0.221	0.230	0.232	0.224	0.220	0.221	0.230	0.220	0.223
400	0.281	0.178	0.211	0.154	0.208	0.220	0.221	0.209	0.222	0.221	0.230	0.231	0.223	0.223	0.224	0.228
500	0.200	0.204	0.198	0.223	0.253	0.221	0.206	0.210	0.231	0.216	0.222	0.220	0.227	0.221	0.224	0.226
1000	0.202	0.191	0.218	0.209	0.241	0.219	0.227	0.217	0.231	0.227	0.225	0.224	0.226	0.225	0.227	0.227
2000	0.223	0.208	0.211	0.217	0.228	0.225	0.232	0.230	0.231	0.228	0.227	0.225	0.224	0.224	0.225	0.225
3000	0.199	0.231	0.232	0.221	0.218	0.222	0.227	0.224	0.221	0.233	0.221	0.224	0.226	0.227	0.223	0.226
4000	0.155	0.231	0.227	0.216	0.215	0.209	0.221	0.223	0.225	0.228	0.223	0.225	0.225	0.226	0.225	0.226
5000	0.195	0.226	0.217	0.224	0.222	0.221	0.225	0.225	0.224	0.224	0.225	0.225	0.226	0.226	0.225	0.225
10000	0.200	0.220	0.210	0.223	0.219	0.217	0.226	0.226	0.225	0.228	0.225	0.225	0.225	0.225	0.225	0.226

Table 3.8: Polynomial Problem Parameter x_2 LANOVA Index Convergence

Simulation Population Size \ Number of Monte Carlo Simulations	1	2	3	4	5	10	20	30	40	50	100	200	300	400	500	1000
10	0.178	0.375	0.373	0.522	0.368	0.557	0.510	0.468	0.562	0.553	0.524	0.553	0.551	0.554	0.564	0.552
20	0.589	0.390	0.574	0.562	0.584	0.596	0.605	0.554	0.535	0.569	0.561	0.560	0.554	0.546	0.544	0.556
30	0.288	0.666	0.486	0.439	0.609	0.441	0.542	0.533	0.581	0.522	0.526	0.559	0.552	0.555	0.554	0.548
40	0.233	0.528	0.487	0.475	0.495	0.505	0.555	0.516	0.542	0.537	0.554	0.546	0.550	0.557	0.555	0.547
50	0.376	0.450	0.556	0.536	0.558	0.511	0.572	0.537	0.538	0.573	0.551	0.557	0.547	0.550	0.547	0.551
100	0.246	0.380	0.528	0.525	0.466	0.512	0.526	0.523	0.537	0.560	0.556	0.542	0.551	0.555	0.554	0.555
200	0.251	0.444	0.514	0.569	0.512	0.549	0.552	0.541	0.549	0.541	0.552	0.552	0.553	0.555	0.553	0.552
300	0.385	0.420	0.535	0.517	0.537	0.535	0.539	0.553	0.553	0.538	0.544	0.548	0.553	0.553	0.552	0.551
400	0.439	0.437	0.521	0.494	0.515	0.538	0.546	0.539	0.542	0.542	0.551	0.555	0.553	0.555	0.551	0.551
500	0.442	0.485	0.513	0.503	0.502	0.531	0.542	0.541	0.556	0.552	0.552	0.549	0.554	0.553	0.549	0.552
1000	0.403	0.483	0.503	0.520	0.509	0.540	0.546	0.554	0.557	0.555	0.552	0.553	0.553	0.552	0.555	0.552
2000	0.430	0.490	0.517	0.502	0.514	0.545	0.546	0.549	0.552	0.552	0.551	0.554	0.552	0.553	0.551	0.552
3000	0.445	0.479	0.499	0.517	0.525	0.535	0.541	0.546	0.544	0.549	0.550	0.552	0.552	0.552	0.552	0.552
4000	0.406	0.484	0.513	0.515	0.525	0.539	0.541	0.545	0.549	0.548	0.552	0.553	0.552	0.552	0.553	0.553
5000	0.407	0.486	0.509	0.514	0.518	0.540	0.545	0.549	0.550	0.551	0.550	0.551	0.551	0.553	0.552	0.553
10000	0.433	0.472	0.500	0.518	0.524	0.537	0.543	0.548	0.549	0.551	0.550	0.551	0.552	0.552	0.552	0.553

Table 3.9: Polynomial Problem Parameter x_1 Sobol Index Convergence

Simulation Population Size \ Number of Monte Carlo Simulations	1	2	3	4	5	10	20	30	40	50	100	200	300	400	500	1000
10	-2.89	-0.05	0.38	0.41	-0.03	0.09	0.11	0.09	0.29	0.22	0.20	0.08	0.16	0.20	0.19	0.22
20	0.52	-0.79	-0.17	0.25	0.12	0.22	0.20	0.30	0.16	0.19	0.17	0.22	0.21	0.20	0.22	0.20
30	-1.56	0.08	-0.05	0.03	0.16	0.09	0.21	0.27	0.24	0.13	0.10	0.21	0.19	0.19	0.19	0.20
40	-0.49	-0.63	0.23	-0.14	0.20	0.13	0.27	0.05	0.18	0.14	0.18	0.18	0.21	0.20	0.19	0.19
50	-0.93	-0.25	0.12	0.13	0.23	0.03	0.11	0.16	0.18	0.23	0.20	0.19	0.20	0.20	0.19	0.20
100	-1.00	-0.09	-0.07	0.04	-0.54	0.13	0.11	0.09	0.15	0.26	0.21	0.17	0.22	0.18	0.20	0.19
200	-0.62	-0.03	-0.06	0.13	0.08	0.17	0.20	0.17	0.19	0.15	0.20	0.19	0.19	0.20	0.20	0.20
300	-0.68	-0.06	0.07	0.02	0.08	0.11	0.17	0.21	0.16	0.18	0.18	0.18	0.20	0.20	0.20	0.20
400	-0.43	-0.28	0.09	-0.06	0.03	0.18	0.16	0.15	0.14	0.15	0.21	0.19	0.20	0.20	0.20	0.20
500	-0.42	-0.01	-0.03	0.06	0.03	0.14	0.16	0.17	0.21	0.19	0.18	0.19	0.21	0.20	0.19	0.20
1000	-0.48	0.02	0.02	0.12	0.07	0.19	0.17	0.19	0.22	0.21	0.18	0.20	0.20	0.20	0.20	0.20
2000	-0.63	-0.06	0.05	0.00	0.04	0.17	0.18	0.20	0.20	0.20	0.19	0.20	0.20	0.20	0.20	0.20
3000	-0.34	-0.18	0.07	0.11	0.10	0.13	0.16	0.18	0.18	0.19	0.20	0.20	0.20	0.20	0.20	0.20
4000	-0.58	-0.08	0.02	0.05	0.09	0.15	0.16	0.17	0.19	0.19	0.20	0.20	0.20	0.20	0.20	0.20
5000	-0.53	-0.10	0.05	0.08	0.10	0.16	0.17	0.19	0.19	0.19	0.19	0.20	0.20	0.20	0.20	0.20
10000	-0.55	-0.14	0.05	0.08	0.10	0.16	0.17	0.19	0.19	0.19	0.20	0.20	0.20	0.20	0.20	0.20

Table 3.10: Polynomial Problem Parameter x_2 Sobol Index Convergence

Simulation Population Size \ Number of Monte Carlo Simulations	1	2	3	4	5	10	20	30	40	50	100	200	300	400	500	1000
10	-3.56	0.59	0.19	0.49	0.45	0.64	0.54	0.42	0.57	0.53	0.57	0.57	0.61	0.58	0.62	0.59
20	0.27	0.36	0.55	0.55	0.71	0.66	0.69	0.61	0.43	0.61	0.62	0.60	0.60	0.60	0.59	0.61
30	-0.14	0.62	0.58	-0.03	0.71	0.52	0.55	0.57	0.61	0.55	0.55	0.61	0.61	0.60	0.59	0.59
40	0.32	0.58	0.47	0.48	0.45	0.45	0.58	0.56	0.60	0.61	0.59	0.57	0.60	0.60	0.60	0.59
50	0.03	0.48	0.50	0.55	0.60	0.55	0.65	0.59	0.57	0.64	0.59	0.60	0.60	0.59	0.58	0.59
100	-0.16	0.31	0.58	0.52	0.43	0.57	0.58	0.55	0.56	0.59	0.61	0.60	0.60	0.61	0.60	0.60
200	0.05	0.34	0.45	0.59	0.55	0.58	0.63	0.58	0.62	0.60	0.60	0.60	0.59	0.60	0.60	0.59
300	0.13	0.45	0.54	0.49	0.51	0.56	0.57	0.58	0.59	0.57	0.58	0.60	0.60	0.60	0.60	0.60
400	0.35	0.36	0.61	0.43	0.51	0.57	0.57	0.58	0.58	0.58	0.59	0.61	0.60	0.60	0.59	0.60
500	0.34	0.49	0.49	0.53	0.50	0.56	0.54	0.58	0.59	0.60	0.59	0.59	0.60	0.60	0.59	0.60
1000	0.26	0.46	0.53	0.53	0.53	0.57	0.59	0.60	0.60	0.60	0.60	0.60	0.60	0.60	0.60	0.60
2000	0.28	0.43	0.53	0.52	0.52	0.57	0.59	0.59	0.60	0.59	0.60	0.60	0.60	0.60	0.60	0.60
3000	0.32	0.45	0.49	0.52	0.54	0.57	0.58	0.58	0.59	0.59	0.60	0.60	0.60	0.60	0.60	0.60
4000	0.20	0.44	0.49	0.52	0.54	0.57	0.58	0.58	0.59	0.59	0.60	0.60	0.60	0.60	0.60	0.60
5000	0.20	0.45	0.48	0.52	0.51	0.57	0.58	0.59	0.59	0.59	0.60	0.60	0.60	0.60	0.60	0.60
10000	0.24	0.40	0.48	0.52	0.54	0.56	0.58	0.59	0.59	0.60	0.59	0.60	0.60	0.60	0.60	0.60

Table 3.11: Beam Problem Parameter b LANOVA Index Convergence

Simulation Population Size \ Number of Monte Carlo Simulations	1	2	3	4	5	10	20	30	40	50	100	200	300	400	500	1000
10	0.565	0.478	0.121	0.338	0.368	0.127	0.247	0.256	0.207	0.224	0.231	0.255	0.264	0.259	0.258	0.251
20	-0.051	0.016	0.013	-0.001	-0.002	-0.009	0.021	0.026	0.013	0.007	0.019	0.018	0.016	0.020	0.018	0.017
30	0.045	0.028	0.027	0.064	0.020	0.010	0.010	0.020	0.013	0.013	0.017	0.017	0.015	0.015	0.019	0.018
40	0.053	0.045	0.022	0.005	0.009	0.017	0.030	0.012	0.026	0.017	0.013	0.019	0.020	0.019	0.015	0.017
50	0.003	0.015	0.039	0.044	0.018	0.019	0.022	0.006	0.019	0.021	0.018	0.017	0.015	0.018	0.019	0.017
100	-0.010	-0.013	0.017	0.023	0.025	0.010	0.011	0.013	0.017	0.013	0.017	0.019	0.017	0.020	0.018	0.017
200	0.034	0.011	0.021	0.019	0.009	0.029	0.016	0.016	0.019	0.015	0.018	0.019	0.017	0.018	0.017	0.017
300	0.033	0.005	0.006	0.009	0.015	0.019	0.020	0.020	0.016	0.019	0.016	0.017	0.018	0.018	0.018	0.017
400	0.013	0.008	0.014	0.018	0.014	0.024	0.019	0.017	0.016	0.019	0.019	0.018	0.017	0.017	0.018	0.017
500	0.006	0.005	0.011	0.019	0.014	0.019	0.017	0.017	0.017	0.016	0.018	0.017	0.017	0.017	0.017	0.017
1000	0.018	0.024	0.020	0.020	0.016	0.018	0.019	0.017	0.017	0.017	0.018	0.018	0.017	0.017	0.018	0.017
2000	0.006	0.013	0.020	0.021	0.020	0.019	0.016	0.017	0.017	0.017	0.018	0.016	0.017	0.017	0.018	0.017
3000	0.011	0.020	0.017	0.014	0.013	0.017	0.017	0.018	0.018	0.017	0.017	0.018	0.018	0.017	0.017	0.017
4000	0.017	0.016	0.015	0.014	0.018	0.017	0.017	0.017	0.018	0.017	0.017	0.017	0.017	0.018	0.017	0.017
5000	0.011	0.015	0.019	0.017	0.019	0.015	0.017	0.017	0.017	0.017	0.017	0.017	0.017	0.017	0.018	0.017
10000	0.013	0.016	0.015	0.017	0.016	0.017	0.018	0.017	0.017	0.017	0.017	0.017	0.017	0.017	0.017	0.017

Table 3.12: Beam Problem Parameter H LANOVA Index Convergence

Simulation Population Size \ Number of Monte Carlo Simulations	1	2	3	4	5	10	20	30	40	50	100	200	300	400	500	1000
10	-0.006	0.025	0.014	-0.006	-0.003	0.038	0.001	0.021	0.022	0.014	0.016	0.009	0.009	0.012	0.006	0.011
20	0.171	0.136	0.199	0.175	0.148	0.160	0.143	0.125	0.129	0.142	0.150	0.154	0.150	0.160	0.157	0.154
30	0.243	0.127	0.041	0.112	0.132	0.190	0.166	0.108	0.140	0.160	0.159	0.154	0.145	0.155	0.150	0.153
40	0.153	0.205	0.053	0.190	0.092	0.154	0.127	0.167	0.153	0.150	0.157	0.148	0.165	0.149	0.151	0.156
50	0.185	0.063	0.100	0.170	0.131	0.160	0.142	0.155	0.136	0.131	0.145	0.162	0.160	0.153	0.157	0.159
100	-0.026	0.029	0.137	0.121	0.150	0.146	0.153	0.128	0.140	0.152	0.156	0.162	0.152	0.155	0.155	0.153
200	0.194	0.128	0.158	0.134	0.146	0.118	0.131	0.145	0.150	0.147	0.161	0.156	0.155	0.154	0.154	0.155
300	0.152	0.142	0.138	0.145	0.150	0.148	0.141	0.164	0.145	0.162	0.155	0.154	0.155	0.155	0.154	0.152
400	0.106	0.129	0.160	0.161	0.148	0.148	0.142	0.149	0.152	0.155	0.156	0.154	0.153	0.156	0.155	0.156
500	0.128	0.149	0.131	0.135	0.163	0.147	0.149	0.151	0.155	0.150	0.153	0.155	0.154	0.155	0.153	0.155
1000	0.119	0.173	0.138	0.161	0.134	0.139	0.153	0.153	0.153	0.155	0.157	0.158	0.153	0.155	0.154	0.154
2000	0.124	0.157	0.147	0.148	0.152	0.153	0.154	0.154	0.154	0.156	0.155	0.154	0.155	0.154	0.154	0.154
3000	0.123	0.154	0.146	0.145	0.148	0.154	0.151	0.152	0.153	0.153	0.154	0.155	0.155	0.155	0.155	0.155
4000	0.119	0.129	0.142	0.155	0.147	0.154	0.152	0.153	0.155	0.153	0.155	0.155	0.155	0.155	0.155	0.155
5000	0.130	0.137	0.143	0.153	0.144	0.147	0.154	0.153	0.155	0.155	0.155	0.155	0.155	0.155	0.155	0.155
10000	0.136	0.141	0.149	0.144	0.150	0.151	0.154	0.154	0.154	0.154	0.155	0.155	0.155	0.155	0.155	0.155

Table 3.13: Beam Problem Parameter E LANOVA Index Convergence

Simulation Population Size \ Number of Monte Carlo Simulations	1	2	3	4	5	10	20	30	40	50	100	200	300	400	500	1000
10	0.198	0.055	0.281	-0.004	0.313	0.065	0.111	0.202	0.287	0.180	0.163	0.267	0.247	0.239	0.272	0.254
20	0.371	0.285	0.295	0.318	0.329	0.299	0.220	0.233	0.250	0.162	0.233	0.247	0.221	0.251	0.242	0.241
30	-0.065	-0.124	0.349	0.032	0.084	0.237	0.189	0.165	0.313	0.248	0.244	0.244	0.236	0.246	0.253	0.254
40	-0.390	0.088	0.248	-0.069	0.206	0.296	0.236	0.240	0.196	0.246	0.243	0.256	0.248	0.251	0.234	0.251
50	-0.118	-0.279	0.220	0.317	0.377	0.264	0.292	0.242	0.204	0.243	0.246	0.254	0.247	0.235	0.256	0.248
100	-0.331	-0.381	0.079	0.225	0.175	0.300	0.249	0.222	0.212	0.207	0.258	0.240	0.240	0.249	0.243	0.244
200	0.066	0.118	0.242	0.195	0.212	0.233	0.231	0.222	0.218	0.232	0.238	0.247	0.241	0.243	0.250	0.243
300	-0.009	0.101	0.202	0.195	0.239	0.219	0.244	0.239	0.243	0.243	0.236	0.238	0.248	0.244	0.248	0.244
400	-0.138	0.104	0.246	0.181	0.191	0.217	0.232	0.239	0.252	0.228	0.243	0.239	0.249	0.238	0.248	0.246
500	-0.114	0.131	0.226	0.179	0.235	0.227	0.242	0.249	0.240	0.237	0.244	0.237	0.247	0.240	0.244	0.247
1000	0.028	0.132	0.164	0.201	0.193	0.213	0.228	0.251	0.229	0.238	0.248	0.246	0.244	0.239	0.242	0.245
2000	-0.104	0.155	0.166	0.201	0.209	0.213	0.235	0.238	0.240	0.239	0.241	0.241	0.244	0.243	0.244	0.245
3000	-0.108	0.143	0.159	0.177	0.205	0.236	0.245	0.243	0.239	0.237	0.243	0.244	0.243	0.243	0.243	0.244
4000	-0.112	0.115	0.140	0.180	0.180	0.226	0.233	0.234	0.240	0.238	0.241	0.244	0.243	0.244	0.245	0.244
5000	-0.042	0.086	0.152	0.178	0.210	0.213	0.233	0.236	0.241	0.242	0.245	0.242	0.244	0.243	0.246	0.244
10000	-0.060	0.113	0.167	0.184	0.199	0.223	0.234	0.236	0.242	0.242	0.240	0.243	0.243	0.244	0.245	0.244

Table 3.14: Beam Problem Parameter q LANOVA Index Convergence

Simulation Population Size \ Number of Monte Carlo Simulations	1	2	3	4	5	10	20	30	40	50	100	200	300	400	500	1000
10	0.027	0.009	-0.032	-0.083	-0.052	0.040	-0.022	0.031	0.000	0.015	0.009	0.019	0.017	0.021	0.012	0.017
20	0.188	0.361	0.323	0.297	0.259	0.243	0.241	0.255	0.274	0.256	0.263	0.281	0.262	0.268	0.259	0.271
30	0.236	0.344	0.197	0.113	0.165	0.270	0.251	0.242	0.236	0.253	0.259	0.260	0.257	0.259	0.260	0.266
40	0.155	0.162	0.251	0.232	0.286	0.242	0.243	0.273	0.254	0.252	0.272	0.263	0.268	0.272	0.262	0.264
50	0.148	0.189	0.219	0.262	0.294	0.280	0.261	0.273	0.272	0.289	0.263	0.262	0.256	0.261	0.260	0.269
100	0.353	0.205	0.283	0.248	0.226	0.286	0.244	0.250	0.251	0.261	0.263	0.268	0.263	0.260	0.259	0.263
200	0.181	0.235	0.256	0.248	0.241	0.230	0.254	0.244	0.258	0.260	0.258	0.261	0.262	0.268	0.261	0.264
300	0.240	0.241	0.256	0.223	0.274	0.252	0.246	0.260	0.265	0.261	0.263	0.264	0.263	0.262	0.263	0.261
400	0.260	0.274	0.286	0.259	0.250	0.245	0.262	0.258	0.263	0.261	0.259	0.262	0.262	0.261	0.261	0.263
500	0.214	0.245	0.291	0.258	0.256	0.250	0.261	0.266	0.252	0.260	0.262	0.265	0.262	0.263	0.263	0.263
1000	0.243	0.250	0.235	0.263	0.258	0.257	0.261	0.259	0.259	0.260	0.262	0.264	0.262	0.261	0.263	0.263
2000	0.207	0.238	0.250	0.268	0.255	0.253	0.260	0.260	0.260	0.262	0.262	0.263	0.263	0.263	0.263	0.262
3000	0.214	0.241	0.244	0.252	0.263	0.261	0.260	0.260	0.259	0.261	0.263	0.263	0.263	0.263	0.262	0.263
4000	0.212	0.238	0.243	0.261	0.250	0.262	0.262	0.263	0.261	0.262	0.262	0.263	0.262	0.262	0.262	0.263
5000	0.228	0.241	0.249	0.257	0.251	0.263	0.262	0.260	0.262	0.264	0.262	0.262	0.262	0.263	0.263	0.263
10000	0.213	0.235	0.250	0.252	0.251	0.261	0.260	0.261	0.261	0.263	0.261	0.262	0.262	0.263	0.263	0.263

Table 3.15: Beam Problem Parameter L LANOVA Index Convergence

Simulation Population Size \ Number of Monte Carlo Simulations	1	2	3	4	5	10	20	30	40	50	100	200	300	400	500	1000
10	0.247	0.235	0.122	0.132	0.156	0.171	0.191	0.117	0.185	0.159	0.144	0.143	0.150	0.158	0.157	0.158
20	0.070	0.000	0.019	0.050	0.006	0.013	0.017	0.018	0.004	0.015	0.007	0.007	0.008	0.013	0.009	0.010
30	-0.022	0.018	-0.009	0.008	-0.003	0.010	0.015	0.008	0.011	0.010	0.011	0.009	0.012	0.010	0.009	0.009
40	0.008	0.004	0.038	-0.015	-0.008	0.013	0.014	0.008	0.002	0.011	0.013	0.010	0.008	0.012	0.010	0.011
50	0.017	0.002	-0.001	0.012	0.031	0.022	0.000	0.014	0.009	0.014	0.011	0.012	0.011	0.008	0.009	0.008
100	-0.025	0.008	0.017	0.011	0.011	0.013	0.013	0.008	0.013	0.012	0.012	0.010	0.010	0.010	0.010	0.010
200	-0.008	0.006	-0.002	0.005	0.013	0.012	0.013	0.010	0.010	0.009	0.010	0.012	0.010	0.011	0.011	0.011
300	0.009	-0.004	0.014	0.011	0.017	0.005	0.017	0.012	0.007	0.009	0.010	0.009	0.010	0.010	0.010	0.010
400	0.003	0.004	0.007	0.009	0.010	0.016	0.011	0.009	0.011	0.010	0.011	0.010	0.010	0.009	0.010	0.010
500	0.014	0.009	0.017	0.012	0.003	0.009	0.010	0.009	0.009	0.010	0.011	0.010	0.010	0.010	0.010	0.010
1000	0.013	0.011	0.005	0.010	0.013	0.008	0.009	0.010	0.010	0.009	0.010	0.010	0.010	0.010	0.010	0.010
2000	0.009	0.010	0.008	0.008	0.010	0.009	0.010	0.010	0.011	0.010	0.011	0.010	0.010	0.010	0.010	0.010
3000	0.002	0.010	0.012	0.008	0.008	0.011	0.012	0.010	0.011	0.009	0.010	0.010	0.010	0.010	0.010	0.010
4000	0.003	0.009	0.010	0.008	0.008	0.011	0.010	0.011	0.010	0.010	0.010	0.010	0.010	0.010	0.010	0.010
5000	0.012	0.007	0.008	0.009	0.009	0.009	0.011	0.010	0.010	0.010	0.011	0.010	0.010	0.010	0.010	0.010
10000	0.005	0.010	0.009	0.008	0.009	0.010	0.010	0.010	0.010	0.010	0.010	0.010	0.010	0.010	0.010	0.010

Table 3.16: Beam Problem Parameter b Sobol Index Convergence

Simulation Population Size \ Number of Monte Carlo Simulations	1	2	3	4	5	10	20	30	40	50	100	200	300	400	500	1000
10	-0.006	-0.904	-0.153	-0.824	-0.105	-0.182	-0.152	-0.008	0.097	-0.101	-0.034	0.035	0.000	0.025	0.056	0.038
20	-0.223	-0.065	0.137	0.191	0.217	-0.041	0.017	-0.006	-0.027	-0.028	0.008	0.039	-0.002	0.035	0.025	0.041
30	0.028	-0.156	0.151	-0.209	-0.107	-0.040	-0.011	-0.041	0.113	0.042	0.026	0.041	-0.001	0.018	0.031	0.030
40	-1.066	-0.585	-0.031	-0.219	-0.004	0.093	-0.014	0.062	-0.027	0.019	0.028	0.020	0.041	0.038	0.020	0.032
50	-0.363	-0.682	0.027	0.130	0.122	-0.028	0.048	0.057	-0.003	0.054	0.056	0.022	0.018	0.026	0.032	0.036
100	-0.793	-0.318	-0.099	-0.032	-0.159	0.080	0.022	0.035	-0.012	-0.023	0.050	0.036	0.013	0.030	0.024	0.024
200	-0.276	-0.088	-0.081	-0.020	-0.034	0.031	-0.006	-0.007	0.005	0.017	0.032	0.035	0.023	0.028	0.030	0.030
300	-0.284	-0.173	0.035	-0.159	0.019	0.015	-0.003	0.020	0.012	0.039	0.016	0.023	0.029	0.020	0.028	0.028
400	-0.524	-0.058	0.027	-0.042	-0.042	0.021	0.008	0.005	0.021	0.019	0.030	0.022	0.032	0.017	0.032	0.031
500	-0.194	-0.189	-0.004	-0.026	0.019	0.036	0.014	0.025	0.018	0.005	0.018	0.018	0.028	0.020	0.025	0.032
1000	-0.339	-0.103	-0.080	-0.024	-0.015	-0.018	0.007	0.028	0.015	0.022	0.033	0.029	0.025	0.017	0.026	0.029
2000	-0.376	-0.096	-0.047	-0.027	-0.011	-0.009	0.007	0.014	0.017	0.025	0.022	0.022	0.026	0.027	0.026	0.026
3000	-0.398	-0.083	-0.095	-0.049	-0.009	0.009	0.021	0.024	0.019	0.020	0.024	0.029	0.025	0.026	0.026	0.028
4000	-0.396	-0.116	-0.080	-0.066	-0.048	0.003	0.013	0.020	0.022	0.019	0.020	0.026	0.027	0.027	0.027	0.026
5000	-0.294	-0.165	-0.082	-0.047	-0.025	-0.007	0.014	0.013	0.021	0.028	0.028	0.024	0.028	0.027	0.029	0.026
10000	-0.321	-0.121	-0.075	-0.042	-0.038	0.001	0.013	0.015	0.022	0.021	0.021	0.026	0.025	0.028	0.028	0.027

Table 3.17: Beam Problem Parameter H Sobol Index Convergence

Simulation Population Size \ Simulation Iterations	1	2	3	4	5	10	20	30	40	50	100	200	300	400	500	1000
10	0.057	0.204	-0.402	0.184	0.122	0.255	0.247	0.193	0.254	0.164	0.223	0.226	0.226	0.233	0.256	0.241
20	-0.034	0.401	0.101	0.299	0.366	0.174	0.230	0.166	0.224	0.185	0.225	0.275	0.228	0.257	0.240	0.263
30	0.280	0.163	0.223	0.042	0.117	0.232	0.238	0.163	0.261	0.229	0.262	0.270	0.244	0.244	0.250	0.249
40	0.032	0.005	0.147	0.102	0.152	0.216	0.224	0.272	0.205	0.182	0.266	0.251	0.272	0.259	0.241	0.247
50	-0.503	-0.455	0.242	0.230	0.254	0.183	0.248	0.271	0.199	0.264	0.240	0.253	0.237	0.249	0.245	0.262
100	-0.683	-0.012	0.185	0.201	0.080	0.241	0.218	0.225	0.219	0.228	0.252	0.245	0.244	0.257	0.247	0.249
200	0.033	0.220	0.191	0.167	0.171	0.217	0.214	0.226	0.236	0.219	0.251	0.258	0.243	0.247	0.250	0.249
300	0.015	0.088	0.255	0.117	0.249	0.209	0.228	0.262	0.231	0.249	0.237	0.247	0.247	0.243	0.250	0.246
400	-0.134	0.134	0.270	0.182	0.203	0.224	0.233	0.227	0.242	0.238	0.250	0.242	0.248	0.243	0.253	0.249
500	-0.037	0.127	0.186	0.172	0.218	0.211	0.233	0.231	0.239	0.242	0.244	0.245	0.248	0.246	0.244	0.250
1000	-0.037	0.146	0.168	0.192	0.182	0.195	0.231	0.243	0.234	0.251	0.251	0.247	0.245	0.241	0.247	0.247
2000	-0.114	0.136	0.153	0.191	0.204	0.217	0.243	0.234	0.240	0.246	0.246	0.242	0.246	0.247	0.244	0.246
3000	-0.087	0.160	0.170	0.196	0.208	0.235	0.240	0.241	0.244	0.239	0.244	0.249	0.246	0.246	0.246	0.248
4000	-0.060	0.127	0.149	0.190	0.188	0.227	0.237	0.238	0.242	0.241	0.243	0.247	0.247	0.245	0.248	0.247
5000	-0.013	0.091	0.154	0.190	0.192	0.217	0.239	0.234	0.241	0.245	0.248	0.244	0.246	0.246	0.246	0.246
10000	-0.055	0.120	0.165	0.182	0.190	0.227	0.235	0.238	0.242	0.240	0.243	0.246	0.246	0.248	0.248	0.247

Table 3.18: Beam Problem Parameter E Sobol Index Convergence

Simulation Population Size \ Number of Monte Carlo Simulations	1	2	3	4	5	10	20	30	40	50	100	200	300	400	500	1000
10	0.198	0.055	0.281	-0.004	0.313	0.065	0.111	0.202	0.287	0.180	0.163	0.267	0.247	0.239	0.272	0.254
20	0.371	0.285	0.295	0.318	0.329	0.299	0.220	0.233	0.250	0.162	0.233	0.247	0.221	0.251	0.242	0.241
30	-0.065	-0.124	0.349	0.032	0.084	0.237	0.189	0.165	0.313	0.248	0.244	0.244	0.236	0.246	0.253	0.254
40	-0.390	0.088	0.248	-0.069	0.206	0.296	0.236	0.240	0.196	0.246	0.243	0.256	0.248	0.251	0.234	0.251
50	-0.118	-0.279	0.220	0.317	0.377	0.264	0.292	0.242	0.204	0.243	0.246	0.254	0.247	0.235	0.256	0.248
100	-0.331	-0.381	0.079	0.225	0.175	0.300	0.249	0.222	0.212	0.207	0.258	0.240	0.240	0.249	0.243	0.244
200	0.066	0.118	0.242	0.195	0.212	0.233	0.231	0.222	0.218	0.232	0.238	0.247	0.241	0.243	0.250	0.243
300	-0.009	0.101	0.202	0.195	0.239	0.219	0.244	0.239	0.243	0.243	0.236	0.238	0.248	0.244	0.248	0.244
400	-0.138	0.104	0.246	0.181	0.191	0.217	0.232	0.239	0.252	0.228	0.243	0.239	0.249	0.238	0.248	0.246
500	-0.114	0.131	0.226	0.179	0.235	0.227	0.242	0.249	0.240	0.237	0.244	0.237	0.247	0.240	0.244	0.247
1000	0.028	0.132	0.164	0.201	0.193	0.213	0.228	0.251	0.229	0.238	0.248	0.246	0.244	0.239	0.242	0.245
2000	-0.104	0.155	0.166	0.201	0.209	0.213	0.235	0.238	0.240	0.239	0.241	0.241	0.244	0.243	0.244	0.245
3000	-0.108	0.143	0.159	0.177	0.205	0.236	0.245	0.243	0.239	0.237	0.243	0.244	0.243	0.243	0.243	0.244
4000	-0.112	0.115	0.140	0.180	0.180	0.226	0.233	0.234	0.240	0.238	0.241	0.244	0.243	0.244	0.245	0.244
5000	-0.042	0.086	0.152	0.178	0.210	0.213	0.233	0.236	0.241	0.242	0.245	0.242	0.244	0.243	0.246	0.244
10000	-0.060	0.113	0.167	0.184	0.199	0.223	0.234	0.236	0.242	0.242	0.240	0.243	0.243	0.244	0.245	0.244

Table 3.19: Beam Problem Parameter q Sobol Index Convergence

Simulation Population Size \ Number of Monte Carlo Simulations	1	2	3	4	5	10	20	30	40	50	100	200	300	400	500	1000
10	0.206	0.139	0.419	0.366	0.523	0.309	0.348	0.457	0.383	0.382	0.402	0.419	0.444	0.417	0.431	0.431
20	0.038	0.446	0.552	0.608	0.542	0.418	0.306	0.369	0.439	0.397	0.421	0.430	0.419	0.439	0.433	0.442
30	0.339	0.262	0.347	0.064	0.200	0.389	0.431	0.429	0.427	0.436	0.424	0.412	0.414	0.427	0.430	0.434
40	-0.583	-0.227	0.310	0.270	0.423	0.449	0.354	0.448	0.424	0.432	0.447	0.434	0.441	0.441	0.430	0.433
50	0.501	0.344	0.431	0.383	0.472	0.469	0.472	0.447	0.418	0.481	0.452	0.435	0.429	0.434	0.432	0.438
100	0.166	-0.101	0.423	0.409	0.274	0.457	0.391	0.420	0.409	0.420	0.443	0.441	0.430	0.435	0.427	0.435
200	0.160	0.354	0.321	0.407	0.395	0.364	0.435	0.401	0.424	0.437	0.430	0.437	0.437	0.433	0.437	0.439
300	0.290	0.352	0.356	0.350	0.418	0.414	0.387	0.422	0.428	0.447	0.434	0.436	0.434	0.431	0.434	0.434
400	0.218	0.391	0.432	0.421	0.384	0.429	0.421	0.424	0.425	0.435	0.428	0.434	0.436	0.430	0.430	0.438
500	0.218	0.256	0.442	0.379	0.408	0.432	0.423	0.434	0.431	0.419	0.434	0.433	0.432	0.434	0.432	0.436
1000	0.103	0.368	0.332	0.400	0.426	0.400	0.423	0.427	0.426	0.427	0.441	0.435	0.434	0.430	0.434	0.434
2000	0.177	0.347	0.395	0.404	0.410	0.407	0.422	0.425	0.428	0.435	0.432	0.433	0.435	0.434	0.435	0.435
3000	0.172	0.363	0.364	0.381	0.408	0.424	0.426	0.432	0.432	0.427	0.431	0.435	0.434	0.436	0.434	0.435
4000	0.149	0.330	0.361	0.378	0.387	0.417	0.430	0.430	0.431	0.426	0.432	0.435	0.435	0.434	0.434	0.435
5000	0.209	0.314	0.377	0.388	0.401	0.413	0.427	0.425	0.433	0.436	0.434	0.434	0.434	0.435	0.435	0.435
10000	0.175	0.337	0.368	0.380	0.390	0.414	0.422	0.428	0.430	0.433	0.432	0.433	0.433	0.434	0.435	0.435

Table 3.20: Beam Problem Parameter L Sobol Index Convergence

Simulation Population Size \ Number of Monte Carlo Simulations	1	2	3	4	5	10	20	30	40	50	100	200	300	400	500	1000
10	-0.234	-0.632	-0.078	-0.584	-0.018	-0.140	-0.145	-0.009	0.134	-0.095	-0.050	-0.002	-0.001	0.012	0.054	0.029
20	-0.226	0.009	0.099	0.111	0.161	-0.002	-0.039	-0.015	-0.028	-0.032	-0.004	0.027	-0.023	0.028	0.014	0.033
30	0.003	-0.103	0.179	-0.331	-0.200	-0.031	-0.038	-0.045	0.107	0.022	0.019	0.026	-0.006	0.013	0.024	0.021
40	-0.991	-0.711	0.045	-0.256	-0.003	0.079	-0.022	0.012	-0.030	0.012	0.017	0.008	0.026	0.031	0.007	0.024
50	-0.385	-0.593	0.029	0.056	0.132	-0.010	0.033	0.071	-0.005	0.054	0.041	0.013	0.009	0.019	0.025	0.026
100	-0.672	-0.325	-0.118	-0.072	-0.171	0.059	0.012	0.020	-0.027	-0.024	0.037	0.024	0.005	0.019	0.015	0.017
200	-0.370	-0.104	-0.102	-0.037	-0.052	0.018	-0.015	-0.023	-0.009	0.011	0.025	0.026	0.014	0.017	0.022	0.020
300	-0.306	-0.201	0.060	-0.163	0.033	-0.021	0.001	0.010	0.002	0.023	0.011	0.012	0.020	0.010	0.019	0.018
400	-0.551	-0.094	0.011	-0.048	-0.045	0.006	0.009	0.001	0.010	0.008	0.019	0.011	0.022	0.007	0.024	0.021
500	-0.226	-0.185	-0.009	-0.057	0.013	0.003	0.002	0.013	0.004	0.000	0.010	0.007	0.018	0.011	0.014	0.023
1000	-0.375	-0.111	-0.091	-0.030	-0.027	-0.040	-0.006	0.016	0.003	0.012	0.023	0.018	0.015	0.007	0.016	0.018
2000	-0.346	-0.119	-0.063	-0.044	-0.027	-0.014	0.002	0.006	0.010	0.016	0.013	0.014	0.016	0.017	0.016	0.017
3000	-0.384	-0.083	-0.097	-0.057	-0.013	0.004	0.013	0.015	0.012	0.010	0.015	0.018	0.016	0.017	0.016	0.018
4000	-0.423	-0.136	-0.093	-0.070	-0.058	-0.009	0.005	0.010	0.011	0.009	0.011	0.016	0.017	0.017	0.017	0.017
5000	-0.305	-0.187	-0.096	-0.064	-0.036	-0.015	0.005	0.005	0.012	0.019	0.019	0.014	0.018	0.016	0.019	0.017
10000	-0.341	-0.126	-0.083	-0.053	-0.047	-0.011	0.001	0.006	0.012	0.012	0.011	0.016	0.016	0.018	0.018	0.017

Chapter 4

Laminate Studies

4.1 Trial Studies

To perform statistical analysis on a population, it is important to understand the shape of the probability distribution. Parameters for discussing spread and size differ depending on the distribution used to model said population. To understand the shape of laminate stiffness output from the numerical simulation, trial runs were completed for select layups prior to sensitivity analysis. While sensitivity analysis is valid regardless of output shape, other parameters for describing variation such as standard deviation require a normally distributed output. Such an output distribution is not guaranteed for a normally distributed input.

These trial runs were completed for one of the study laminates plus two special cases, shown in Table 4.3. All studied laminates are symmetric, with two additional cross-ply laminates chosen as special cases.

Table 4.1: Output Stiffness Shape Investigation Laminates

Stacking Sequence	Ply Thickness (m)	Mean Angle Variation (°)	Std. Dev. Angle Variation (°)	Data Source
$[0, 90, 90, 0]_s$	1.5E-4	0	3.25	Hyer [6]
$[90, 0, 0, 90]_s$	1.5E-4	0	3.25	Hyer [6]
$[45, 90, -45, 0]_s$	3.0E-4	0	3.25	Amancher [2]

Sample distributions for the symmetric laminates are shown in Fig. 4.1 through Fig. 4.7.

The output of these laminates follows a normal distribution, verified by χ^2 GOF testing. For these laminates mean and standard deviation are good descriptors of the shape of the distribution. This result means that these parameters can be used in the comparison of laminates in the primary study.

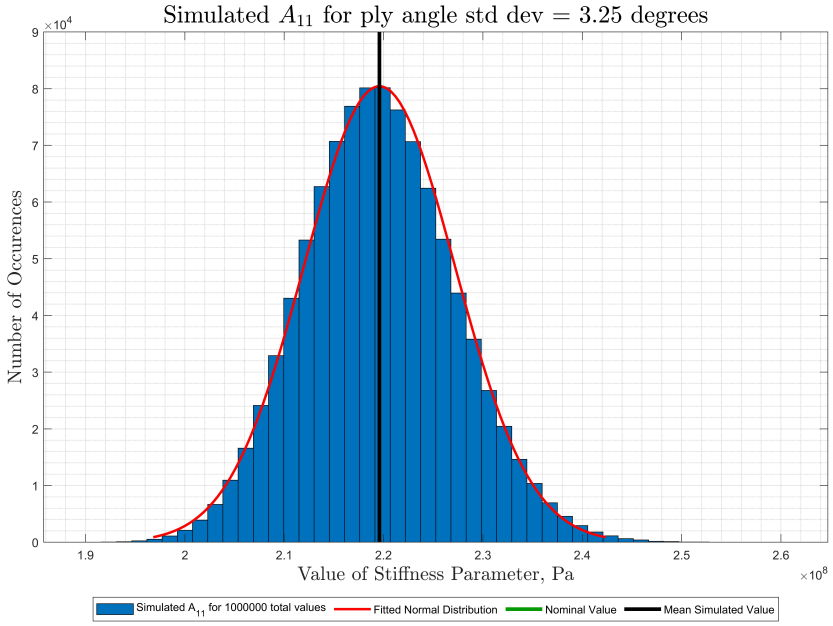

Figure 4.1: Symmetric Laminate Simulated A_{11} for Normally Distributed Ply Angle Variation

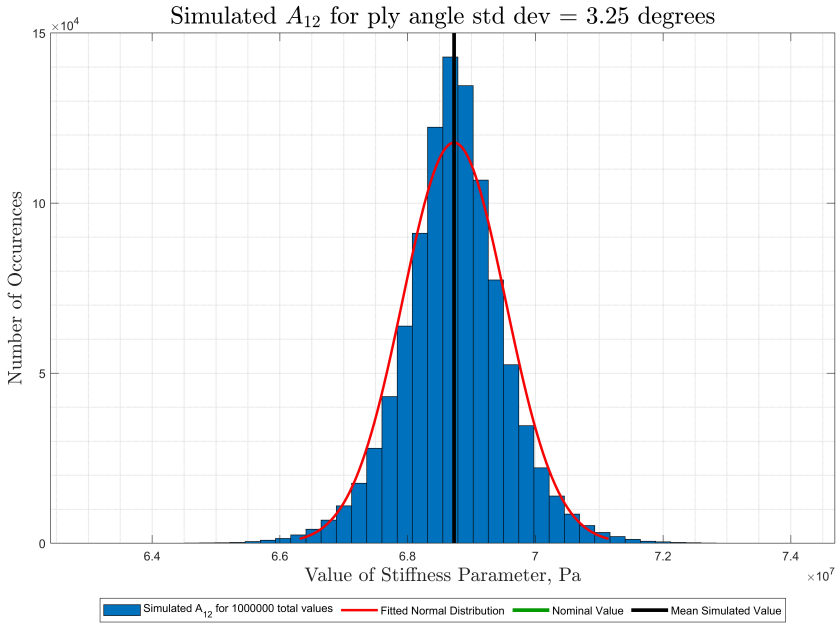

Figure 4.2: Symmetric Laminate Simulated A_{12} for Normally Distributed Ply Angle Variation

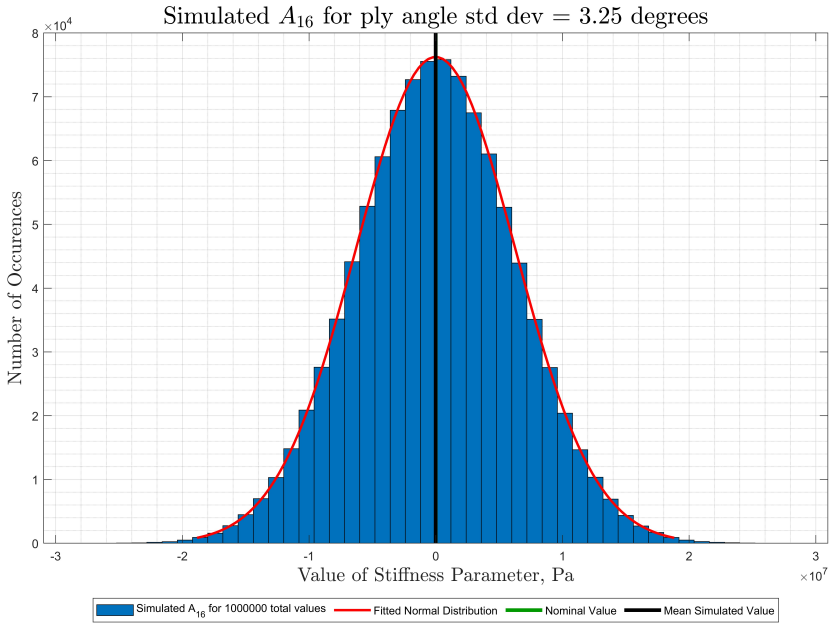

Figure 4.3: Symmetric Laminate Simulated A_{16} for Normally Distributed Ply Angle Variation

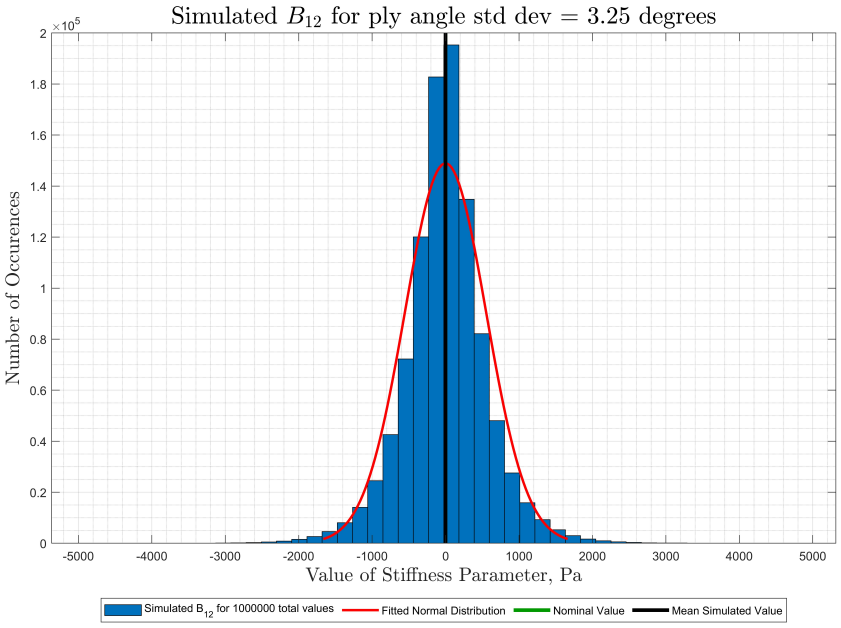

Figure 4.4: Symmetric Laminate Simulated B_{12} for Normally Distributed Ply Angle Variation

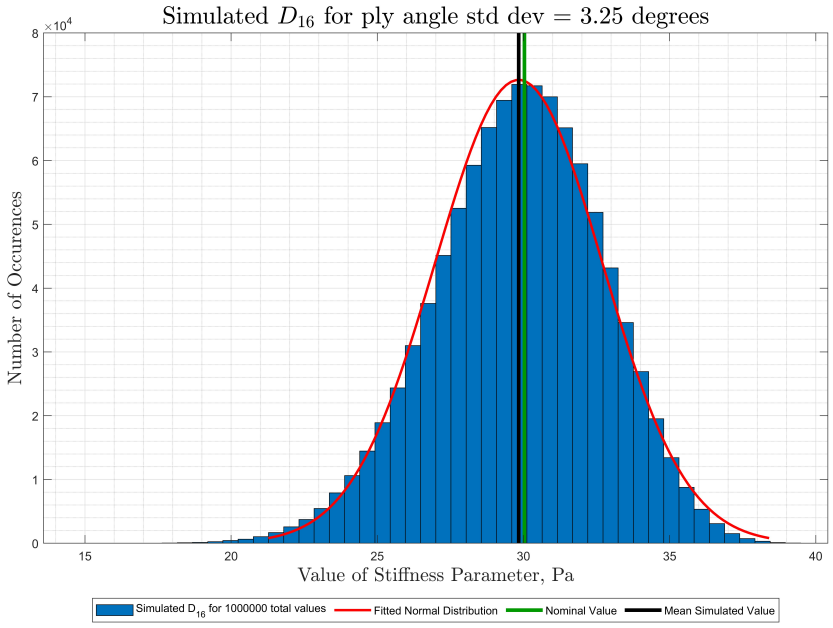

Figure 4.5: Symmetric Laminate Simulated D_{16} for Normally Distributed Ply Angle Variation

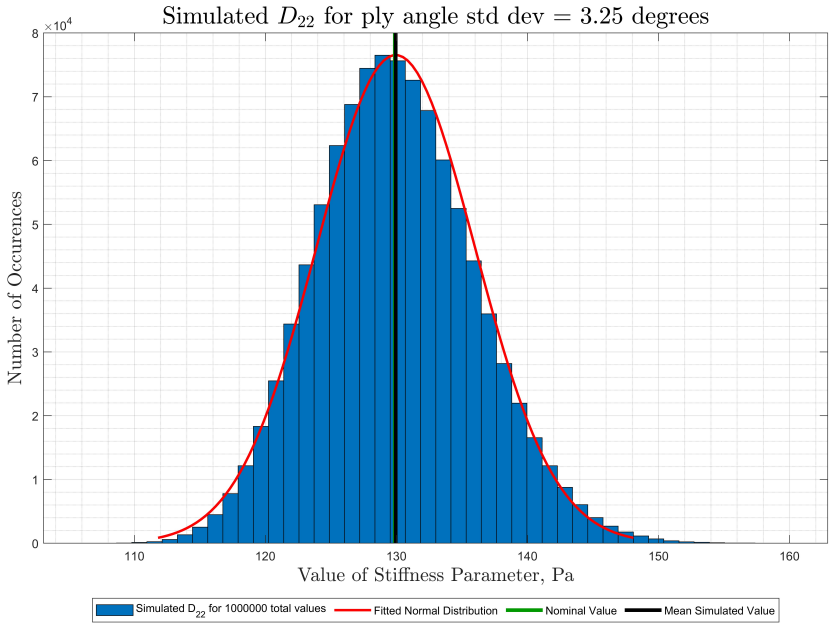

Figure 4.6: Symmetric Laminate Simulated D_{22} for Normally Distributed Ply Angle Variation

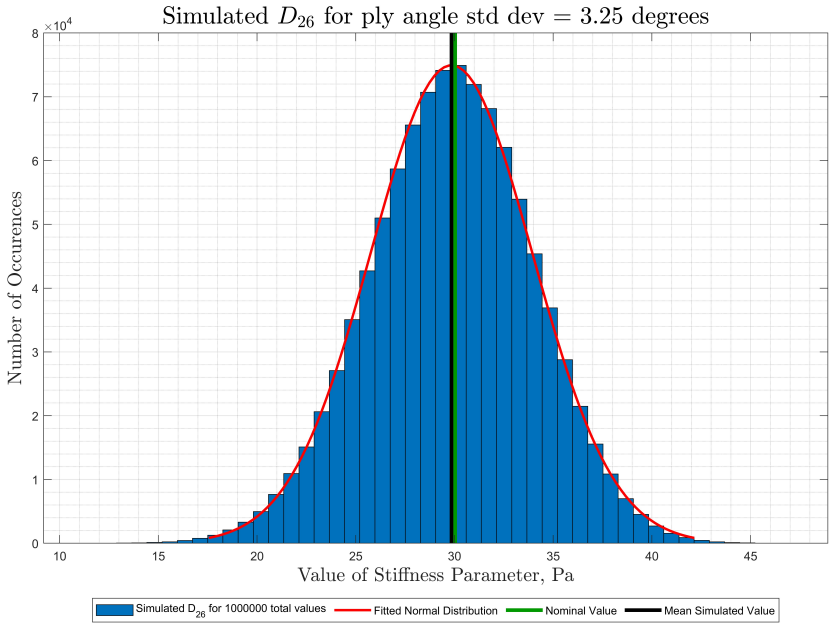

Figure 4.7: Symmetric Laminate Simulated D_{66} for Normally Distributed Ply Angle Variation

Distribution shapes for cross ply laminates, shown in Fig. 4.8 through Fig. 4.14 differ from other laminates. These laminates show skewed distributions for stiffness matrix components with non-zero nominal values. Variance can still be used for sensitivity index calculations, but mean and standard deviation of a normal distribution are not sufficient to describe the shape of the distribution. A fitted distribution would need to be able to describe the skew present in the output. A Weibull distribution could handle these specific cases of skewed distributions for a cross ply laminate. However, the appearance of negative numbers outside this special case means the Weibull distribution is not suited for the general case. An extension of normal distributions, known as skewed normal distributions [1], could describe the output distribution for all laminates. The skewed normal distribution is defined on the whole number line, contains a parameter for describing skew, and maintains use of the standard deviation as a measure of spread. However, methods for solving for the parameters of the skewed normal distribution using maximum likelihood estimation are difficult to implement numerically. As a result, cross ply laminates are handled as a special case where non-zero nominal stiffness values are fitted with a Weibull distribution and zero nominal stiffness values are fitted with a normal distribution. While cross-ply laminates are not studied for the thin-ply results discussion, understanding these special cases is important for building general case suitability of the analysis code.

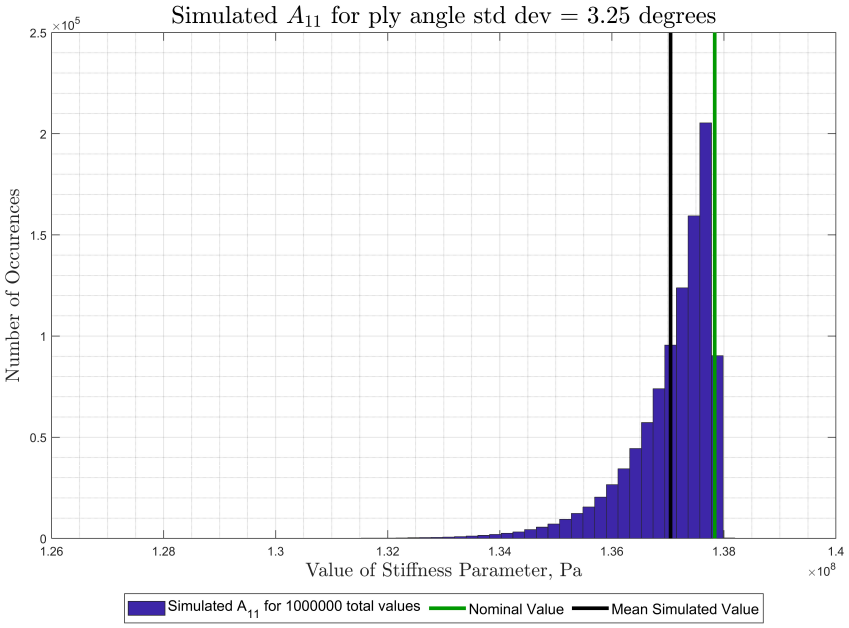

Figure 4.8: Cross Ply Laminate Simulated A_{11} for Normally Distributed Ply Angle Variation

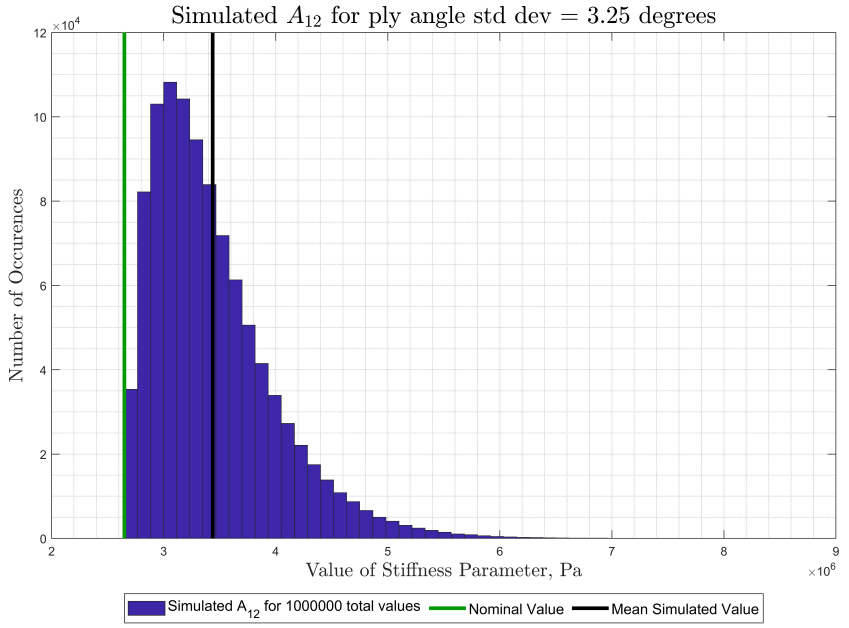

Figure 4.9: Cross Ply Laminate Simulated A_{12} for Normally Distributed Ply Angle Variation

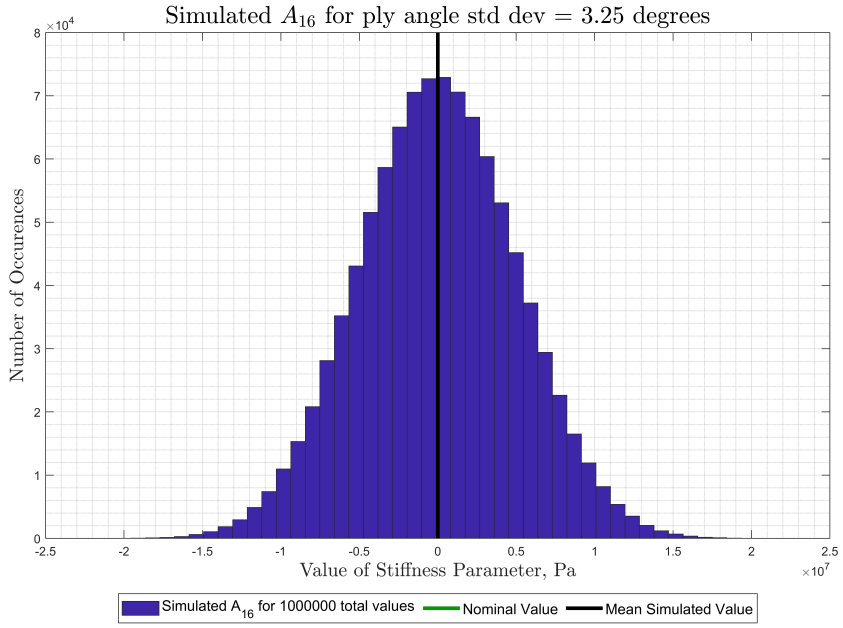

Figure 4.10: Cross Ply Laminate Simulated A_{16} for Normally Distributed Ply Angle Variation

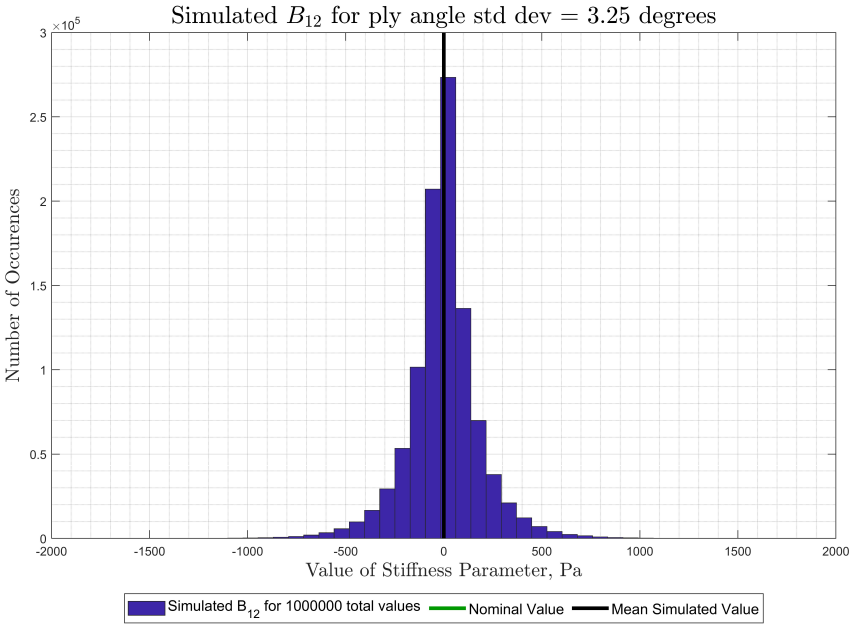

Figure 4.11: Cross Ply Laminate Simulated B_{12} for Normally Distributed Ply Angle Variation

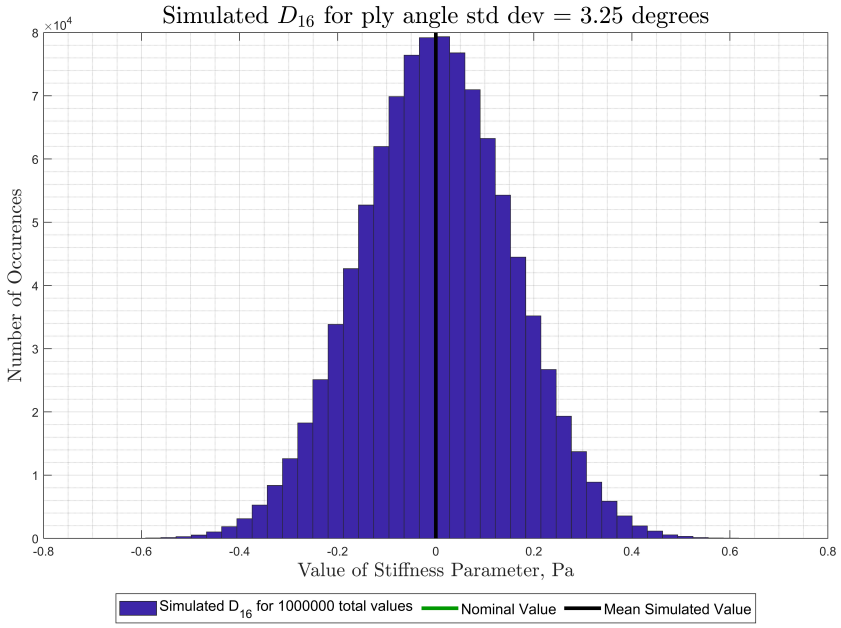

Figure 4.12: Cross Ply Laminate Simulated D_{16} for Normally Distributed Ply Angle Variation

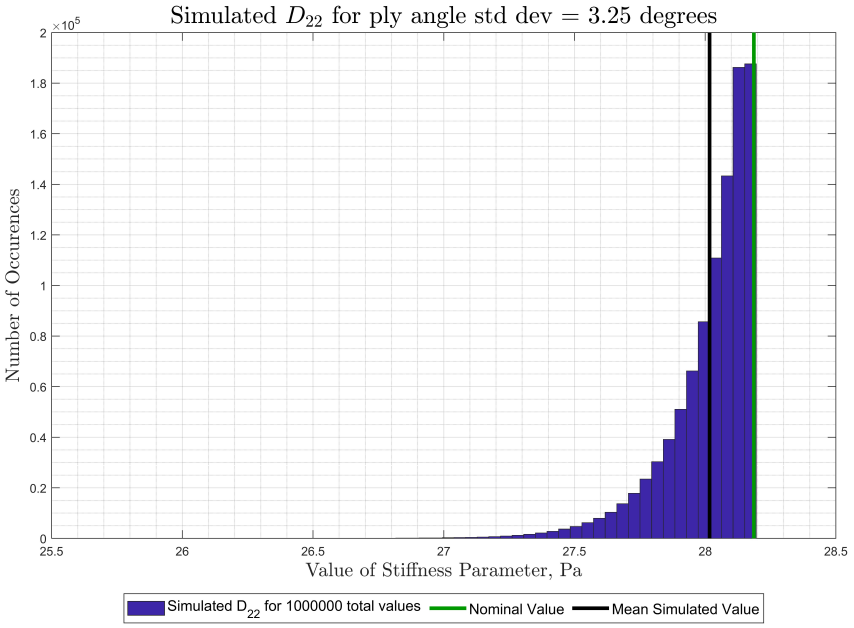

Figure 4.13: Cross Ply Laminate Simulated D_{22} for Normally Distributed Ply Angle Variation

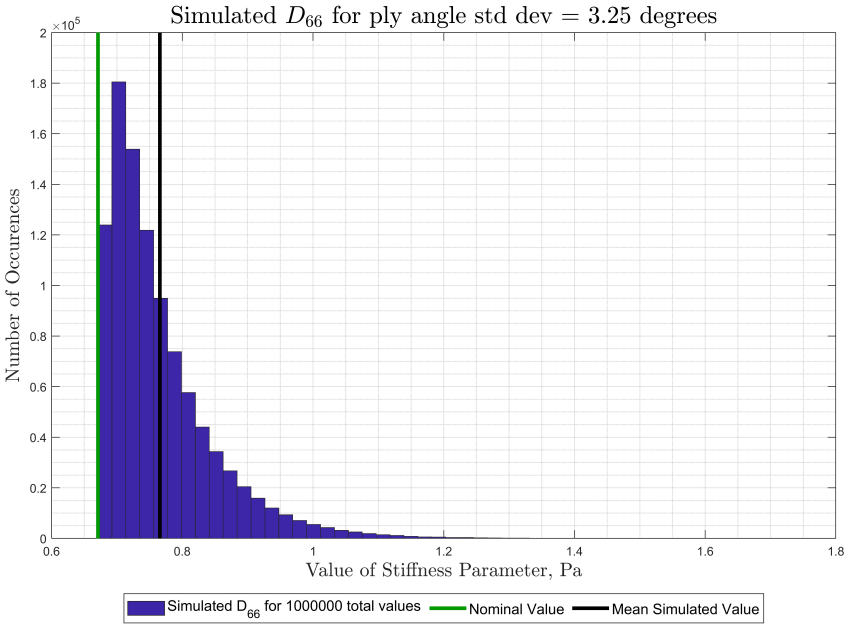

Figure 4.14: Cross Ply Laminate Simulated D_{26} for Normally Distributed Ply Angle Variation

A review of the normalized global reduced stiffnesses and their derivatives, shown in 4.15 and 4.16 respectively, demonstrate why cross-ply laminates can show skewed behavior. The values of $\overline{Q}_{11}$, $\overline{Q}_{22}$, and $\overline{Q}_{66}$ are at their maximum or minimum value at 0° and 90°. Derivatives $d\overline{Q}_{11}/d\theta$, $d\overline{Q}_{22}/d\theta$, and $d\overline{Q}_{66}/d\theta$ are therefore zero at 0° and 90°. These local extrema mean that small perturbations around these points can either only increase or only decrease. The presence of non 0° and 90° plies suppresses this behavior from appearing in non-cross-ply laminates.

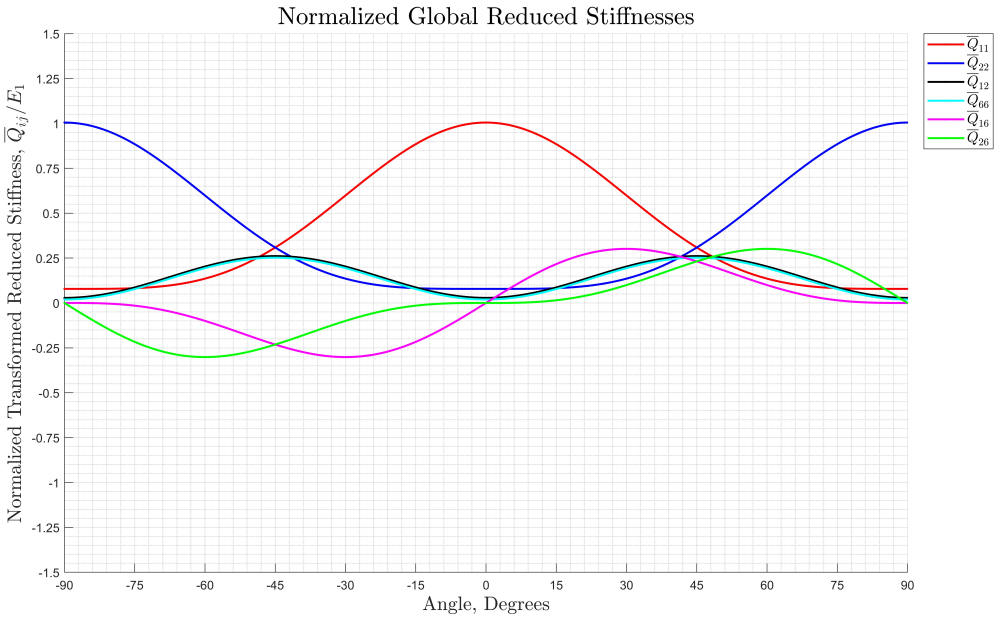

Figure 4.15: Normalized Global Reduced Stiffnesses as a Function of θ

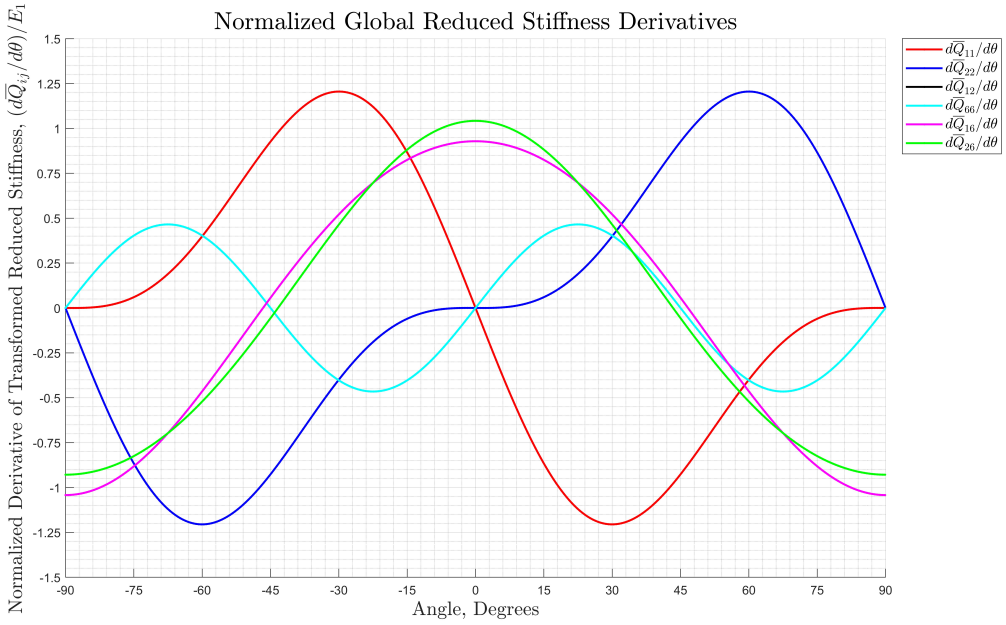

Figure 4.16: Normalized Global Reduced Stiffness Derivatives as a Function of θ

4.2 Results and Discussion

4.2.1 Analysis Parameters

Input parameters for the Monte-Carlo simulation were determined to perform the convergence studies as discussed in section 3.3. Mean ply angle variation and standard deviation were chosen from reference sources [7]. These parameters are summarized in Table 4.2 below. Variations in void content and ply thickness were not considered. In addition, the error in ply angle is assumed to be independent of the nominal ply thickness.

Table 4.2: Output Stiffness Shape Investigation Laminates

Parameter	Value
Number of Simulations	1000
Simulation Population Size	1000
Mean Ply Angle Error	0° [7]
Ply Angle Error Standard Deviation	3.25° [7]

This work focuses on the three laminate designs studied by Amancher et al. [2] for thin, thick, and intermediate ply thicknesses. Lamina properties are taken from the unidirectional laminate testing in the referenced work. To isolate any effect of the different tested properties for each laminate thickness, the thick and intermediate laminates were also studied using the properties obtained from testing of the thin plies. The laminate and property definitions are shown below in Table 4.3 and Table 4.4, respectively.

Table 4.3: Reference Laminates [2]

Classification	Stacking Sequence	Ply Thickness (m)	Material Properties
Thin	$[45, 90, -45, 0]_{10s}$	3.00E-05	Thin
Intermediate	$[45, 90, -45, 0]_{3s}$	1.00E-04	Intermediate and Thin
Thick	$[45, 90, -45, 0]_{s}$	3.00E-04	Thick and Thin
Large Thick	$[45, 90, -45, 0]_{10s}$	3.00E-04	Thick

Table 4.4: Laminate Material Properties [2]

Classification	E_1 (GPa)	E_2 (GPa)	ν_{12}	G_{12} (GPa)
Thin	222	7.01	0.314	4.66
Intermediate	223	7.01	0.274	4.66
Thick	229	7.01	0.266	4.66

Two metrics are used in this work to describe the effect of simulated manufacturing errors on laminate stiffness: standard deviation and sensitivity index. The combination of these two metrics is used to study the impacts both with respect to each individual ply and holistically at the laminate level. Sensitivity indices are excellent for describing effects at the ply level and provide a qualitative means for assessing which individual plies contribute the most to variation seen in the laminate stiffnesses. To simplify analysis of the sensitivity indices for the thin ply laminates with a total ply count of 80, indices are grouped by nominal ply orientation angle. This grouping also allows for better comparison across laminates with different total ply counts. Since the A matrix, and by extension the effective engineering properties, are not impacted by a ply's height within the stack these sensitivity indices do

not vary with height and may be grouped. The individual ply contribution to the B and D matrices are affected by ply height within the laminate. Therefore the sensitivity indices of these stiffness terms cannot be evaluated in this grouped manner. Sensitivity indices of these terms are not assessed in this work.

Standard deviation of the stiffness matrix components and effective engineering properties are used to obtain a quantitative comparison. This metric is normalized by the nominal stiffness values for each respective parameter to allow for comparison across the multiple laminates investigated in this work. This metric does not describe the impact of any individual ply, but allows for quantitative comparison across laminates for overall impact of the ply angle variation.

4.2.2 Uncertainty Analysis

Standard deviation of output stiffness and sensitivity to individual ply changes were analyzed to characterize the size effects of ply thickness. Due to slight differences in nominal stiffness values between the laminate types, the normalized standard deviation is compared. Nominal values, standard deviation, and normalized standard deviation for each type of laminate are discussed in the following, starting with the A matrix and effective engineering properties.

Table 4.5: A Matrix Uncertainty Analysis Summary

Layup		Thin	Interm	Interm	Thick	Thick	Large Thick
Material Property		Thin	Thin	Interm	Thin	Thick	Thick
A_{11} (MN/m)	Nominal	214	214	214	214	220	2196
	RMS Error	2.50	4.53	4.56	7.99	8.08	25.82
	Standard Deviation	2.33	4.24	4.27	7.35	7.59	24.01
	Normalized Std Dev	0.011	0.020	0.020	0.034	0.035	0.011
A_{12} (MN/m)	Nominal	67	67	67	67	69	687
	RMS Error	0.26	0.48	0.50	0.86	0.87	2.73
	Standard Deviation	0.25	0.45	0.45	0.78	0.81	2.55
	Normalized Std Dev	0.004	0.007	0.007	0.012	0.012	0.004
A_{16} (MN/m)	Nominal	0	0	0	0	0	0
	RMS Error	2.06	3.79	3.82	6.50	6.73	21.34
	Standard Deviation	1.92	3.51	3.53	6.07	6.28	19.88
	Normalized Std Dev	N/A	N/A	N/A	N/A	N/A	N/A
A_{22} (MN/m)	Nominal	214	214	214	214	220	2196
	RMS Error	2.49	4.61	4.56	7.95	8.09	25.72
	Standard Deviation	2.33	4.24	4.26	7.35	7.59	24.01
	Normalized Std Dev	0.011	0.020	0.020	0.034	0.035	0.011
A_{26} (MN/m)	Nominal	0	0	0	0	0	0
	RMS Error	2.04	3.83	3.77	6.49	6.73	21.15
	Standard Deviation	1.92	3.51	3.53	6.07	6.28	19.88
	Normalized Std Dev	N/A	N/A	N/A	N/A	N/A	N/A
A_{66} (MN/m)	Nominal	73	73	74	73	75	754
	RMS Error	0.26	0.48	0.50	0.86	0.87	2.73
	Standard Deviation	0.25	0.45	0.45	0.78	0.81	2.55
	Normalized Std Dev	0.003	0.006	0.006	0.011	0.011	0.003

Inspection of the normalized standard deviations of the A matrix terms and effective engineering moduli shows a clear decrease with decreasing ply thickness. This difference is attributable to the increase in ply count as ply thickness decreases. An additional case of the thick ply thickness and thin ply stacking sequence was run to confirm this. For a normally distributed ply angle error, an increase in ply count will lead to a decrease in standard deviation for extensional values as errors average out across the laminate. These trends are shown in bar charts in Fig. 4.17 through Fig. 4.20.

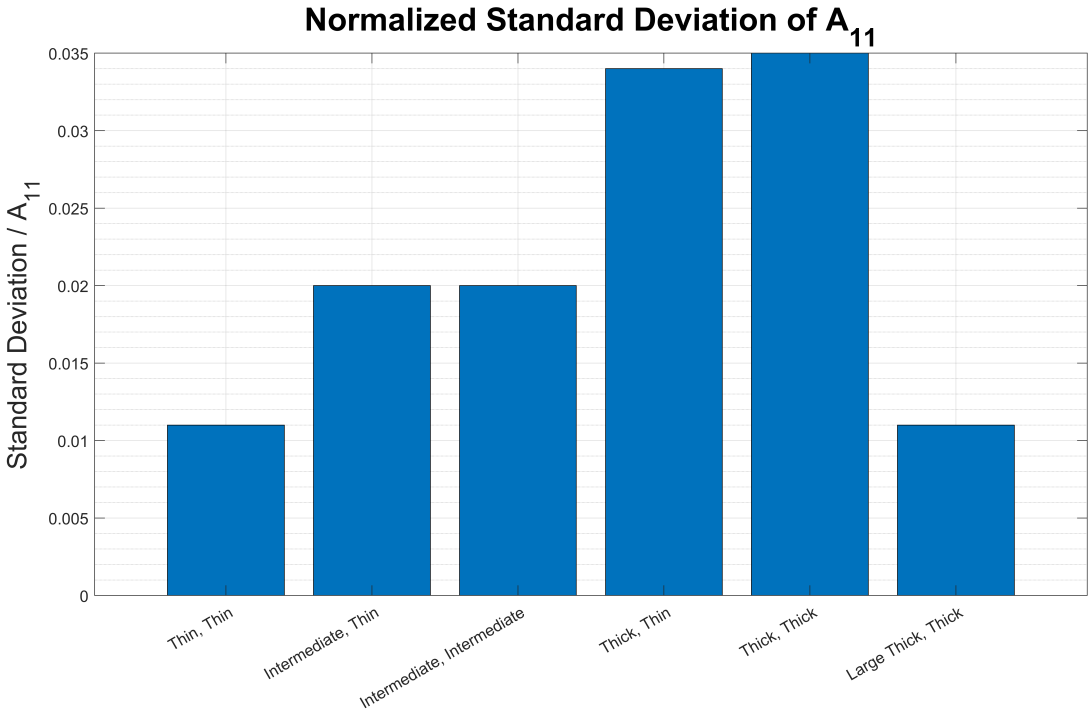

Figure 4.17: Normalized Standard Deviation of A_{11}

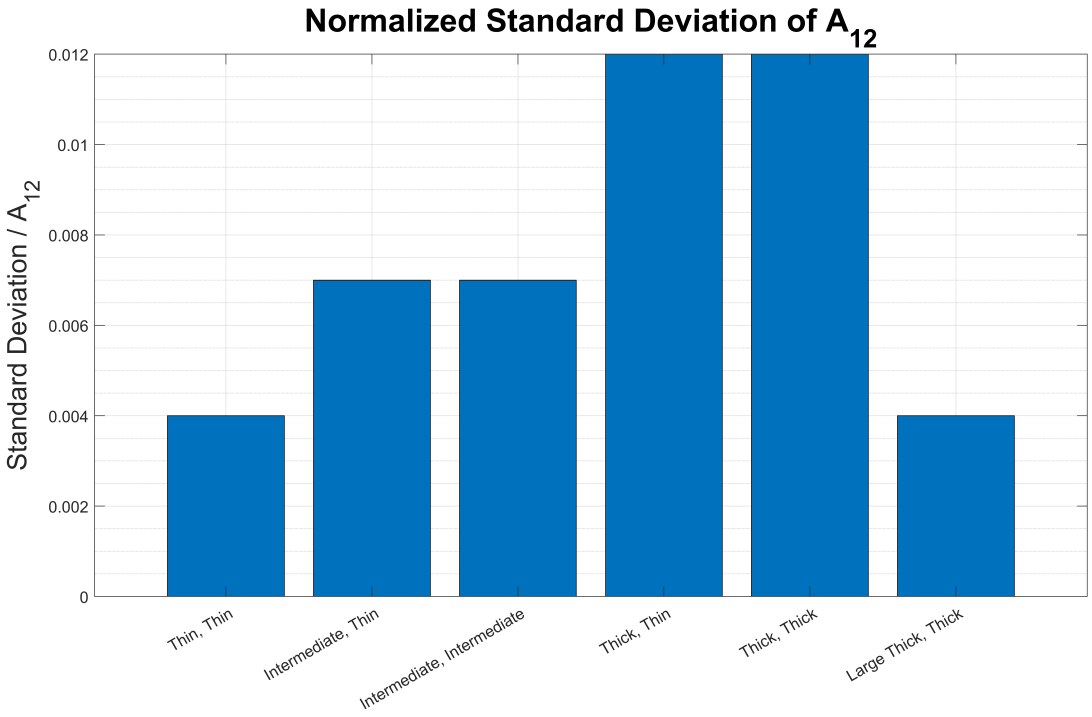

Figure 4.18: Normalized Standard Deviation of A_{12}

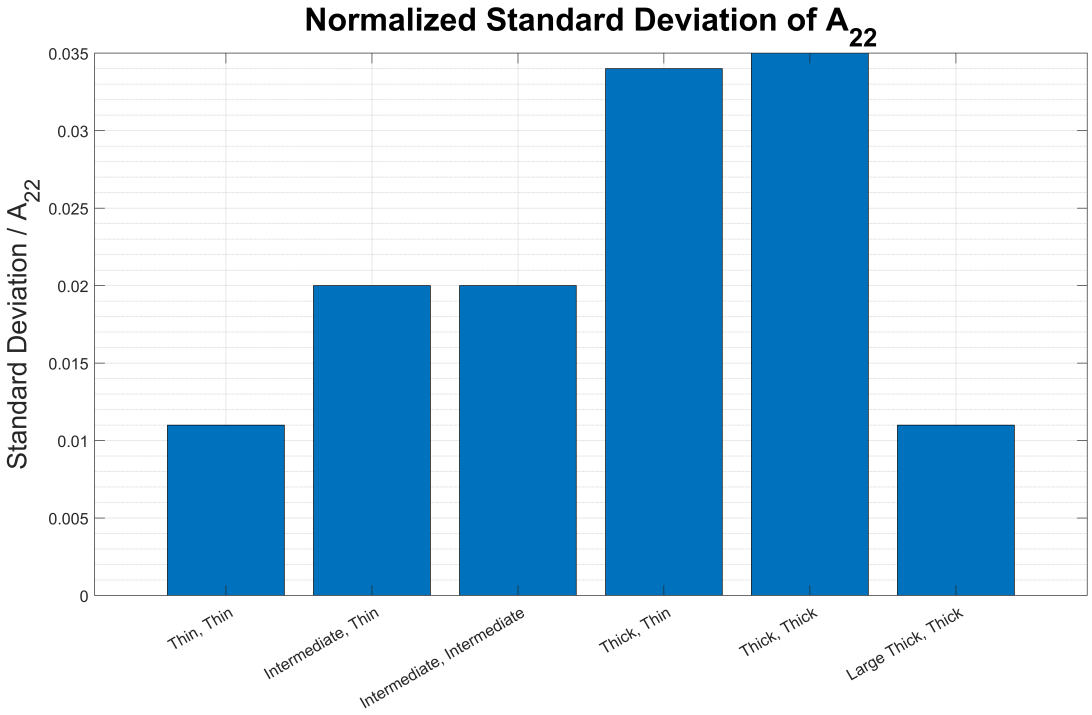

Figure 4.19: Normalized Standard Deviation of A_{22}

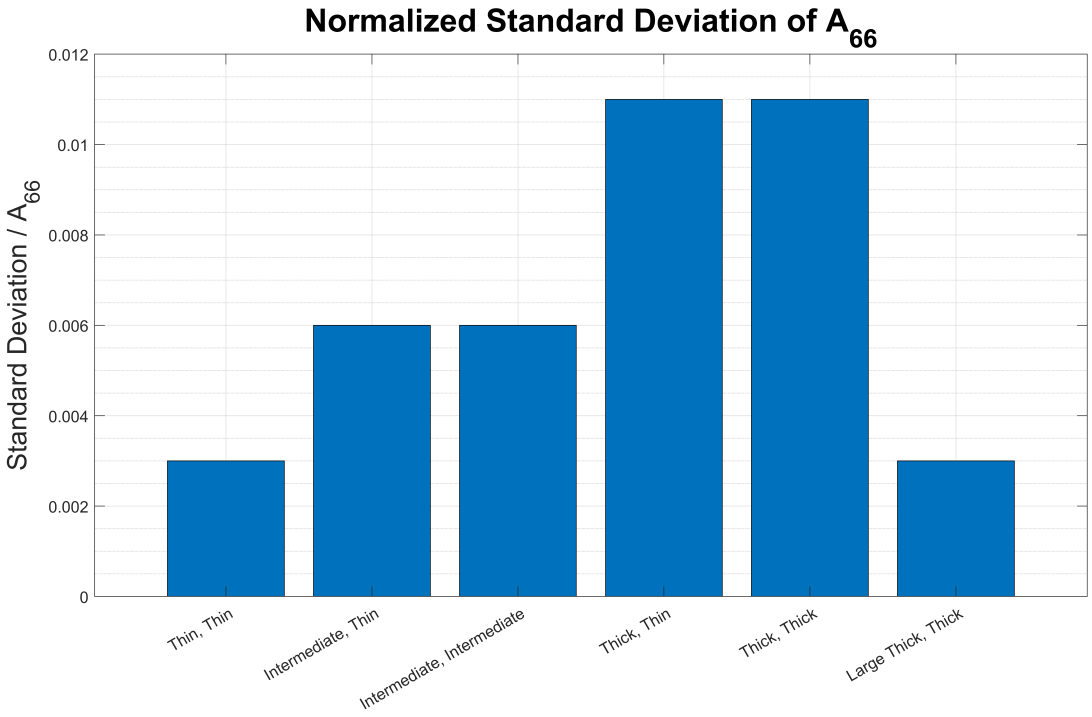

Figure 4.20: Normalized Standard Deviation of A_{66}

It should be noted that the maximum normalized standard deviation of an effective engineering property for the thick ply composite is 4% of the nominal value. This value is low by engineering standards and not likely to have significant impact on laminate performance. A similar trend is observed in the effective engineering properties, which is expected.

Table 4.6: Effective Engineering Property Uncertainty Analysis Summary

Layup		Thin	Interm	Interm	Thick	Thick	Large Thick
Material Property		Thin	Thin	Interm	Thin	Thick	Thick
E_x (GPa)	Nominal	80.2	80.2	80.5	80.2	82.5	82.5
	RMS Error	0.95	1.75	1.75	3.20	3.19	0.98
	Standard Deviation	0.89	1.62	1.64	2.82	2.92	0.92
	Normalized Std Dev	0.011	0.020	0.020	0.035	0.035	0.011
E_y (GPa)	Nominal	80.2	80.2	80.5	80.2	82.5	82.5
	RMS Error	0.95	1.79	1.77	3.18	3.25	0.98
	Standard Deviation	0.89	1.63	1.64	2.88	2.98	0.92
	Normalized Std Dev	0.011	0.020	0.020	0.036	0.036	0.011
ν_{xy}	Nominal	0.31	0.31	0.31	0.31	0.31	0.31
	RMS Error	0.00	0.01	0.01	0.01	0.01	0.00
	Standard Deviation	0.00	0.01	0.01	0.01	0.01	0.00
	Normalized Std Dev	0.012	0.022	0.022	0.040	0.041	0.012
G_{xy} (GPa)	Nominal	30.5	30.5	30.7	30.5	31.4	31.4
	RMS Error	0.12	0.26	0.26	0.75	0.77	0.12
	Standard Deviation	0.11	0.21	0.21	0.51	0.53	0.11
	Normalized Std Dev	0.003	0.007	0.007	0.017	0.017	0.003

The dependence of standard deviation on ply count is also observed for the B and D matrices. The opposite trend is observed of the normalized standard deviation for D_{16} and D_{26}. This trend for the twisting terms D_{16} and D_{26} is attributable to the small nominal value and is not thought to be a size effect of the laminate.

Table 4.7: B Matrix Uncertainty Analysis Summary

Layup		Thin	Interm	Interm	Thick	Thick	Large Thick
Material Property		Thin	Thin	Interm	Thin	Thick	Thick
B_{11} (N)	Nominal	0	0	0	0	0	0
	RMS Error	1,757	3,322	3,334	6,322	6,506	181,222
	Standard Deviation	1,641	3,115	3,128	5,905	6,103	169,318
	Normalized Std Dev	N/A	N/A	N/A	N/A	N/A	N/A
B_{12} (N)	Nominal	0	0	0	0	0	0
	RMS Error	181	338	336	597	610	18791
	Standard Deviation	170	311	313	533	555	17,649
	Normalized Std Dev	N/A	N/A	N/A	N/A	N/A	N/A
B_{16} (N)	Nominal	0	0	0	0	0	0
	RMS Error	1,392	2,327	2,350	3,089	3,212	144,065
	Standard Deviation	1,288	2,174	2,184	2,880	2,985	133,212
	Normalized Std Dev	N/A	N/A	N/A	N/A	N/A	N/A
B_{22} (N)	Nominal	0	0	0	0	0	0
	RMS Error	1,767	3,313	3,333	6,352	6,671	182,315
	Standard Deviation	1,643	3,123	3,135	5,935	6,130	169,509
	Normalized Std Dev	N/A	N/A	N/A	N/A	N/A	N/A
B_{26} (N)	Nominal	0	0	0	0	0	0
	RMS Error	1,448	2,735	2,791	5,004	5,142	149,816
	Standard Deviation	1,353	2,561	2,574	4,669	4,834	140,007
	Normalized Std Dev	N/A	N/A	N/A	N/A	N/A	N/A
B_{66} (N)	Nominal	0	0	0	0	0	0
	RMS Error	181	338	336	597	610	18,791
	Standard Deviation	170	311	313	533	555	17,649
	Normalized Std Dev	N/A	N/A	N/A	N/A	N/A	N/A

Table 4.8: D Matrix Uncertainty Analysis Summary

Layup		Thin	Interm	Interm	Thick	Thick	Large Thick
Material Property		Thin	Thin	Interm	Thin	Thick	Thick
D_{11} (N.m)	Nominal	97	85	85	56	58	99,558
	RMS Error	1.7	3.2	3.2	6.3	6.5	1,721.6
	Standard Deviation	1.5	3.0	3.0	5.8	6.0	1,591
	Normalized Std Dev	0.016	0.035	0.035	0.103	0.104	0.016
D_{12} (N.m)	Nominal	33	36	36	43	45	34,146
	RMS Error	0.2	0.3	0.3	0.6	0.7	178.9
	Standard Deviation	0.2	0.3	0.3	0.5	0.5	164.1
	Normalized Std Dev	0.005	0.008	0.008	0.011	0.011	0.005
D_{16} (N.m)	Nominal	2	8	8	29	30	2,463
	RMS Error	1.3	2.0	2.1	3.0	3.1	1,299.1
	Standard Deviation	1.2	1.9	1.9	2.8	2.9	1,213
	Normalized Std Dev	0.491	0.224	0.224	0.095	0.095	0.492
D_{22} (N.m)	Nominal	106	113	113	126	130	108,929
	RMS Error	1.7	3.2	3.2	6.2	6.6	1730
	Standard Deviation	1.5	3.0	3.0	5.9	6.0	1593
	Normalized Std Dev	0.015	0.027	0.027	0.046	0.047	0.015
D_{26} (N.m)	Nominal	2	8	8	29	30	2,463
	RMS Error	1.3	2.6	2.6	4.2	4.4	1396.3
	Standard Deviation	1.3	2.4	2.4	4.0	4.1	1,316
	Normalized Std Dev	0.533	0.288	0.288	0.136	0.136	0.534
D_{66} (N.m)	Nominal	36	39	39	46	48	37,362
	RMS Error	0.2	0.3	0.3	0.6	0.7	178.9
	Standard Deviation	0.2	0.3	0.3	0.5	0.5	164.1
	Normalized Std Dev	0.004	0.007	0.007	0.011	0.011	0.004

While normalized standard deviations are generally low, a clear improvement can be observed for thin ply laminates due to the increased ply count for equal laminate thickness. Decreased ply thickness allows for this ply count increase within the same design space, and therefore is projected to provide significant benefits in resilience against ply angle errors for error sensitive applications.

4.2.3 Sensitivity Analysis

Similar trends to those discussed above are observed when investigating sensitivity indices. Thin ply laminates have lower sensitivity indices on each individual ply, which is consistent with the observations made on standard deviations. Maximum indices for a given ply orientation are shown in Table 4.9 through Table 4.12 for Sobol's method.

Table 4.9: E_x FOSI Laminate Comparison

E_x Max Index Compare, FOSI			
Angle (°)	Thin	Interm	Thick
45	0.023	0.082	0.231
90	-0.001	0.002	0.000
-45	0.023	0.082	0.231
0	0.000	0.008	0.020

Table 4.10: E_y FOSI Laminate Comparison

E_y Max Index Compare, FOSI			
Angle (°)	Thin	Interm	Thick
45	0.023	0.080	0.225
90	0.000	0.007	0.034
-45	0.023	0.080	0.223
0	-0.002	0.000	0.000

Table 4.11: ν_{xy} FOSI Laminate Comparison

ν_{XY} Max Index Compare, FOSI			
Angle (°)	Thin	Interm	Thick
45	0.021	0.072	0.196
90	0.002	0.014	0.053
-45	0.021	0.071	0.189
0	-0.001	0.003	0.007

Table 4.12: G_{xy} FOSI Laminate Comparison

G_{xy} Max Index Compare, FOSI			
Angle (°)	Thin	Interm	Thick
45	0.013	0.057	0.220
90	0.010	0.027	0.002
-45	0.012	0.050	0.092
0	0.010	0.027	0.018

These observations support the conclusion that ply count, which for a fixed laminate thickness is a result of decreased ply thickness, is the driving factor for the observed differences. The values shown in Table 4.9 through Table 4.12 for Sobol's method are presented in graphical form in Fig. 4.21 through Fig. 4.28. Values are consistent with standard deviations obtained in uncertainty analysis.

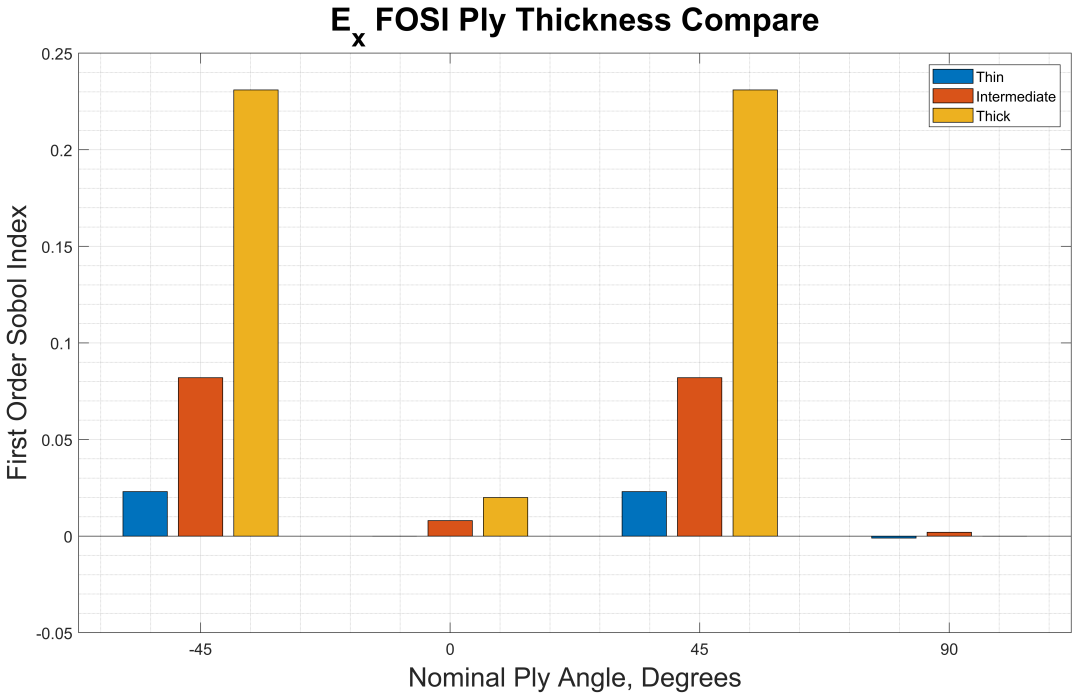

Figure 4.21: E_x FOSI vs Ply Thickness

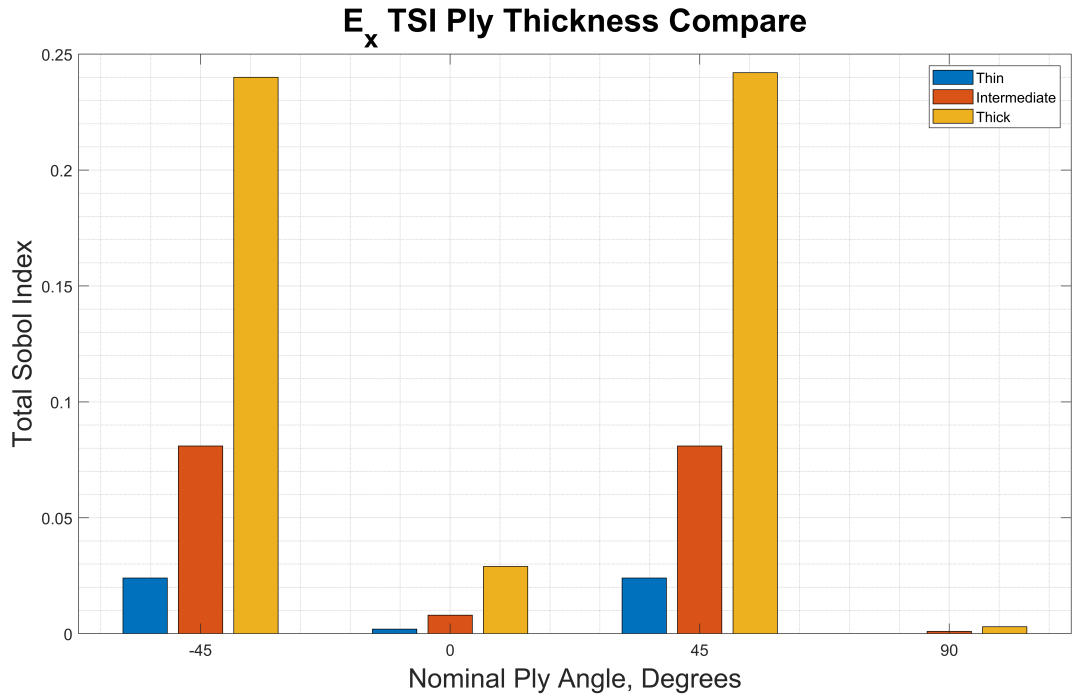

Figure 4.22: E_x TSI vs Ply Thickness

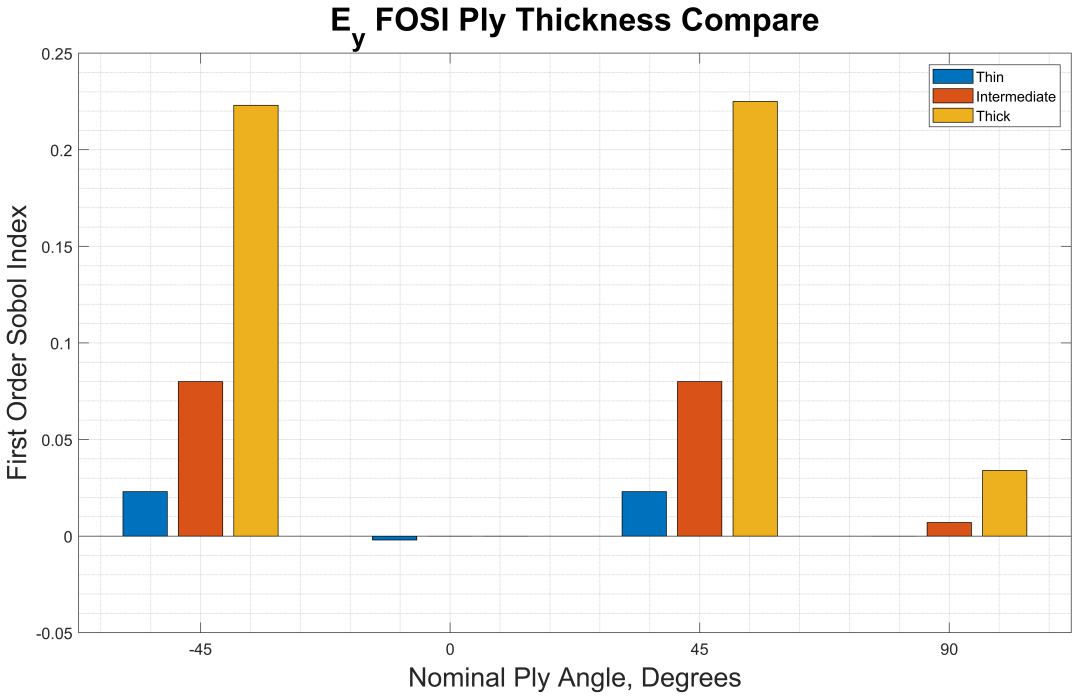

Figure 4.23: E_y FOSI vs Ply Thickness

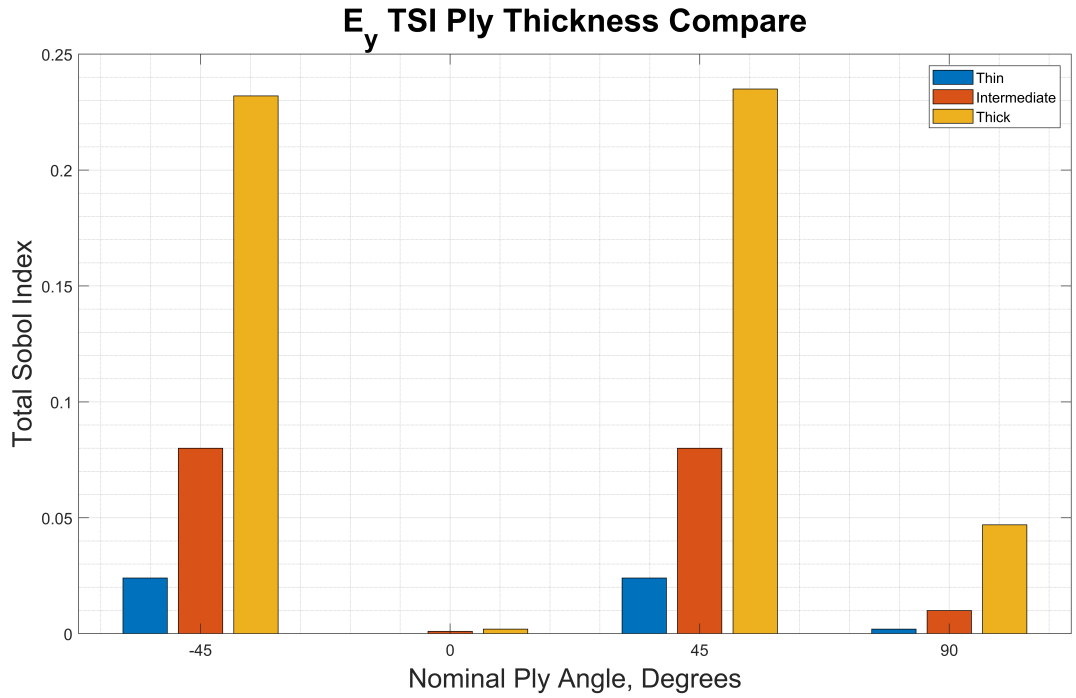

Figure 4.24: E_y TSI vs Ply Thickness

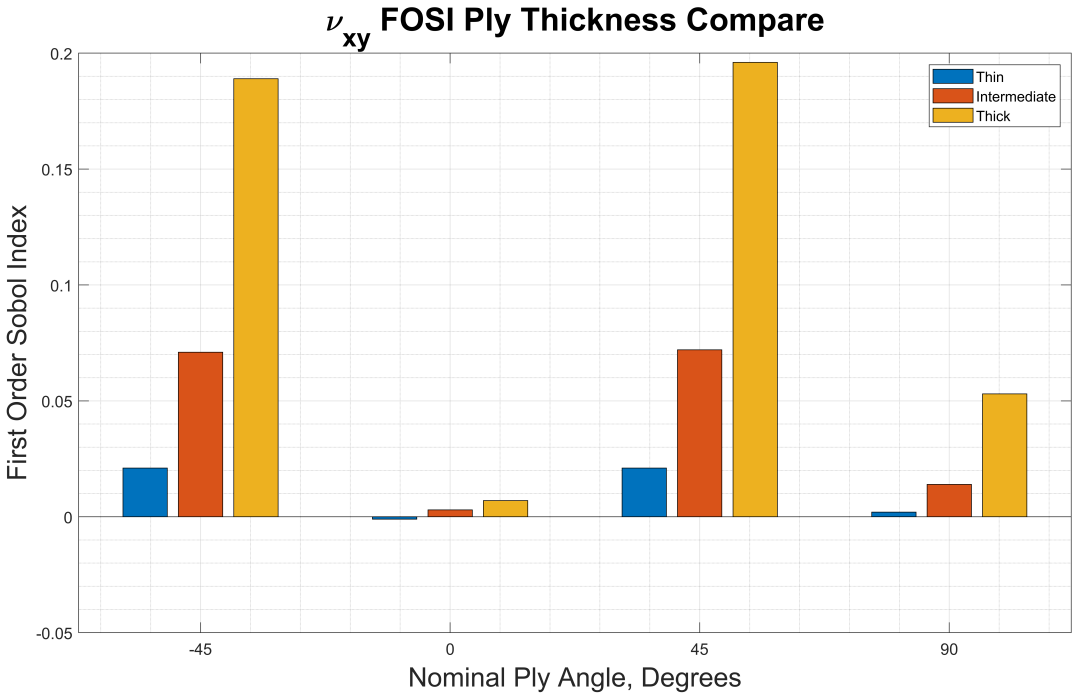

Figure 4.25: ν_{xy} FOSI vs Ply Thickness

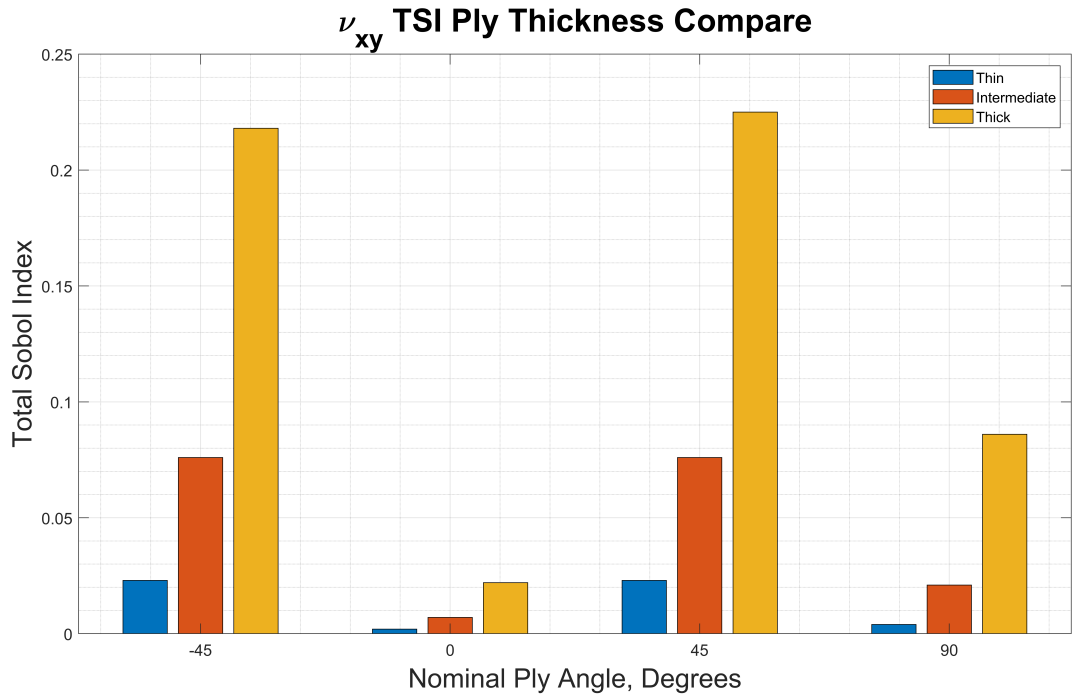

Figure 4.26: ν_{xy} TSI vs Ply Thickness

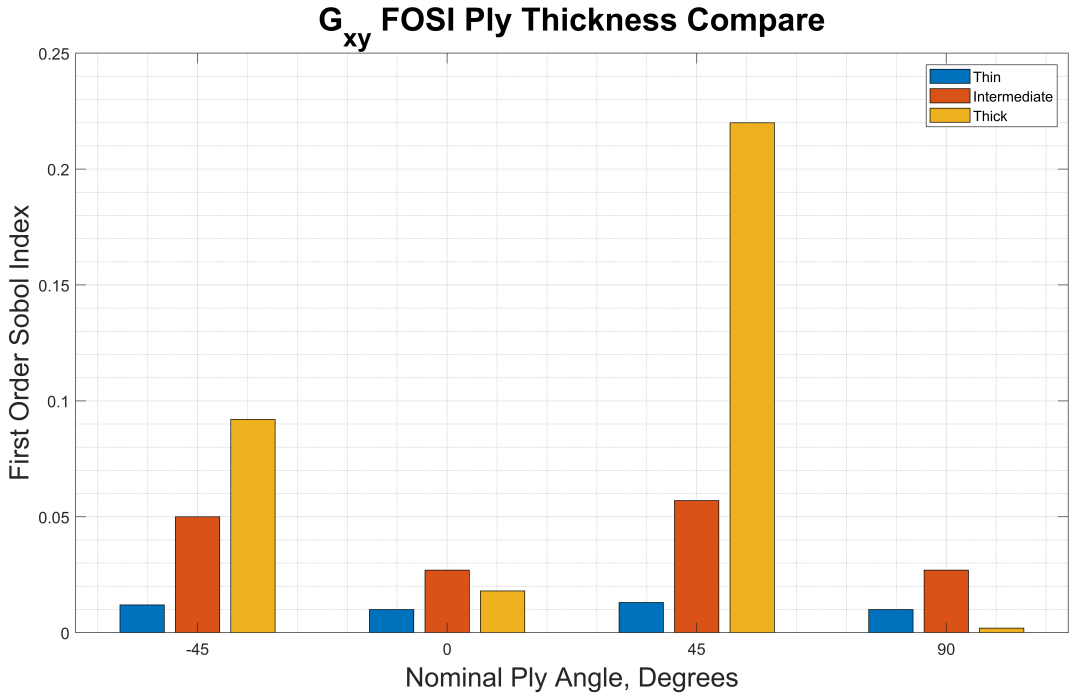

Figure 4.27: G_{xy} FOSI vs Ply Thickness

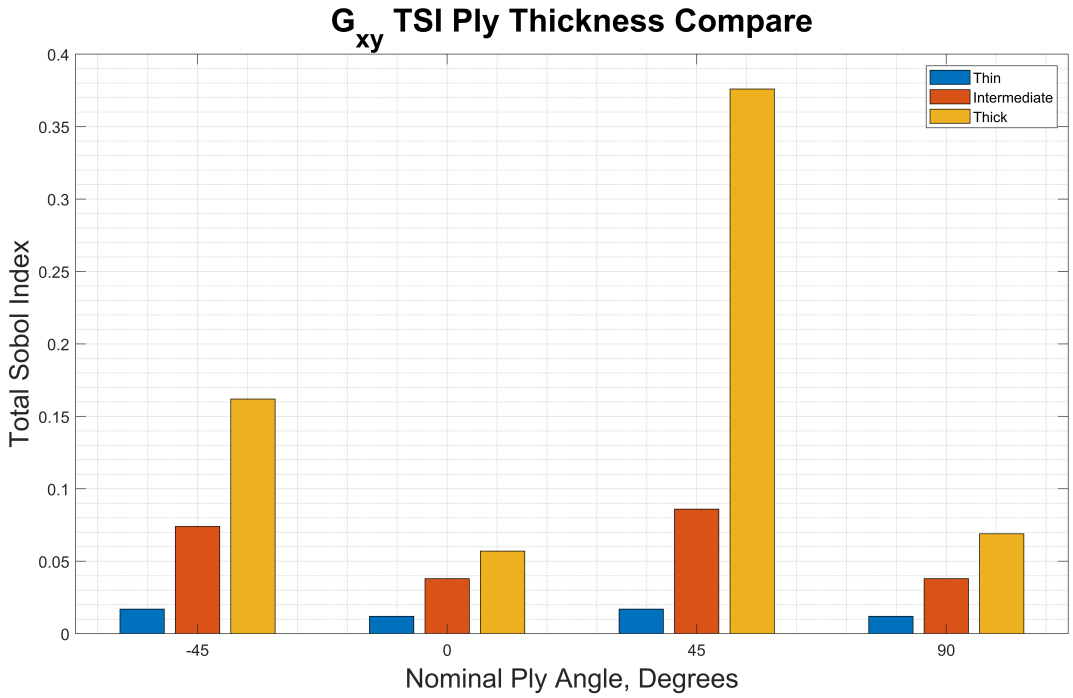

Figure 4.28: G_{xy} TSI vs Ply Thickness

first-order and total Sobol's indices give similar results for thick and intermediate laminates, suggesting most of the variation is due to first-order effects. As ply count increases with the thin ply laminate, larger differences can be observed between first-order and total effects. The comparison of sensitivity indices for the different methods studied in this work for thin ply laminates is shown in Fig. 4.29 through Fig. 4.32. Local analysis of variance shows good agreement with first-order Sobol's indices, suggesting that the simplified method is adequate for studying first-order effects. Relative ranking shows good agreement between all three presented indices. This agreement indicates that all 3 indices are sufficient for drawing conclusions about the relative impact of ply angle error for each nominal orientation angle.

Additionally, a comparison of total and first-order indices from Sobol's method shows that the majority of the impact of the variation in ply angle on the effective engineering properties is a first-order effect and not from interaction between plies, as measured by the elements of the ABD matrix.

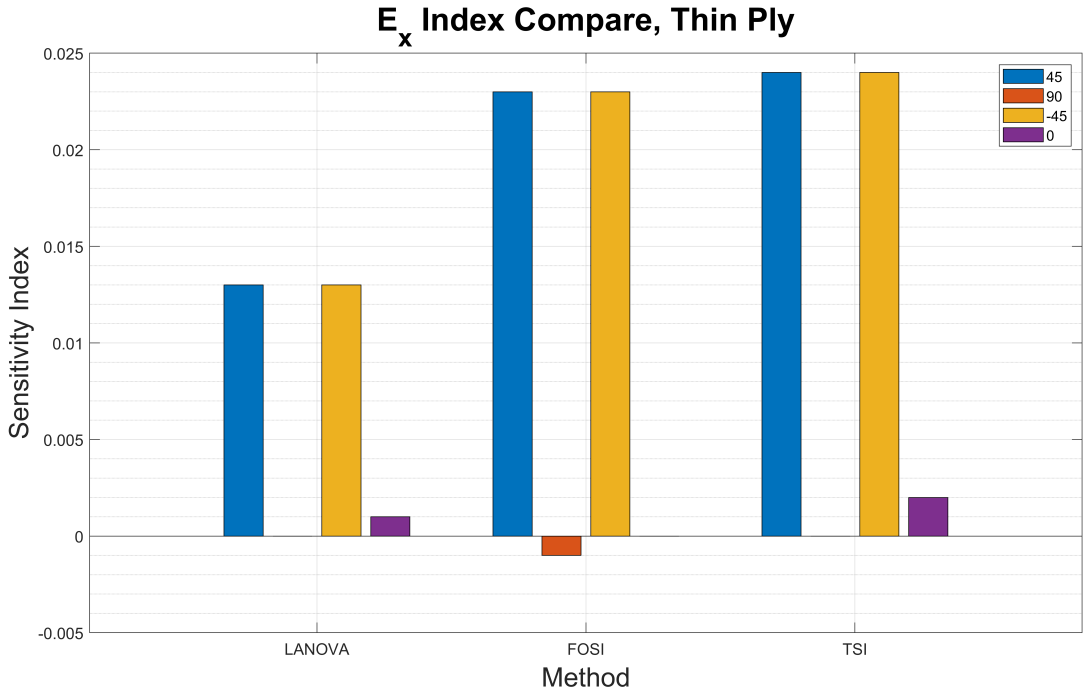

Figure 4.29: E_x Sensitivity Index Method Comparison

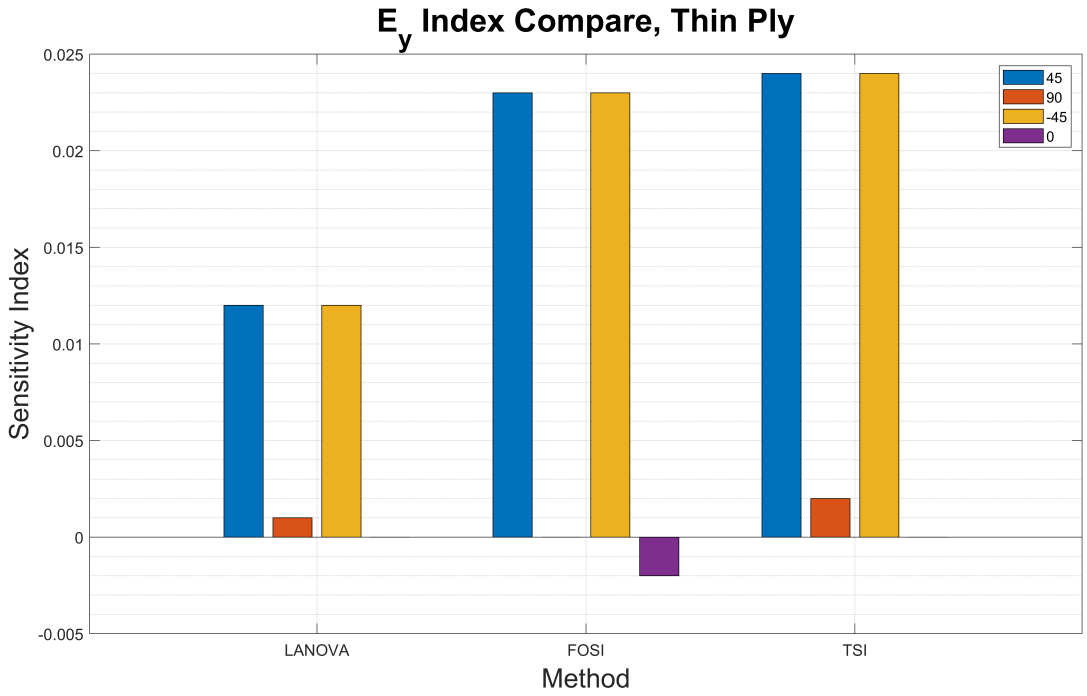

Figure 4.30: E_y Sensitivity Index Method Comparison

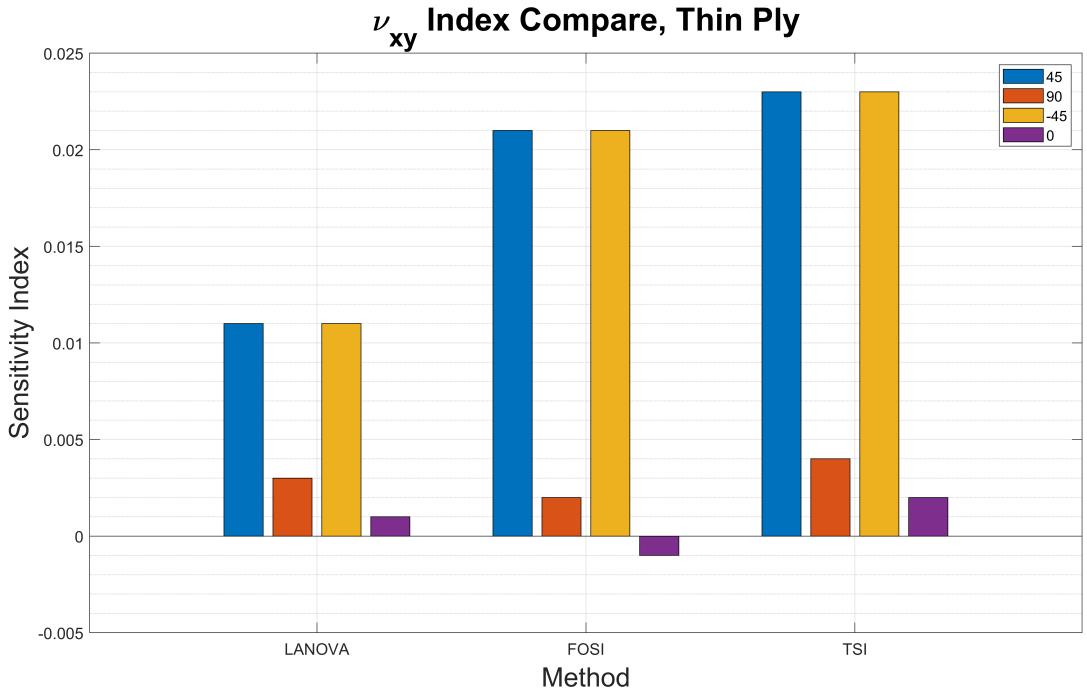

Figure 4.31: ν_{xy} Sensitivity Index Method Comparison

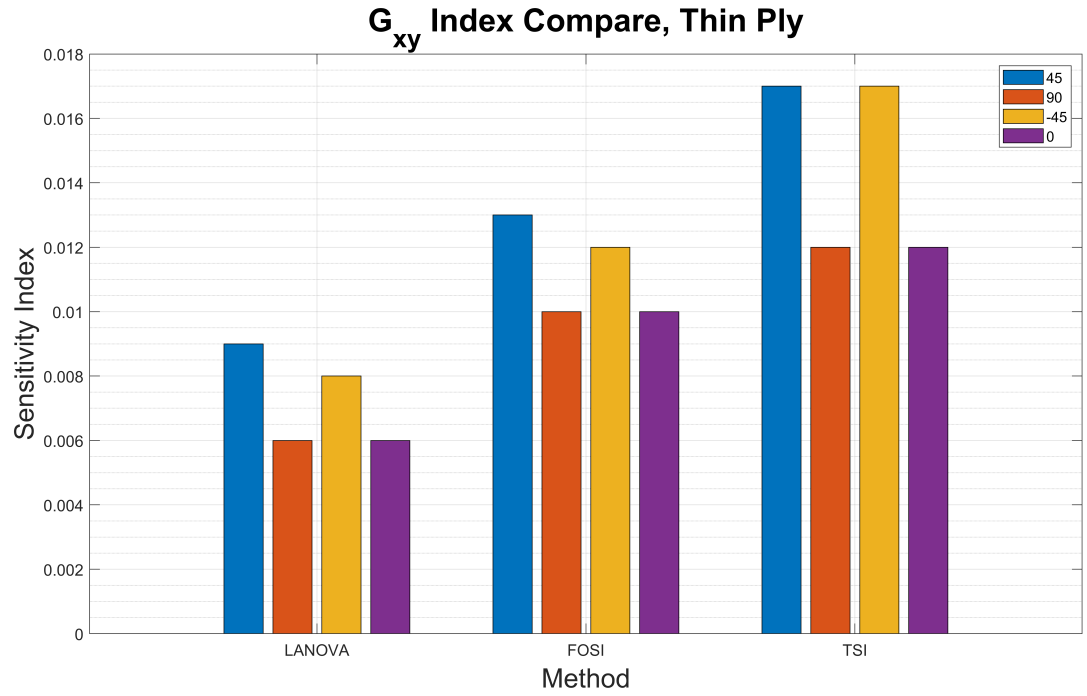

Figure 4.32: G_{xy} Sensitivity Index Method Comparison

The material parameter G_{xy} exhibits different behavior from the other effective engineering properties, due to the difference in the derivative of A_{66} and A11/22 as shown in Fig. 4.16. The derivative of A_{66} experiences stationary points at 45° intervals. Inspection of sensitivity indices of extensional terms A_{11} and A_{22} suggest that ply orientations at the stationary points of the derivative of the Q matrix terms will present a lower sensitivity index compared to ply angles which are not at a stationary point. Given that all four ply orientations present in the cross-ply laminates are stationary points for A_{66}, it is reasonable to obtain similar sensitivity indices for each of the ply orientations for the laminated studies in this work.

Chapter 5

Conclusions

5.1 Summary

This work has shown, that for an assumed 3.25°[7] standard deviation in ply orientation angle, the maximum observed normalized standard deviation in effective engineering stiffness is 3.5% of the nominal value. For 3σ bounds, this would equate to a maximum expected 10.5% change from nominal. This bounding case assumes a hand layup of a prepreg. Machine-based laminate construction is expected to have tighter tolerances on this error, which would further decrease the 3σ bounds.

Sensitivity analysis performed in this work has shown that the most critical plies to variation in the effective engineering properties for a quasi-isotropic layup are the +45° and -45° plies. These results indicate that when specifying tolerances on such laminates, the tolerance on ply angle of such plies is more important than the tolerance for the 0° and 90° plies. This insight is critical during the early stage in laminate design for determining which plies are most sensitive to manufacturing errors. This technique could be applied to additional laminates, and include additional input variables such as ply thickness or void content could be included to develop a better understanding as to which plies are critical to design when assessing manufacturing errors in built up laminates.

The completion of both uncertainty analysis and sensitivity analysis allows for information

about both laminate level performance and critical plies for performance to be obtained. While uncertainty analysis, assessing both mean and standard deviation, is useful for determining expected laminate performance, it does not provide information on which ply's variation is most critical to the expected performance. Adding sensitivity analysis allows for this additional information to be captured. The results obtained from both LANOVA and Sobol's method for sensitivity analysis in this work has shown that first-order sensitivity analysis techniques are sufficient for assessing sensitivity of a quasi-isotropic laminate to ply angle variation. Therefore any repeated analyses could be completed using the local technique to save computational cost and time. This sufficiency should be re-validated if different laminates or output quantities are introduced.

In addition to the overall low total variation observed in Table 4.6 a distinct decrease in variation of the ABD matrix terms was observed in the thin ply laminates. This decrease in variation, captured in both the uncertainty and sensitivity analyses, is linked to the increase in ply count attained by using thin plies within the same design thickness as a thick ply laminate. Investigation of a laminate with large ply thickness and ply level properties confirmed that this behavior is a result of the increase in ply count and not inherently connected to smaller ply thickness. A layup with the same ply count as a thick ply laminate and thinner plies would be expected to have the same variation as its thick ply counterpart. In the case of a laminate of fixed thickness, a decrease in ply thickness allows for an increase in ply count. Additionally, this increase in ply count increases the ability of the designer to tailor the layup for their intended application. Furthermore, the resulting decreased sensitivity to ply angle manufacturing errors provides a more robust laminate.

Based on the review of literature and the analyses performed in this work, thin ply laminates using sublaminar stacking are of significant interest for engineering applications. In these applications first-ply failure stress drives design. Thin ply laminates have been shown in

literature to suppress delamination and other transverse failure modes, resulting in an increased first ply failure strength. In addition, these laminates have shown to be less sensitive to manufacturing defects due to their higher ply count for a fixed laminate height. These qualities make thin ply laminates appealing for engineering applications.

5.2 Future Work

Multiple opportunities exist to further expand this work. Additional laminate types, sources of variation, and/or extension of the composite analysis could be performed to expand the scope of the simulations performed in this work.

While laminates studied to date are repeated quasi-isotropic layups, thin-ply composites are not restricted to such designs. Other layups should be studied to confirm that the observations made in this work extend to other laminate types. Composite tubes are often designed from axially biased symmetric laminates, and other special applications may call for asymmetric laminates, neither of which are assessed here. While the classical definition of effective engineering properties would not work for asymmetric laminates, analysis of ABD matrix terms and other output quantities such as strength could still be performed to assess the laminate's design.

In addition to other laminate types, the analysis performed in this work could be extended to simple structures such as sandwich panels. These panels are common in space structures, and may consist of composite facesheets separated by a metallic core. Appropriate modeling of the core as a uniform orthotropic material would allow for direct integration into the analyses performed in this work and lend to an application to engineering structures.

This work only considers the effect of ply angle variation on laminate stiffness. To extend this

work in assessment of manufacturing errors beyond ply thickness, additional input variables could be considered in the simulation. Variation in individual ply thickness, as well as void content in a ply modeled in the form of a penalty to that ply's stiffness properties, could be included in the simulation to assess the impact of other types of manufacturing errors. Uncertainty analysis would immediately consider their additional effects in overall laminate performance, and sensitivity analysis of these new input variables could be performed to identify which plies are most sensitive to these defects.

Laminate stiffness properties are the only output assessed in this work. The next logical step after laminate stiffness is laminate strength. Given a set of loads or displacements the laminate will be subjected to, the stiffness properties obtained in this work could be used to perform laminate analysis using CLT. Uncertainty analysis could be completed to obtain a 3σ confidence interval on expected stress/strain response, with sensitivity analysis identifying critical plies. With increasing complexity, Sobol's method for sensitivity analysis would be recommended to ensure that all interactions are captured when identifying critical plies. In addition to the above description of how this work could be extended to thermal loading and/or assessments of laminate stability under loading. The techniques presented in this work are a probabilistic approach to laminate analysis that can be expanded to additional applications beyond laminate stiffness.

Bibliography

[1] Chris Adcock and Adelchi Azzalini. "A selective overview of skew-elliptical and related distributions and of their applications". In: *Symmetry* 12.1 (2020), p. 118.

[2] R Amacher et al. "Thin ply composites: Experimental characterization and modeling of size-effects". In: *Composites Science and Technology* 101 (2014), pp. 121–132.

[3] Nasir Bilal. "Implementation of Sobol's method of global sensitivity analysis to a compressor simulation model". In: International Compressor Engineering Conference. 2014.

[4] Pedro P Camanho et al. "Prediction of in situ strengths and matrix cracking in composites under transverse tension and in-plane shear". In: *Composites Part A: Applied Science and Manufacturing* 37.2 (2006), pp. 165–176.

[5] Dassault Systèmes Simulia Corp. *ABAQUS/CAE User's Manual, (Abaqus 2016)*. English. United States.

[6] Michael W Hyer and Scott R White. *Stress analysis of fiber-reinforced composite materials*. DEStech Publications, Inc, 2009.

[7] Cornelia Jareteg et al. "Variation simulation for composite parts and assemblies including variation in fiber orientation and thickness". In: *Procedia CIRP* 23 (2014), pp. 235–240.

[8] Christopher Z Mooney. *Monte carlo simulation*. 116. Sage, 1997.

[9] D Novák, B Teplỳ, and N Shiraishi. "Sensitivity analysis of structures: a review". In: *Proceedings of CIVIL COMP*. Vol. 93. 1993, pp. 201–207.

[10] Lixia Pan et al. "Neural network ensemble-based sensitivity analysis in structural engineering: Comparison of selected methods and the influence of statistical correlation". In: *Computers & Structures* 242 (2021), p. 106376.

[11] R Byron Pipes and NJ Pagano. "Interlaminar stresses in composite laminates under uniform axial extension". In: *Journal of composite materials* 4.4 (1970), pp. 538–548.

[12] Sohel Rana and Raul Fangueiro. *Advanced composite materials for aerospace engineering: processing, properties and applications*. Woodhead Publishing, 2016.

[13] Reuven Y Rubinstein and Dirk P Kroese. *Simulation and the Monte Carlo method*. John Wiley & Sons, 2016.

[14] Hardeo Sahai and Mohammed I Ageel. *The analysis of variance: fixed, random and mixed models*. Springer Science & Business Media, 2012.

[15] Andrea Saltelli et al. *Global sensitivity analysis: the primer*. John Wiley & Sons, 2008.

[16] Sangwook Sihn et al. "Experimental studies of thin-ply laminated composites". In: *Composites Science and Technology* 67.6 (2007), pp. 996–1008.

[17] M SOBOL'I. "Sensitivity estimates for nonlinear mathematical models". In: *Mathematical Modelling Computational Experiments* 1.4 (1993), pp. 407–414.

[18] Kamran Tavakoldavani. *Composite materials equivalent properties in lamina, laminate, and structure levels*. The University of Texas at Arlington, 2014.

[19] *Thin-ply composite technology and applications*. 2019. URL: https://sbir.nasa.gov/content/thin-ply-composite-technology-and-applications-1.

[20] Stephen Tsai, Sangwook Sihn, and Ran Kim. "Thin ply composites". In: *46th AIAA/ASME/ASCE/AHS/ASC Structures, Structural Dynamics and Materials Conference*. 2005, p. 2005.

[21] MR Wisnom, B Khan, and SR Hallett. "Size effects in unnotched tensile strength of unidirectional and quasi-isotropic carbon/epoxy composites". In: *Composite Structures* 84.1 (2008), pp. 21–28.

[22] Y Zheng and A Rundell. "Comparative study of parameter sensitivity analyses of the TCR-activated Erk-MAPK signalling pathway". In: *IEE Proceedings-Systems Biology* 153.4 (2006), pp. 201–211.